TURUN
YLIOPISTO
UNIVERSITY
OF TURKU

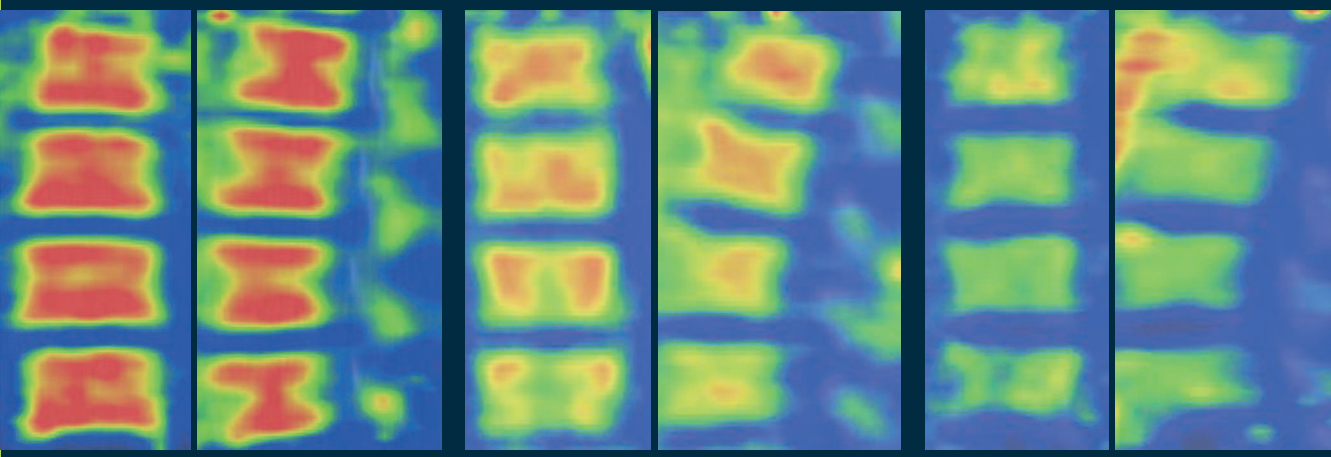

DIAGNOSTIC CHALLENGES IN THE EVALUATION OF RENAL OSTEODYSTROPHY

A Study Using ^{18}F-Sodium Fluoride Positron Emission Tomography

Louise Aaltonen

TURUN YLIOPISTON JULKAISUJA – ANNALES UNIVERSITATIS TURKUENSIS
SARJA – SER. D OSA – TOM. 1622 | MEDICA – ODONTOLOGICA | TURKU 2022

TURUN
YLIOPISTO
UNIVERSITY
OF TURKU

DIAGNOSTIC CHALLENGES IN THE EVALUATION OF RENAL OSTEODYSTROPHY

A Study Using ^{18}F-Sodium Fluoride Positron Emission Tomography

Louise Aaltonen

TURUN YLIOPISTON JULKAISUJA – ANNALES UNIVERSITATIS TURKUENSIS
SARJA – SER. D OSA – TOM. 1622 | MEDICA – ODONTOLOGICA | TURKU 2022

University of Turku

Faculty of Medicine
Department of Internal Medicine
Doctoral Programme in Clinical Research
Turku PET Centre

Supervised by

Docent Kaj Metsärinne, MD, PhD
Kidney Center
Department of Internal Medicine
Turku University Hospital
University of Turku
Turku, Finland

Docent Niina Koivuviita, MD, PhD
Kidney Center
Department of Internal Medicine
Turku University Hospital
University of Turku
Turku, Finland

Reviewed by

Docent Daniel Gordin, MD, PhD
Department of Nephrology
Helsinki University Hospital
University of Helsinki, Finland
Minerva Foundation Institute for
Medical Research
Helsinki, Finland

Professor Eero Honkanen, MD, PhD
University of Helsinki
Helsinki University Hospital
Helsinki, Finland

Opponent

Docent Satu Mäkelä, MD, PhD
Department of Internal Medicine
Tampere University Hospital
Tampere University
Tampere, Finland

The originality of this publication has been checked in accordance with the University of Turku quality assurance system using the Turnitin OriginalityCheck service.

ISBN 978-951-29-8820-4 (PRINT)
ISBN 978-951-29-8821-1 (PDF)
ISSN 0355-9483 (Print)
ISSN 2343-3213 (Online)
Painosalama, Turku, Finland 2022

To Jarkko, Ada and Filip

UNIVERSITY OF TURKU
Faculty of Medicine
Department of Internal Medicine
LOUISE AALTONEN: Diagnostic Challenges in the Evaluation of Renal Osteodystrophy – A Study Using ^{18}F-Sodium Fluoride Positron Emission Tomography
Doctoral Dissertation, 000 pp.
Doctoral Programme of Clinical Investigation
April 2022

ABSTRACT

The majority of patients with end-stage kidney disease develop abnormalities in bone metabolism, referred to as renal osteodystrophy. Bone abnormalities are associated with cardiovascular morbidity and mortality. The diagnosis of the subgroups of renal osteodystrophy, such as low- and high-turnover bone disease, is challenging. Bone biopsy is the gold standard, but it is invasive and not easily available. Biomarkers, such as parathyroid hormone and alkaline phosphatase, diagnostic accuracy is insufficient. A noninvasive diagnostic tool in the evaluation of renal osteodystrophy would be highly welcomed. ^{18}F-sodium fluoride positron emission tomography (^{18}F-NaF PET) is an imaging method that measures osteoblast activity and remodeling of bone.

The aims of this study were to (a) assess the usability of ^{18}F-NaF PET and (b) to assess the possible correlation between tracer activity and findings obtained from bone biopsy (c) evaluating whether ^{18}F-NaF PET imaging could replace bone biopsies in clinical practice. In addition, (d) the association between arterial calcification and bone metabolism was evaluated.

We observed a correlation between tracer activity measured by dynamic ^{18}F-NaF PET and parameters obtained by bone biopsy (a). The sensitivity and specificity of the method to distinguish between high- and low-turnover bone disease was good (b). Fluoride activity measured in the static ^{18}F-NaF PET scan showed good correlation with the fluoride activity measured in the dynamic scan, after correction for tracer activity in the blood (c). A weak association between arterial calcification and bone metabolism was also established (d).

^{18}F-NaF PET presents as a promising diagnostic tool in the evaluation of renal osteodystrophy. Our research suggests that a static ^{18}F-NaF PET scan obtained after a single injection of tracer generates usable images of bone metabolism and could also work in a clinical setting.

KEYWORDS: ^{18}F-NaF PET, positron emission tomography, bone histomorphometry, renal osteodystrophy, vascular calcification, dialysis

TURUN YLIOPISTO
Lääketieteellinen tiedekunta
Sisätautioppi
LOUISE AALTONEN: Diagnostiset haasteet munuaispotilaiden luustotaudin arvioinnissa – Tutkimus, jossa käytetään ^{18}F-NaF positroniemissiotomografia
Väitöskirja, 000 s.
Turun Yliopiston kliininen tohtoriohjelma
Huhtikuu 2022

TIIVISTELMÄ

Suurimmalle osalle potilaista, jotka sairastavat vaikeaa munuaisten vajaatoimintaa, kehittyy poikkeavuuksia luun aineenvaihduntaan. Luustohäiriöiden tiedetään liittyvän myös sydän- ja verisuonisairauksiin sekä kuolleisuuteen. Luustohäiriöiden alaryhmien kuten hitaan ja nopean aineenvaihdunnan luutaudin diagnosointi on haastavaa. Nykyisin katsotaan luubiopsian olevan diagnostiikan kultainen standardi, mutta se on kajoava ja käytössä vain muutamissa keskuksissa. Laboratoriokokeiden, kuten alkalisen fosfataasin tai parathormonin diagnostinen tarkkuus tiedetään puolestaan riittämättömäksi. Näin ollen erityisesti kliinisessä työssä kaivattaisiin uutta kajoamatonta menetelmää munuaistaudin aiheuttamien luustomuutosten arviointiin. ^{18}F-NaF positroniemissiotomografia (^{18}F-NaF PET) on kuvantamismenetelmä, joka kuvastaa luuta muodostavien solujen aktiivisuutta ja luun uudelleenmuodostumista.

Tämän tutkimuksen tavoitteena oli (a) arvioida ^{18}F-NaF PET -kuvantamisen käytettävyyttä ja (b) arvioida merkkiaineaktiivisuuden mahdollista korrelaatiota luubiopsiasta saatujen parametrien välillä. Lisäksi arvioitiin, voisiko (c) ^{18}F-NaF PET korvata luubiopsian kliinisessä työssä. Myös (d) valtimokalkkeutumien ja luun aineenvaihdunnan häiriöiden välistä yhteyttä selvittiin.

Dynaamisen ^{18}F-NaF PET kuvauksen mitatun merkkiaineaktiivisuuden ja luubiopsialla saatujen parametrien välillä oli vahva korrelaatio (a). Menetelmä todettiin sekä herkäksi että tarkaksi kyvyssään erottaa luun alentunut ja kiihtynyt aineenvaihdunta (b). Staattisen ja dynaamisen ^{18}F-NaF PET –kuvauksen fluoriaktiivisuus korreloivat hyvin veren merkkiaineen aktiivisuuden korjaamisen jälkeen (c). Valtimoiden kalkkeutumisasteen ja luun aineenvaihdunnan välillä puolestaan pystyttiin osoittamaan heikko assosiaatio (d).

^{18}F-NaF PET on lupaava diagnostinen työkalu munuaispotilaiden luustotaudin arvioinnissa. Tutkimuksemme viittaa siihen, että yhden merkkiaineinjektion jälkeen saatu staattinen ^{18}F-NaF PET kuvaus voisi toimia myös kliinisessä työssä.

AVAINSANAT: ^{18}F-NaF PET, positroniemissiotomografia, luun histomorfometria, renaalinen osteodystrofia, vaskulaarinen kalsifikaatio, dialyysi

Table of Contents

Abbreviations

AAC	Abdominal aortic calcification
Ac.f	Activation frequency
AIF	Arterial input function
Aj.AR	Adjusted apposition rate
ASBMR	American Society of Bone and Mineral Research
AUC	Area under the curve
BFR	Bone formation rate
BFR/BS	Bone formation rate per bone surface
BMD	Bone mineral density
BMU	Basic multicellular unit
BSAP	Bone-derived alkaline phosphatase
BV/TV	Bone volume per tissue volume
CAC score	Coronary artery calcium score
CaSR	Calcium-sensing receptors
CKD	Chronic kidney disease
CKD-MBD	Chronic kidney disease–mineral and bone disorder
CT	Computed tomography
CTX	Collagen type 1 crosslinked C-telopeptide
CVD	Cardiovascular disease
DXA	Dual-energy X-ray absorptiometry
ES/BS	Eroded surface per bone surface
ESRD	End-stage kidney disease
HR-pQCT	High-resolution peripheral computed tomography
^{18}F-FDG	^{18}F-fluorodeoxyglucose
FGF-23	Fibroblast growth factor 23
FGFR	Fibroblast growth factor receptor
^{18}F-NaF-PET	^{18}F-sodium fluoride positron emission tomography
FUR	Fractional uptake rate
GFR	Glomerular filtration rate
HSC	Hematopoietic stem cells
IQR	Interquartile range
KDIGO	Kidney Disease Improving Global Outcomes
K_i	Blood clearance to bone

LVH	Left ventricular hypertrophy
MAR	Mineral apposition rate
MBq	Megabecquerel
Mlt	Mineralization lag time
MRI	Magnetic resonance imaging
MS/BS	Mineralized surface per bone surface
NaPi-2	Sodium phosphate (NaPi-2) transporter
NCC	NaCl cotransporter
NFAT	Nuclear factor of activated T-cells
OPG	Osteoprotegerin
Ob.S/BS	Osteoblast surface per bone surface
Oc.S/BS	Osteoclast surface per bone surface
OS/BS	Osteoid surface per bone surface
O.Th	Osteoid thickness
OV/BV	Osteoid volume per bone volume
PET	Positron emission tomography
Pit-1	NaPi cotransporter
P1NP	Procollagen type 1 N-terminal propeptide
PTH	Parathyroid hormone
RAAS	Renin-angiotensin-aldosterone system
RANK	Receptor activator of NF-jB
RANKL	Receptor activator of NF-jB ligand
ROC	Receiver operating characteristics
ROD	Renal osteodystrophy
ROI	Region of interest
SD	Standard deviation
SNA	Sympathetic nerve system
SUV	Standardized uptake values
TAC	Time uptake curve
TBS	Trabecular bone score
Tb.Th	Trabecular thickness
TMV	Bone turnover, mineralization and volume
TRAP5b	Tartrate-resistant acid phosphatase
Wnt	Wingless/int-1
W.Th	Wall thickness
25(OH)D	25-hydroxyvitamin D
1.25$(OH)_2$D	1.25-dihydroxyvitamin D

List of Original Publications

This dissertation is based on the following original publications, which are referred to in the text by their Roman numerals:

I. Aaltonen L, Koivuviita N, Seppänen M, Tong X, Kröger H, Löyttyniemi E, Metsärinne K. Correlation between 18F-Sodium Fluoride positron emission tomography and bone histomorphiometry in dialysis patients. BONE 2020 May;134:115267. DOI: 10.1016/j.bone.2020.115267

II. Aaltonen L, Koivuviita N, Seppänen M, Burton IS, Kröger H, Löyttyniemi E, Metsärinne K. Bone Histomorphometry and 18F-Sodium Fluoride Positron Emission Tomography Imaging: Comparison between only Bone Turnover -based and Unified TMV -based Classification of Renal Osteodystrophy. Calcif Tissue Int 2021 Jun 17. DOI: 10.1007/s00223-021-00874-9

III. Aaltonen L, Koivuviita N, Seppänen M, Kröger H, Tong X, Löyttyniemi E, Metsärinne K. Association between bone mineral metabolism and vascular calcification in end-stage renal disease. BMC Nephrol. 2022 Jan 3;23(1)12. DOI: 10.1186/s12882-021-02652-z

IV. Aaltonen L, Koivuviita N, Seppänen M, Oikonen V, Kirjavainen A, Kröger H, Löyttyniemi E, Metsärinne K. Measuring bone metabolic activity in CKD5D patients with renal osteodystrophy using 18F-sodium fluoride positron emission tomography – comparison between static and dynamic measurements.

1 Introduction

Even in the early stages of chronic kidney disease, disturbances in mineral homeostasis start to develop, leading to abnormalities in bone remodeling and mineralization (1). The pathophysiology behind these abnormalities is complex and not fully understood. Chronic kidney disease–mineral and bone disorder is associated with increased cardiovascular morbidity and mortality (2, 3). Cardiovascular morbidity is highly prevalent in the CKD population, and disturbances in mineral homeostasis, including rising levels of fibroblast growth factor 23, eventually leading to hyperphosphatemia, accelerate mineral deposition in both the vessels and heart valves (4). Disturbance in bone metabolism, especially high turnover disease, increase fracture risk in end-stage renal disease (5). Fractures are associated with both increased morbidity and mortality (6).

The underlying bone abnormalities linked to this disorder are referred to as renal osteodystrophy. Renal osteodystrophy include changes in bone turnover, bone mineralization and bone volume (1). The underlying subtype of renal osteodystrophy guide medication decisions and potential surgical interventions. However, the diagnosis of the underlying bone disorder is challenging. Bone biopsy is the gold standard for diagnosing the subtypes of renal osteodystrophy, but it is not easily available. It is invasive, requires expertise regarding quantitative histomorphometry and is limited to a single site of the skeleton. Biomarkers in clinical use have limited ability to correctly estimate the underlying bone disorder in advanced kidney disease (7).

The link between arterial calcification and abnormalities in bone metabolism is also well acknowledged, even though the underlying mechanisms are not yet fully understood. Several cross-sectional studies indicate a connection between arterial calcification and impaired bone metabolism in patients with end-stage kidney disease (8). Reduced progression of vascular calcification linked to improvement in bone turnover shown in one small prospective study, strengthens this assumption (9). However, there are no large longitudinal studies to confirm the link between changes in bone metabolism and development or progression of vascular calcification.

^{18}F-sodium fluoride positron emission tomography (^{18}F-NaF PET) is a noninvasive quantitative imaging technique that in a unique way enables studies of

regional bone metabolism (10). ^{18}F-NaF is a bone-seeking tracer that reflects remodeling of bone and osteoblast activity (11). It serves as an efficient tracer to measure metabolic changes in bone. A non-invasive imaging method measuring bone turnover would be a valuable tool in clinical practice. Quantitative dynamic positron emission tomography scans are used in the research setting, for example, when measuring the treatment effect of osteoporosis medication (12) but are not feasible in clinical practice. Measuring standardized uptake values from static scans would be a more suitable method.

Coronary artery calcification is highly prevalent in advanced kidney disease. Coronary calcification is associated with cardiovascular disease, myocardial infarction and all-cause mortality (13). Non-contrast cardiac computed tomography is highly sensitive for detection of coronary artery calcification (14)

The aim of this study was to assess a possible correlation between histomorphometric markers obtained by bone biopsy and tracer activity in the ^{18}F-sodium fluoride positron emission tomography scan. This study also aimed to evaluate the diagnostic accuracy of the method when evaluating dialysis patients with renal osteodystrophy and to assess its feasibility in clinical practice. Cardiovascular morbidity is strongly linked to renal osteodystrophy, and this study also evaluated the possible association between bone metabolism and arterial calcification.

2 Review of the Literature

2.1 Chronic kidney disease–mineral and bone disorder (CKD-MBD)

Chronic kidney disease (CKD) affects 8–16% of the population worldwide (15, 16) and is an increasing health problem. Chronic kidney disease is a significant contributor to excess morbidity and mortality (17, 18). As kidney function declines, a disturbance in mineral homeostasis progressively develops, leading to a complex disorder called chronic kidney disease–mineral and bone disorder (CKD-MBD) (1). CKD-MBD is defined as a disorder of mineral and bone metabolism due to CKD manifested by either one or a combination of the following: 1) abnormalities of calcium, phosphorus, parathyroid hormone (PTH) or vitamin D metabolism, 2) abnormalities in bone turnover, mineralization, volume, linear growth, or strength or 3) vascular or other soft-tissue calcification (1, 19). CKD-MBD is a unique disorder linked to chronic kidney disease.

The disturbance in mineral homeostasis in patients with chronic kidney disease affects bone remodeling. Bone abnormalities are found in a majority of patients with end-stage kidney disease (1, 20–22). Abnormal bone turnover is associated with an increased risk of fractures (5, 23–24), and fractures are a major cause of morbidity and increased mortality (4, 25). Impaired bone metabolism is also associated with vascular calcification and cardiovascular morbidity and mortality (8, 9, 26).

2.1.1 Classification of chronic kidney disease (CKD)

According to the KDIGO (Kidney Disease Improving Global Outcomes) guidelines (27), the definition of chronic kidney disease is kidney damage for three months or more, as defined by structural or functional abnormalities of the kidney that can lead to decreased glomerular filtration rate (GFR). These abnormalities can be manifested by either pathological abnormalities, markers of kidney damage (including abnormalities in the composition of the blood or urine or in imaging tests) or GFR < 60mL/min/1.73m^2 for three months or more, with or without kidney damage. The estimated glomerular filtration rate is eGFR.

The classification of CKD is based on the level of GFR. Based on severity, CKD is classified into five stages; see Table 1. The prevalence of complications linked to chronic kidney disease increases with declining GFR.

Table 1. Stages of chronic kidney disease.

Stage	Qualitative Description	Renal function, GFR mL/min/1.73m^2
1	Kidney damage with normal or ↑ GFR	90
2	Kidney damage with mild ↓ GFR	60–89
3a	Mild to moderate ↓ GFR	45–59
3b	Moderate to severe ↓ GFR	30–44
4	Severe ↓ GFR	15–29
5	Kidney failure	< 15 (or dialysis)

2.1.2 Normal physiology of bone

The mature adult skeleton consists of 80 percent cortical bone and 20 percent trabecular bone (28). Different bones have different ratios of cortical and trabecular bone. For example, in the vertebra, the ratio of trabecular and cortical bone is 75:25, in the femoral neck 50:50 and in the radial diaphysis 5:95. The cortical bone provides maximum resistance to torsion or bending and gives the compressive strength of the bone. Trabecular bone is metabolically more active than cortical bone and responds more rapidly to mechanical stimuli (29).

Both trabecular and cortical bone are composed of osteons. Cortical osteons are called Haversian systems; they are cylindrical in shape and form a branching network within the cortical bone (28). Trabecular osteons are called packets and are semilunar in shape. Both cortical and trabecular bone are normally formed in a lamellar pattern. Collagen fibrils are laid down in variable orientations within the pattern (28, 29). One can see the lamellar pattern during microscopic examination with polarized light.

Bone is a combination of osteoid matrix and hydroxyapatite crystal. In addition, bone contains water, non-collagenous proteins and specialized bone cells. About 10 percent of the bone volume consists of bone cells. The bone cells arise from two lines, osteoprogenitor cells from mesenchymal stem cells, which differentiate into osteoblasts and osteocytes, and the osteoclasts, which are hematopoietic cells (29). *Osteoblasts* are considered the bone-forming cells and line the surfaces of bone. Osteoblasts synthesize new bone matrix. Within the osteoblast lineage, subpopulations of osteoblasts respond to various hormonal, mechanical or cytokine signals. When osteoblasts are activated, they may remain quiescent osteoblasts lining

bone, become osteocytes or return to the osteoprogenitor cell line (29). *Osteocytes* account for 90% of all bone cells. Osteocytes are osteoblasts that have surrounded themselves with organic matrix and live within vacuoles called lacunae. Osteocytes can communicate with each other, and they contribute to maintenance of calcium homeostasis. *Osteoclasts* are the only cells that can resorb bone. They are multinucleated cells derived from mononuclear precursor cells of the monocyte-macrophage lineage (30). Figure 1 shows the different bone cells.

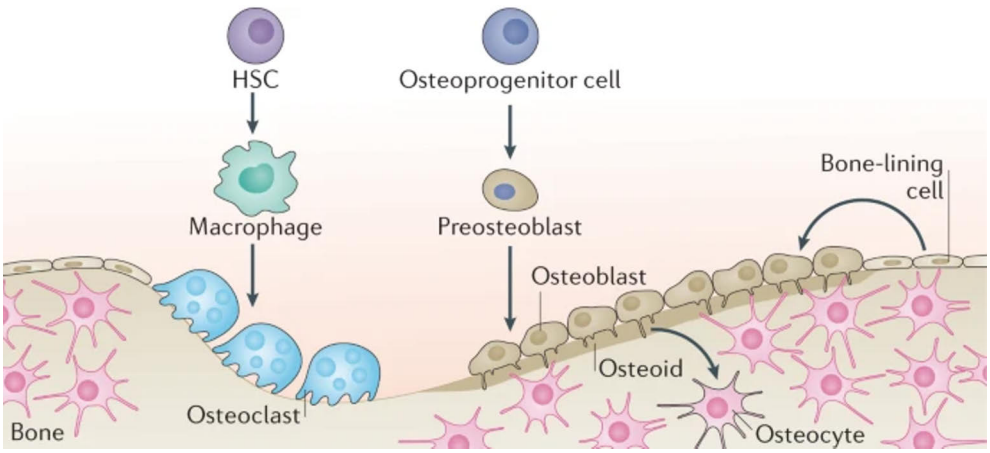

Figure 1. Bone homeostatis. Figure reproduced from Nature Reviews Molecular Cell Biology 2020 Nov;21(11):696. Reproduced with permission. HSC = hematopoietic stem cells.

Bone undergoes dynamic modeling, remodeling and growth throughout life (31). Both modeling and remodeling involve osteoclastic bone resorption and osteoblastic bone formation. *Bone modeling* is the process in which bones change their overall shape in response to mechanical forces or physiological influences. Bone modeling is less frequent than remodeling in adults but can still occur in adulthood as an adaptive response to mechanical loading (32, 33). *Bone remodeling* is the system's way of maintaining bone strength and mineral homeostasis. It is a tightly regulated process of resorption and replacement of bone and is essential for keeping the bones healthy. Remodeling also assists in the regulation of calcium and phosphate metabolism and in the repair of microdamaged bone (34). Anatomically, the remodeling cycle takes place within a basic multicellular unit (BMU), which consists of a tightly coupled group of osteoblasts and osteoclasts, which carry out formation of new bone and resorption of old bone (35). Each BMU undergoes its functions in the same order: 1) origination and organization of the BMU, 2) activation of osteoclasts and resorption of old bone, 3) recruitment of osteoblasts and formation of new bone matrix, and 4) mineralization (36). The end result of each bone

remodeling cycle, which takes approximately 120–200 days, is production of a new osteon (37). Osteocytes regulate differentiation of osteoclasts and osteoblasts and thus regulate bone resorption and formation. The remodeling process is basically the same in cortical and trabecular bone (38). Bone remodeling increases in early postmenopausal women, then slows with further aging but stays increased. Bone remodeling in aging men is thought to increase only mildly.

The remodeling cycle is tightly regulated by signaling pathways and endocrine regulation (39). There are two major signaling pathways that regulate the resorption and formation within the remodeling cycle: osteoprotegerin/receptor activator of NF-jB ligand/receptor activator of NF-jB (OPG/RANKL/RANK) and wingless/int-1 (Wnt) pathways. Osteoblasts and osteocytes stimulate RANK expression. RANKL binding to its receptor RANK activates osteoclasts and the expression of osteoclast genes (30, 37). OPG inhibits osteoclastic bone resorption by binding to RANKL and thereby preventing its binding to RANK (37). OPG has proven to increase the risk for CVD morbidity and mortality, probably by direct actions on vascular function and the effects on the OPG/RANKL/RANK pathway (40). Wnt pathways again are major regulators of osteoblastic bone formation. PTH is an endocrine regulator of the bone remodeling cycle. PTH stimulates bone resorption and is a key physiological mechanism in calcium homeostasis. Continuous PTH excretion induces both trabecular and cortical bone loss because of modulation of the OPG/RANKL/RANK signaling system (41). Cortical bone loss is usually more severely affected. Vitamin D, calcitonin, growth hormone and several other hormones also affect the remodeling cycle. In addition, glucocorticoids inhibit osteoblast differentiation and increase osteoblast apoptosis (42). Prostaglandins also regulate bone resorption and formation, even though the exact role in the remodeling cycle remains uncertain.

2.1.3 Pathophysiology of CKD-MBD

The pathophysiology of mineral and bone disorder is complex, and even though information and new published data have broadened our understanding of the disorder, further studies are needed to better understand the major impact on both bone health and cardiovascular disease.

The parathyroid gland is important in regulating mineral homeostasis by cross-talking with bone and kidneys. As renal function declines, the kidney´s ability to appropriately excrete excess phosphate load declines, usually beginning by the CKD stages 2–3. This initiates rising levels of fibroblast growth factor 23 (FGF-23), a bone-derived hormone (43). FGF-23 normally acts to decrease serum PTH (44, 45), but in CKD, FGF-23 receptors are downregulated in both the kidney and the parathyroid gland (klotho-FGFR1 receptors) (46-48). FGF-23 increases phosphorus

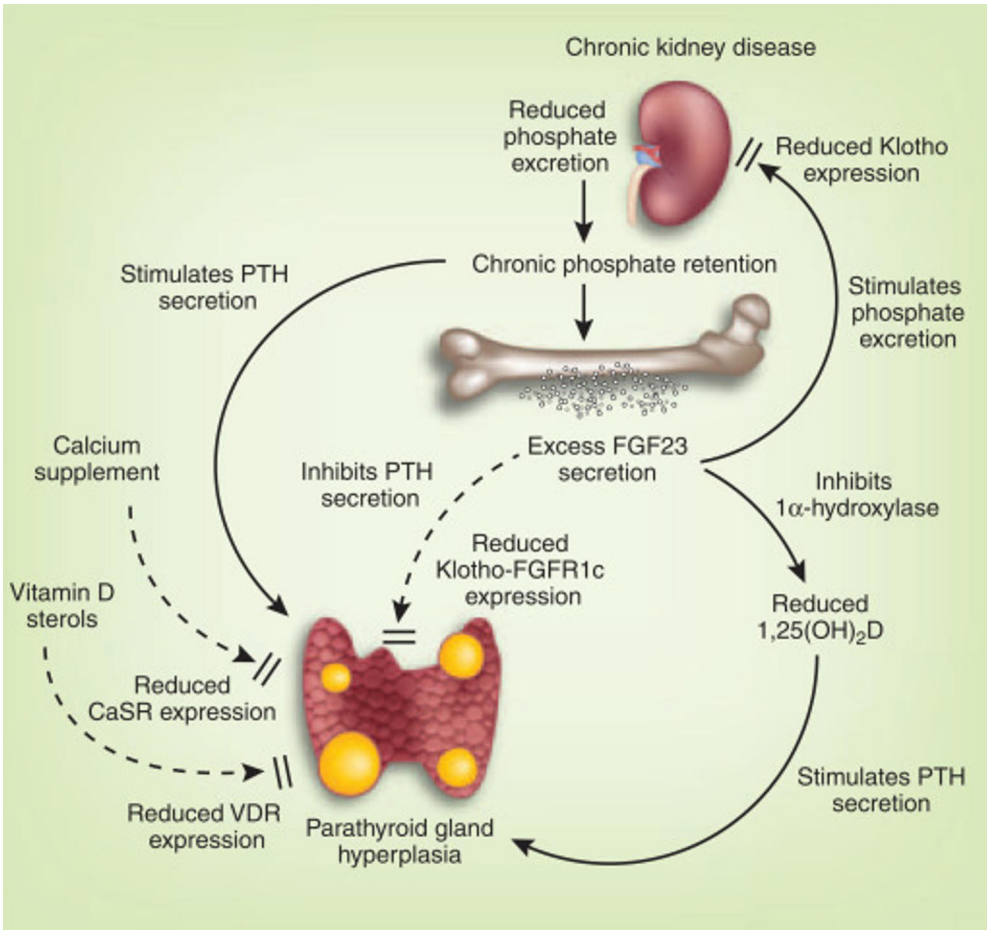

Figure 2. The development of secondary hyperparathyroidism in chronic kidney disease. Figure reproduced from Kidney International 2010 Feb;77(4):292-8. Reproduced with permission

excretion by the kidneys and decreases calcitriol synthesis by inhibiting 1α-hydroxylase (49, 50). The enzyme 1α -hydroxylase converts 25-hydroxyvitamin D (25(OH)D) to 1.25-dihydroxyvitamin D ($1.25(OH)_2D$), which is the active form. Lower levels of $1.25(OH)_2D$ decrease the absorption of calcium from the intestine leading to hypocalcemia, which stimulates the secretion of PTH from the parathyroid gland. One of the main functions of PTH is to correct hypocalcemia. Calcium ion levels are sensed by the parathyroid calcium-sensing receptors (CaSRs), which also regulate the synthesis and secretion of PTH (51). PTH acts on bone by activating both osteoclasts and osteoblasts to increase the efflux of calcium and phosphate. PTH also acts on the kidney to increase reabsorption of calcium and to increase excretion of phosphorus. In addition, PTH stimulates the production of $1.25(OH)_2D$. At an

early stage, the system can correct hyperphosphatemia and hypocalcemia by the mechanisms described above, but when CKD progresses and kidney function declines, the remedial mechanisms are exceeded, and persistent hyperphosphatemia develops. Elevated phosphorus levels also stimulate PTH excretion and this vicious circle eventually leads to parathyroid cell proliferation (52). As a contributory mechanism, down-regulation of calcium-sensing receptors, vitamin D receptors and klotho-FGFR1 receptors contribute to the development of PTH resistance (53, 54). The chain of events leading to secondary hyperparathyroidism in CKD is shown in Figure 2.

2.1.3.1 Phosphorus metabolism in CKD

In chronic kidney disease, the disturbance in phosphorus metabolism and the adaptive mechanisms that are activated due to hyperphosphatemia are likely involved in several key features of CKD, including cardiovascular complications. High serum phosphate levels are associated with cardiovascular disease and increased mortality in patients with CKD (55) and in the general population (56, 57). High phosphate levels are also an independent risk factor for the development and progression of renal disease (58, 59). Also, in patients on dialysis, high phosphate levels independently associate with all-cause and cardiovascular mortality (60, 61). However, there is a lack of large longitudinal intervention trials that would clarify the impact of lowering phosphate levels on cardiovascular outcomes.

Phosphorus is a crucial factor for cell life and function, and phosphate balance is carefully regulated to maintain sufficient phosphate levels. Phosphate uptake from the intestine occurs via the phosphate channel NaPi-2b. Upregulation of NaPi-2b in response to $1.25(OH)_2D$ leads to an increase in phosphate absorption from the intestine. Chronic kidney disease does not significantly affect the intestinal uptake of phosphate, but hyperphosphatemia causes retrieval of NaPi-2b channels in the kidney (62), leading to increased phosphaturia. FGF-23 and PTH act on the kidney to achieve NaPi-2b retrieval (49, 63) and hereby increase excretion of phosphate. As GFR declines, these adaptive mechanisms are exceeded, leading to hyperphosphatemia. Experimental studies have demonstrated that phosphate induces vascular calcification and cardiovascular abnormalities in vitro (64, 65), and these results have also been confirmed in vivo (66). The rising levels of FGF-23 due to hyperphosphatemia induce additional pathologies, as discussed in the next section.

2.1.3.2 Fibroblast growth factor 23 and α-Klotho

FGF-23 is a key factor in the pathophysiology of CKD-MBD, and elevated levels of FGF-23 are the first sign of development of secondary hyperparathyroidism in CKD.

FGF-23 levels start to rise before increases in phosphate and PTH levels can be detected (67, 68). FGF-23 levels continue to rise along with phosphate and PTH as CKD progresses, eventually reaching their peak level during dialysis (68). FGF-23 is secreted mainly by osteocytes in bone (69). Its physiological effect is to maintain the balance of phosphorus and vitamin D homeostasis. FGF-23 is also a suppressor of PTH. FGF-23 actions on the kidney and parathyroid gland are mediated through FGF receptor 1 (FGFR1). Transmembrane α-Klotho, a co-receptor, is required for FGF-23 to bind to its receptor (70, 71). As a contributor to excess cardiovascular morbidity linked to CKD-MBD, FGF-23's association with a numerous different manifestations of cardiovascular disease (CVD) have been documented. In animal studies, a direct toxicity of FGF-23 given as an infusion was detected, causing myocyte hypertrophy resulting in the induction and exacerbation of left ventricular hypertrophy (LVH) (72). This effect was independent of α-klotho and was explained by the finding that FGF-23 effects on myocardium are mediated through FGFR4, not FGFR1 (73). The rapid elevations of FGF-23 when CKD progresses correlate with further progression of left ventricular hypertrophy (72, 74). Several studies reveal a relationship between elevated FGF-23 levels and congestive heart failure and atherosclerosis (75, 76), and elevated FGF-23 levels have also been associated with hypertension (77)

Alpha-Klotho, the co-receptor when FGF-23 binds to its receptor, also has FGF-23 independent effects. It was originally discovered in 1997 as a gene linked to aging and has been identified as membrane-bound α-Klotho, which is the co-receptor of FGF-23, and soluble α-Klotho, which has hormone-like properties (78). Alpha-Klotho is highly expressed in the kidney (79), and it has multifaceted functions as an inhibitor of apoptosis and fibrosis and an inducer of autophagy (80, 81). Most experimental data suggest that α-Klotho has vasoprotective properties (82, 83). It also causes phosphaturia (84) and has also shown anti-calcifying and antioxidant properties (85).

2.1.3.3 Wnt signaling pathways and sclerostin

Wnt signaling pathways are important in many biological processes—for example, in cell proliferation, growth, migration, and differentiation (86). Wnt signaling plays a key role in bone physiology and in the regulation of cellular activities and mineralization processes in bone (87). Recent research has focused on understanding Wnt signaling pathways and their part in the pathophysiology of CKD-MBD and vascular calcification. It is clear that the balanced activity of Wnt pathways is important for bone health.

In CKD, the Wnt pathways are disturbed, partly because of increased circulating concentrations of sclerostin. Sclerostin is a Wnt inhibitor (87) and is produced almost exclusively from osteocytes. Sclerostin was recently presented as a new possible biomarker for bone and vascular disease, but further research is needed to establish

its role in the pathophysiology of CKD-MBD. Sclerostin reduces bone formation by inhibiting Wnt pathways in the osteoblasts (88). Regulation of sclerostin in bone is not yet fully understood, but both growth factors and hormones, including PTH, impact the secretion of sclerostin (87). There is experimental evidence of crosstalk between PTH and Wnt signaling actions, mediated by sclerostin (89). Sclerostin showed a negative correlation with PTH and a strong negative association with parameters of bone turnover in dialysis patients (90).

2.1.4 CKD-MBD and vascular calcification

It is well acknowledged that vascular calcification and cardiovascular disease are overrepresented in patients with chronic kidney disease. CVD is the leading cause of morbidity and mortality in patients with end-stage renal disease. The prevalence of vascular calcification increases with decreasing kidney function. In addition to traditional risk factors of cardiovascular disease (91), multiple non-traditional risk factors such as uremic toxins, oxidative stress and inflammation, together with abnormal bone and mineral metabolism, contribute to the excess cardiovascular burden in patients on dialysis (2, 92). The presence of vascular calcification is also a non-traditional risk-factor in the CKD population. Vascular calcification is highly predictive of CVD and mortality (93–95). The risk factor profile of cardiovascular disease seems to differ in the CKD population compared to the general population (96), which is supported by the fact that several large randomized controlled trials have found no survival benefit of different treatment strategies, including lipid-lowering treatment (97), treatment with angiotensin-converting enzyme inhibitors (98) and increased dialysis dose (99). CKD and the progression of kidney disease seem to affect several pathways involved in different tissues' healthy homeostasis contributing to the excess development of vascular calcification in the CKD population.

Pathophysiologically there are two types of vascular calcification: deposition of calcium-phosphate salts occurring in the intima of the blood vessels and deposition of calcium-phosphate salts in the media of the blood vessels (94). In addition, valvular calcification, often observed in calcific aortic valve disease, is characterized by the deposition of calcium salts in the heart valves (100). The impact of vascular calcification on cardiovascular outcomes depends on the location of the mineral deposition. Intimal calcification reflects atherosclerosis plaque burden and is a predictor of cardiovascular events and mortality (101). Medial calcification induces stiffness of the vessels and left ventricular hypertrophy and can result in heart failure (102). Vascular calcification of the media is more specific to CKD (103), even though all types are common in CKD patients. Valvular calcification causes valve stenosis, and this can contribute to the development of cardiac hypertrophy and valve and heart failure (104).

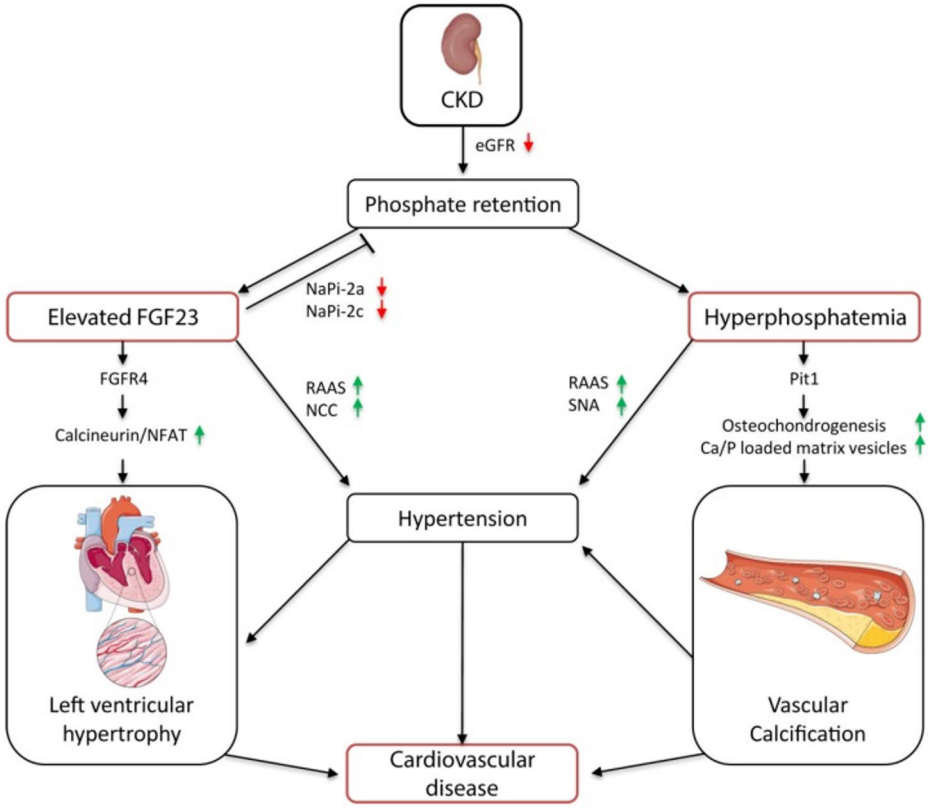

Figure 3. Cardiovascular pathomechanisms of elevated FGF-23 and hyperphosphatemia in chronic kidney disease. Figure reproduced from Toxins (Basel). 2019 Nov 6;11(11):647. Reproduced with permission. FGFR4 is the fibroblast growth factor receptor 4 situated in the heart. NFAT is the nuclear factor of activated T-cells involved in the FGFR4-calcineurin-NFAT signaling. NaPi is the sodium-phosphate transporter. RAAS stands for renin-angiotensin-aldosterone system. NCC is a NaCl cotransporter and Pit-1 is a NaPi cotransporter. SNA means the sympathetic nerve system. Ca=calcium and P = phosphate.

The development of vascular calcification in the CKD population is strongly interconnected with disturbance in mineral and bone metabolism (19). The cardiovascular consequences of elevated FGF-23 and hyperphosphatemia are shown in Figure 3. The development of vascular calcification is an actively cell-regulated pathology, and the understanding of the complex molecular mechanisms regulating this process have increased due to advances in research in this field (105, 106). In the CKD population, a number of calcification inducers are increased, and at the same time, active inhibitors are decreased (107, 108). Inducers of calcification include hypercalcemia as well as increased levels of PTH, uremic toxins and oxidative stress, and, perhaps most importantly, phosphate (105). As discussed above, hyperphosphatemia is strongly associated with vascular calcification and

CVD morbidity and mortality. The mechanisms by which phosphate promotes vascular calcification are linked to the sodium-dependent Pi cotransporter expressed by the vascular smooth cells (109). This cotransporter utilizes phosphate uptake and promote osteochondrogenic phenotype changes, synthesis of bone-related proteins and calcification of the extracellular matrix (110, 111). Phosphate is also a major part of hydroxyapatite, and increases in calcium-phosphate product may also contribute to crystal precipitation in the vasculature (112).

FGF-23 is strongly related to phosphate homeostasis. FGF-23´s role in the pathophysiology of CKD-MBD is more closely explained in Section 2.1.2.2. In addition to hyperphosphatemia, high FGF-23 levels have a central role in pathological cardiovascular remodeling (67, 113). Higher FGF-23 levels are associated with increased risk of developing hypertension (114, 115), and elevated FGF-23 levels might also be a causal factor in the development of hypertension in CKD patients. One theory is that FGF-23, by causing $1.25(OH)_2D$ deficiency, activates the renin-angiotensin-aldosterone system (RAAS), causing hypertension (116). FGF-23 is also thought to activate RAAS by suppressing the angiotensin-converting enzyme 2, which eventually results in increased angiotensin II levels (117). The direct effect of FGF-23 on vascular calcification is controversial. There are both studies that indicate and that rule out an association of elevated FGF-23 levels and vascular calcification (118, 119). There is strong evidence that FGF-23 contributes to the development of left ventricular hypertrophy, especially under uremic conditions, where Klotho defiance is also present (68, 120, 121).

Because both phosphate and FGF-23 contribute to the development of cardiovascular disease in the CKD population by distinct mechanisms, both are considered as therapeutic targets to improve CKD-associated cardiovascular morbidity. FGF-23 has been presented as a novel biomarker of cardiovascular risk (122). Therapeutic options such as blockage of FGFR4 and blockage FGF-23 antibodies in X-linked hypophosphatemia have been considered. The FGFR4 receptor is situated in the heart and is therefore an interesting target. Pre-treatment with anti-FGFR4 can prevent the hypertrophic effect of FGF-23 in vitro (123). Ongoing safety trials of FGFR4 blockade are reported at clinicaltrials.gov: NCT02476019.

2.1.4.1 Detection of vascular calcification

Vascular calcification is associated with, and predictive of, worse prognoses in patients with chronic kidney disease. Several noninvasive imaging techniques can provide useful prognostic information about the degree of vascular calcification in CKD patients. Imaging markers of vascular calcification represent the cumulative results of prolonged exposure to one or several risk factors and might therefore be

better outcome predictors than serological markers (124). KDIGO (1) suggests a lateral abdominal radiograph or an echocardiogram as reasonable alternatives to computed tomography-based imaging for detection of arterial calcification and as a marker of risk in CKD. KDIGO also suggests that patients with detected vascular or valvular calcification should be considered at high cardiovascular risk.

Coronary artery calcification as assessed by computed tomography (CT) represents the golden standard for vascular calcification imaging (125). Non-contrast CT of the heart used to assess coronary calcification is highly sensitive for detection of coronary disease (14, 126), and coronary calcification is associated with cardiovascular disease, myocardial infarction and all-cause mortality in patients with chronic kidney disease, including patients on dialysis (13, 127, 128). Coronary artery calcium score (CAC), is the sum of all areas of calcification in the coronary artery tree and represents the risk for cardiovascular disease in an individual patient, not the risk for plaque rupture (129). However, among patients on dialysis, both the total CAC and the CAC calculated from each epicardial coronary artery predicted a reduced survival (130). In the CKD population, even a minimal amount of calcification is associated with increased risk of cardiovascular events during follow-up (131). However, even though computed tomography (CT) shows good sensitivity and specificity for detecting coronary calcification, simpler imaging tools might be more eligible in clinical practice when screening these patients.

Lateral abdominal X-rays are a simple imaging method that can be used to detect abdominal aortic calcification. KDIGO has since 2009 recommended routine lateral plain radiography in patients with CKD stage 3-5D (1), and it is used in clinical practice to provide information about aortic calcification and cardiovascular risk (132). Abdominal aortic calcification (AAC) increases with age (133) and is also associated with cardiovascular morbidity and cardiovascular outcomes in the CKD population and in patients on dialysis (95, 134-136). AAC correlates with CAC and is an independent predictor of obstructive coronary disease (135, 137, 138).

Standard transthoracic echocardiograms can detect cardiac valve calcification and can discriminate between patients with extensive vascular calcification burden (139). Cardiac valve calcification is common in patients on dialysis, and up to a 40% incidence of either mitral or aortic valve calcification has been shown in patients on hemodialysis (140). Cardiac valve calcification predicts poor outcome in patients on dialysis, but only mitral valve calcification showed significance association with all-cause mortality (140).

In summary, the literature available suggests that detection of vascular calcification as well as detection of vascular calcification progression identify CKD patients with greater risk of cardiovascular events or of death and can help in the management of this patient group.

2.1.4.2 Calciphylaxis

Calciphylaxis is a rare condition typically affecting patients with end-stage kidney disease (141), but it can also occur in earlier stages of kidney disease (141) and in acute kidney injury (142). In rare cases, calciphylaxis can occur in patients with normal kidney function (143). The pathogenesis of calciphylaxis is uncertain but is linked to the disturbance in calcium and phosphate homeostasis in CKD patients and depends on the balance between calcification inducers and inhibitors (144, 145). Calciphylaxis is characterized by occlusion of microvessels in the subcutaneous adipose tissue and in the dermis leading to ischemic skin lesions. Histological analysis suggest that narrowed microvessels lead to chronic ischemia and further occlusion of the vessels leads to infarction and necrosis of the skin (146). The lesions are very painful and the prognosis is in general poor (147). A one-year mortality rate of 45 to 80% has been reported, and sepsis is the leading cause of death. Risk factors for calciphylaxis include female sex, obesity, diabetes mellitus and dependence on dialysis for more than two years. Both severe secondary hyperparathyroidism and oversuppressed PTH due to medication are risk factors for calciphylaxis (141, 148). Hypercalcemia is also an identified risk factor (148). The use of warfarin increases the risk of calciphylaxis (149). Warfarin is a vitamin K antagonist, and there is evidence that endogenous inhibitors of vascular activation also are K-vitamin-dependent for activation, even though the mechanisms are not fully understood (150).

The diagnosis of calciphylaxis is confirmed by skin biopsy, even though the clinical manifestations often evoke the suspicion. The treatment includes sufficient analgesia and wound management including antibiotic and surgical interventions. In addition, avoiding risk factors and treating secondary hyperparathyroidism appropriately, even though the optimal level for PTH in calciphylaxis is unknown, is part of treatment. Intake of vitamin D and calcium substitute should be avoided, and in patients on dialysis, increasing the length or frequency of dialysis sessions might accelerate wound healing (151). Warfarin treatment should be avoided. Sodium thiosulphate has been used as a pharmacotherapeutic agent for the treatment of calciphylaxis with promising results (152). There are several ongoing intervention trials evaluating different treatments, such as vitamin K1 and sodium thiosulphate (clinicaltrials.gov: NCT05018221 and NCT02278692).

2.1.5 Renal osteodystrophy (ROD)

The term renal osteodystrophy is used to describe the large range of bone abnormalities associated with kidney disease and abnormalities in bone and mineral homeostasis. Bone disease resulting from CKD was first noticed in 1890, and already by the 1940s, the term renal osteodystrophy was used (153). During the last centuries, our understanding about the complexity of the pathophysiology of this

bone disease has developed greatly. Renal osteodystrophy is responsible for major morbidity in CKD patients, including fractures. The classification has been updated, and the description and terminology have evolved. Still, one problem has been that different investigators use non-standardized nomenclature. In addition, universal reference values for different stages of the bone disease in different patient groups are lacking, which challenges research settings in this field.

2.1.5.1 Classification of renal osteodystrophy

The classification of renal osteodystrophy is based on determining bone turnover, bone mineralization and bone volume, the TMV classification (19). These parameters are obtained from bone biopsies. The subgroups of renal osteodystrophy can be divided into high-turnover, low-turnover, and normal-turnover bone disease. In the literature, high-turnover bone disease is often referred to as hyperparathyroid bone disease or osteitis fibrosa cystica in severe cases. Low-turnover bone disease is referred to as adynamic bone disease. In addition, the patient can have a mineralization defect or increased or decreased bone volume. In *high-turnover bone disease*, bone formation rate is elevated, and PTH and alkaline phosphatase levels are typically elevated. PTH activates osteoclasts and osteoblasts in the bone and increases calcium and phosphate release from the bone into the circulation. PTH secretion has an anabolic effect on bone, but sustained elevated levels lead to excess bone resorption (154) and increased disordered bone formation (155), which impact both the quality and the quantity of bone. High levels of PTH are also associated with low bone density in CKD (156). Low-turnover bone disease is a medically induced state. In *low-turnover bone disease,* the bone formation rate is low, and PTH levels are also low, leading to excess calcium and phosphate in circulation because of diminished uptake into bone. Both high- and low-turnover bone disease impact the quality and strength of bone and contribute to increased vascular calcification. Histomorphometric findings of each category of renal osteodystrophy are described in detail in Section 2.3.2.3.

2.1.5.2 Renal osteodystrophy and osteoporosis

Fracture risk increases with decreasing kidney function four- to six-fold in end-stage kidney disease (157). Also, many other conditions common in CKD patients such as diabetes, malnutrition and advanced age contribute to fracture risk. Fractures are a major cause of morbidity in the CKD population, and fractures are associated with hospitalization and mortality (158). The World Health Organization defines osteoporosis as a T-score ≤ 2.5; also, the presence of low trauma fracture regardless of bone density can be defined as osteoporosis. However, T-score is not validated in the CKD population.

CKD-related osteoporosis is a state of bone fragility, with reduced skeletal resistance to trauma. Multiple risk factors, both traditional and non-traditional, contribute to the increased fracture risk in CKD patients (159). As the prevalence of CKD increases with age, there is a significant overlap with primary age-related osteoporosis. In addition, oxidative stress caused by kidney insufficiency accelerates the aging process, further increasing the impact on bone. Kidney patients have multiple comorbidities, such as inflammatory diseases and diabetes that impact bone health, as well as medication (160). In kidney disease, the uremic environment includes time spent on dialysis, uremic toxins, chronic metabolic acidosis, ongoing inflammation, and disturbed mineral metabolism, all of which contribute to the metabolic bone disease renal osteodystrophy (159). Abnormal turnover can affect both the quantity and the quality of bone. High turnover causes excess bone resorption and accumulation of unmineralized osteoid (161). In the case of low turnover, which is a medically induced state, both bone resorption and formation are depressed (162), and this combined suppression might be harmful to bone health (163). Bone histomorphometry also reveals lower trabecular volume and reduced trabecular thickness in low-turnover bone (164). Mineralization defects have diminished significantly due to improved dialysis, water purification and discontinuation of aluminum-based phosphate binders (165). Vitamin D deficiency can contribute to a mineralization defect (166), and sufficient phosphate levels are needed for proper mineralization, but this is rarely a problem in CKD patients.

The relationship between bone histomorphometry in renal osteodystrophy and fracture risk is not yet fully established. A small study shows more axial fractures in patients with low-turnover disease and more peripheral fractures in high-turnover (167), but in a recent published study there was no association between subtypes of ROD and fractures (168). However, the incidence of fracture in this study was low, and this may have underpowered the endpoint.

The evaluation and treatment of end-stage kidney disease patients with fractures is challenging. KDIGO guidelines (169) from 2017 recommended that bone density measured by dual-energy X-ray absorptiometry (DXA) can be used in fracture risk assessment, together with other risk factors for osteoporosis. DXA, however, cannot estimate the underlying bone disease. The fracture risk assessment tool (FRAX) can also be used to assess fracture risk in CKD patients, but again, it is not validated in this population.

The treatment of osteoporosis and fractures in ESKD is a matter of contradiction. Also, antifracture agents have not been developed for or adequately studied in patients with mineral and bone metabolism disorder, which is a challenge in clinical decision-making. In addition, data on the effect to prevent fractures is lacking. Treating secondary hyperparathyroidism through control of vitamin D deficiency, hyperphosphatemia, and hyperparathyroidism is recommended before initiating

osteoporosis therapy (170). In patients with CKD grades 1–3, antiresorptive osteoporosis treatment—that is, bisphosphonates—can be used safely. However, in patients with CKD 4–5D, the role of the subgroups of renal osteodystrophy and bone turnover becomes more important. Bone biopsy is not easily available in many units, and reliable biomarkers of turnover are not yet in clinical use. The use of antiresorptive medication in this patient group needs further clarification.

2.2 Biomarkers in renal osteodystrophy

Many available treatments for renal osteodystrophy target bone turnover, such as calcimimetics, bisphosphonates, denosumab and teriparatide. The effects on mineralization and volume are a result of the intervention on osteoclasts and osteoblasts. Bone biopsy is the gold standard for assessing dynamic parameters of bone, but it has several limitations, including taking into consideration that bone formation is a cyclic process (171), that bone biopsy is not easily repeated and that it is not available in every unit. Therefore, circulating biomarkers that measure bone turnover are needed in longitudinal assessment of bone turnover for clinical decision-making to select and initiate treatment and to monitor treatment effects. A few biomarkers of renal osteodystrophy are already in clinical use, such as PTH and bone-specific alkaline phosphatase, even though the ability to reliably estimate high or low turnover is limited. Several biomarkers are used only in clinical studies. CKD diminishes the clearance of many biomarkers or alters their metabolism, which is important to remember. It is also important to remember that even though bone formation and bone resorption usually are in balance in renal osteodystrophy (171, 172), there are stages, such as postmenopause (173), and situations, such as the use of glucocorticoids (174), where this might differ.

2.2.1 Parathormone

Parathormone, PTH is the most frequently used biomarker in clinical practice for estimating bone turnover. In contrast to most other biomarkers of bone turnover, PTH is not produced in bone tissue but in the parathyroid glands. Guidelines in nephrology provide PTH target ranges for CKD grade 5D patients (1); the definition of these ranges is, however, predominantly based on studies that show association between PTH levels and mortality (175). There is limited information about the optimal PTH level in patients not on dialysis. There is also lack of evidence when it comes to what PTH level would be optimal in order to prevent fractures. KDIGO recommends a target range of PTH of 2–9 times the upper normal limit for CKD stage 5D patients. However, PTH´s ability to correctly estimate turnover in bone being in this range is limited (7). In cases of extremely

high or low PTH levels, the accuracy of predicting the underlying bone disorder improves (176, 177). Sprague et al. (7) showed in a study of 492 dialysis patients a sensitivity of 65% and specificity of 67% for low-turnover bone disease when using cut-off levels recommended by KDIGO. The sensitivity for high-turnover bone disease was 37% and specificity of 84%. In a study of 69 CKD stages 4–5D patients, PTH´s sensitivity and specificity to recognize low-turnover bone disease was 70 and 53% and 53 and 96%, respectively, to recognize high-turnover bone disease (178). Still, up-to-date PTH is currently the most useful biomarker for measuring bone turnover in CKD.

2.2.2 Bone-specific alkaline phosphatase

A little less than 50% of circulating alkaline phosphatase is bone-derived alkaline phosphatase (BSAP) (179). BSAP is produced by the osteoblasts, and it serves as a marker of bone turnover and bone formation. Both BSAP and total alkaline phosphatase are associated with both cardiovascular and all-cause mortality and with fractures (180, 181). When it comes to the diagnostic accuracy of BSAP, the evidence is controversial. In recent studies, (7, 178) BSAP seems to recognize low-turnover bone disease slightly better that PTH, but PTH was better in recognizing high-turnover bone disease. The study of Sprague (7) did not support the combined use of PTH and BSAP for better diagnostic accuracy. BSAP might be useful in clinical practice, especially when evaluating patients with low-turnover bone disease.

2.2.3 Tartrate-resistant acid phosphatase

Tartrate-resistant acid phosphatase 5b (TRAP5b) is mainly an osteoclast-derived enzyme (182), which is directly released during the process of bone resorption. TRAP5b is not affected by CKD (174), not even by hemodialysis or peritoneal dialysis (183, 184), and therefore makes it an attractive biomarker for measuring bone resorption in CKD. In the study of Salam and co-workers (178), TRAP5b showed a positive correlation with bone-formation rate. The sensitivity and specificity for recognizing low turnover disease was 89 and 71% and for recognizing high-turnover bone disease 81 and 58%, respectively. Further research is needed to establish whether TRAP5b could work in a clinical setting in the diagnosis of the subtypes of renal osteodystrophy in CKD patients.

2.2.4 Procollagen type 1 N-terminal propeptide

Procollagen type 1 N-terminal propeptide (P1NP) is formed by the osteoblasts and is a marker of bone formation (185). When using P1NP, it is important to know the

specific assay characteristics, thus only intact P1NP assay is reliable in the CKD population (186). P1NP showed a positive correlation with bone-formation rate in the study of Salam and co-workers (178). P1NP diagnostic accuracy to recognize low-turnover bone disease was better than PTH, and P1NP diagnostic accuracy to recognize high turnover was the same as PTH. More research is needed to establish whether P1NP could work also in a clinical setting.

2.2.5 Collagen type 1 crosslinked C-telopeptide

Collagen type 1 crosslinked C-telopeptide (CTX) is a marker of bone resorption and is used in clinical practice in patients with normal kidney function when evaluating treatment response of osteoporosis. Unfortunately, CTX has kinetic characteristics that limit its use in the CKD population. Its removal from the circulation is highly dependent on kidney function (185), and therefore it cannot be recommended as a biomarker in the evaluation of renal osteodystrophy.

2.3 Bone biopsy in renal osteodystrophy

Bone biopsy is the gold standard in the characterization of renal osteodystrophy. Despite this, only a limited number of centers in Europe perform bone biopsies. The bone biopsy procedure is experienced as painful, costly and time consuming, and the histopathological expertise is lacking in many countries (187). In Finland, bone biopsies are available routinely in Turku and Helsinki.

The KDIGO 2017 guideline update (169) on diagnosis, evaluation, prevention and treatment of CKD-MBD suggest that a bone biopsy is indicated in CKD 3–5D patients when the knowledge of the type of ROD impacts treatment decisions. A European expert group of CKD-MBD agreed upon the following clinical indications for performing a bone biopsy (187):

1. low-impact fracture
2. unexplained bone pain prior to parathyroidectomy, to confirm high-turnover bone disease before a surgical intervention
3. unexplained hypercalcemia or radiologic abnormality
4. before initiation of antiresorptive drug, to exclude low-turnover bone disease
5. suspected or proven overload or toxicity from heavy or rare metals

Part of the expert group also suggested a bone biopsy if there is a discordance between PTH and alkaline phosphatase. In addition, KDIGO (169) suggests considering a bone biopsy in cases of suspicion of osteomalacia, inconsistent PTH

trends, unexplained fractures, refractory hypercalcemia or atypical response to standard therapies for elevated PTH. KDIGO guidelines do not suggest a bone biopsy before initiating antiresorptive medicine in CKD stages 3–4. In summary one can state that the goal of taking a bone biopsy would be to determine if the patient has high- or low-turnover disease before treatment decisions, especially before parathyroidectomy, to identify a mineralization defect or to rule out unexplained bone pathology.

2.3.1 Bone biopsy techniques

The preferred site for a bone biopsy when evaluating renal osteodystrophy is the anterior iliac crest. The technique has been proven safe in clinical practice and is associated with minimal morbidity. Anticoagulation medication is disrupted before the biopsy, and routine laboratory tests are obtained, including full blood count and coagulation screen. The bone biopsy is usually performed under local anesthesia in outpatient facilities. Bone biopsies from the anterior iliac crest can be obtained either in a horizontal or a vertical direction. The most widely used approach is the horizontal transiliac approach (187, 188), even though some physicians prefer the vertical approach, which might be safer and the bone samples might be less damaged (189). The horizontal direction provides information about both outer and inner cortices. The vertical direction allows assessment of both subcortical and deep cancellous bone.

Bone biopsies should be obtained with minimal surgical invasiveness but still be sufficient for histomorphometric analysis. Previously, bone samples of ± 8mm in diameter and 1.5–2 cm in length were considered appropriate, but current knowledge indicates that bone samples of a diameter between 4.0 and 4.5 mm may be sufficient. Smaller needles may decrease complication rates, even though they are low even using larger needles (190). Anyhow, operator skills and the use of appropriate instruments determine adequate quality of bone sampling.

2.3.2 Bone histomorphometry

Bone histomorphometry allows the assessment of both qualitative and quantitative qualities of bone. In order to obtain information about dynamic histomorphometric parameters, such as mineralization state, bone formation rate and bone turnover, double labeling of the bone surface with fluorochrome compounds needs to be performed prior to the bone biopsy. As fluorochrome compounds, demeclocycline or tetracycline can be used; these compounds are incorporated into bone. Usually, the schedule consists of a few days of the dosing period, then a drug-free interval of

ten days and then further a few days of the dosing period. The bone biopsy is then performed 7–14 days after the second dosing period.

After the procedure, the samples are immediately transferred to 70% ethanol for fixation (191). Bone sections must be conserved without previous decalcification in order to do complete evaluation of the bone biopsy sample. Thus, after ethanol fixation the samples are dehydrated and embedded in polymethyl methacrylate. Bone histomorphometric measurements are obtained numerically by using computerized image analysis systems, and they should be reported according to the nomenclature recommended by the American Society of Bone and Mineral Research (191). Histomorphometric parameters are derived from primary measurements such as perimeter, thickness and area and can be divided into remodeling parameters and structural parameters (191, 192). Standard bone histomorphometry is typically limited to the analysis of cancellous bone.

KDIGO (19) suggests that bone biopsies in patients with CKD should be characterized by bone turnover, mineralization, and volume (TMV). The exact methods of ensuring these parameters or universal reference values were, however, not reported.

2.3.2.1 Remodeling parameters

Static parameters provide information about the extent of absorption cavities and the amount of unmineralized bone. Osteoid volume (OV/BV, %) means the percent of a given volume of bone tissue that consists of osteoid (unmineralized bone). Osteoid surface (OS/BS, %) is the percent of bone surface covered in osteoid, and osteoid thickness (O.Th) is the thickness for osteoid seams. Eroded surface (ES/BS, %) is the percent of bone surface occupied by resorption cavities. Large resorption cavities are characteristic to hyperparathyroidism. Also, osteoblast and osteoclast surfaces (Ob.S/BS and Oc.S/BS) are static parameters. They reflect the percent of bone surface covered with osteoblasts or osteoclasts.

Dynamic parameters give information about bone-formation rate and bone turnover. These parameters can only be measured after double-labeling with tetracycline or demeclocycline prior to the bone biopsy. Dynamic parameters are measured on the unstained sections, viewed under UV light. The basic parameters follow. Mineralizing surface (MS/BS, %), which is the percent of the bone that displays a tetracycline label, reflects active mineralization. It is a measure of the proportion of the bone surface upon which new mineralized bone is being deposited during a period of tetracycline labeling. Mineral apposition rate (MAR, microm/day) is a measurement of linear rate of new bone deposition. It is measured by calculating the mean distance between double labels divided by the time interval between them. Bone formation rate (BFR/BS microm^3/microm^2/day) is the amount of new bone formed in unit time per

unit of bone surface. It is calculated by multiplying the mineral apposition rate and mineralizing surface (*MS/BS % x MAR um/d)*. Adjusted apposition rate (Aj.AR) indicates the amount of new bone being reported per unit of osteoid surface (when BFR is adjusted to the entire osteoid surface) per unit of time. Mineralization lag time (Mlt/day) represents the average time interval between osteoid formation and its mineralization. It is calculated by dividing the osteoid width by the apposition rate. Activation frequency (Ac.f) estimates bone remodeling rate and is calculated by dividing BFR/BS by wall width. Activation frequency represents the probability that a new remodeling cycle will be initiated on the bone surface at any point.

2.3.2.2 Structural parameters

Structural parameters are related to the three-dimensional geometry of the bone, and they are calculated from measurements of the total bone perimeter and the total area. Structural parameters can provide information about bone mass and structure. The bone structure is associated with bone strength (193). One structural parameter is cancellous bone volume (BV/TV %), which is the percent of marrow cavity that is occupied by cancellous bone. Also trabecular thickness (Tb.Th) and wall width or thickness (W.Th) are structural parameters. W.Th means the distance from the cement line to the marrow of space of completed bone osteons. There is a large error from one biopsy to another when measuring bone volume (194), and even though volume is recommended in the TMV classification of bone biopsies (19), there is no research linking bone volume to the subgroups in renal osteodystrophy; each category may have patients with high or low bone volume (195). However, it is expected that patients with low bone volume have higher fracture risk, even though more research is needed in this area

2.3.2.3 Histomorphometric parameters in renal osteodystrophy

In general, bone abnormalities related to renal osteodystrophy may be categorized under three headings: 1) abnormalities of turnover; 2) abnormalities of bone balance, in other words bone volume, which gives information about whether the patients is losing or gaining bone; and 3) abnormalities in mineralization (19); see Figure 4. In renal osteodystrophy, the patient can have high-turnover bone disease or low-turnover bone disease with or without a mineralization defect. In addition, the patient can, for example, have loss of bone volume that is negative bone balance, as in osteoporosis. These three categories tell the physician whether the patients have abnormal bone remodeling, bone loss or bone gain or abnormalities in mineralization (21).

High-turnover bone disease refers to the term hyperparathyroid bone disease, which is still used in the literature. Severe cases are referred to as osteitis fibrosa

cystica. High-turnover bone disease is defined by increased turnover, demonstrated by high bone formation rate, and increased eroded, osteoid and mineralizing surfaces. In addition, osteoclast and osteoblast activities are elevated, and osteoid width and peritrabecular fibrosis are increased (172, 196-198). The double tetracycline labels are usually seen clearly in high-turnover bone disease; see Figure 5Ab.

Low-turnover bone disease refers to the term adynamic bone disease. Low-turnover bone disease is defined by low turnover, demonstrated by low bone formation and low erosion rates and reduced osteoblast and osteoclast activities (Figure 5Ba). When the bone formation is very slow, the tetracycline labels do not show separation, and it is difficult to tell if a label is a double or a single label (Figure 5Bb). The labels can also be missing when bone formation is very low (199). If a mineralization defect is observed together with high-turnover disease, it is called mixed uremic osteodystrophy. If a mineralization defect is observed together with low-turnover bone disease (200, 201), it is called osteomalacia. The osteoid is thickened when there is a mineralization defect (171, 202).

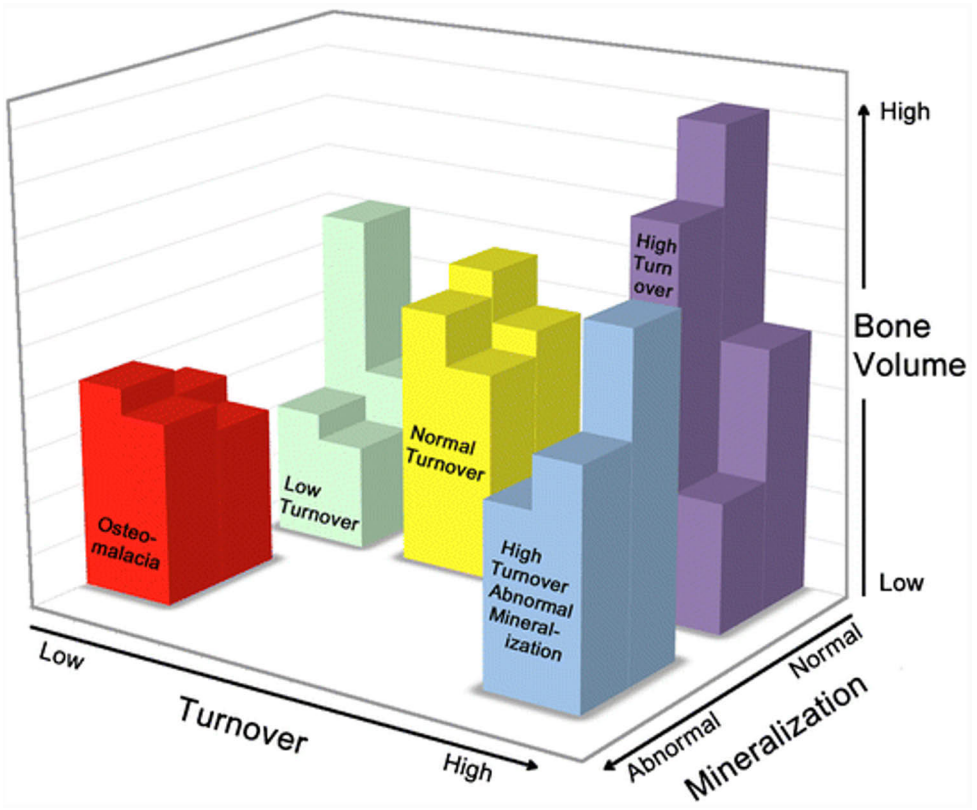

Figure 4. Theoretical construction of the Turnover-Mineralization-Volume framework in renal osteodystrophy. Figure reproduced from Curr Osteoporos Rep. 2017 Jun;15(3):187-193. Reproduced with permission.

2.3.2.4 Histomorphometric reference values

The assessment of normal values of histomorphometric parameters is challenging. Race, gender, and age may cause variance in these parameters, making it difficult to set normal values. The range of different histomorphometric parameters varies in different studies (21, 161, 200, 201, 203-205). In the field of nephrological research, Malluche's reference values are the most cited (21, 197, 204). The static histomorphometric parameters are based on biopsies from 84 normal American subjects, but the dynamic parameters are based on bone biopsies taken from 14 healthy men and 14 healthy women, ages 20–83 years (204). Malluche et al. have suggested reference values for bone turnover, bone balance and bone mineralization (149): 1) bone turnover: Ac.f: 0.49–0.72 /year, BFR 1.8–3.8 $mm^3/mm^2/y$, 2) bone balance: BV/TV 16.8–22.9%, and 3) bone mineralization: Mlt < 50 days, O.th < 20 um. However, in the studies of Recker, for example (200, 201), where both healthy men and women (before and after menopause) underwent bone biopsies, bone-formation rate values were substantial lower than in the studies of Malluche (21, 203, 204). In the studies of Recker and co-workers, altogether 96 healthy men and women underwent biopsies. Many histomorphometric parameters show differences in men and women (164, 206), and the result of statics parameters such as osteoclast and osteoblast activity also show variation with age. In addition, the microarchitecture in different sites of the skeleton shows intra-individual variability (207). Universal reference values for different histomorphometric parameters, especially the dynamic parameters, would be helpful in the comparability of research results in this field.

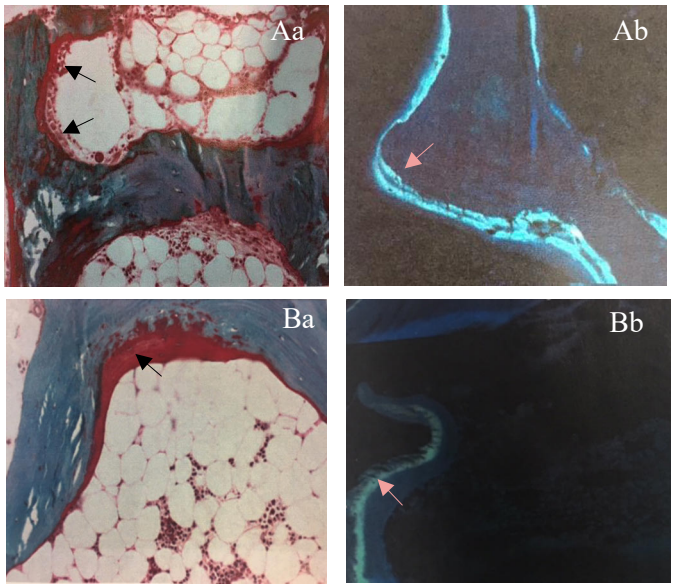

Figure 5. Histomorphometric images of a patient with high turnover bone disease (A) and low-turnover bone disease (B). In high-turnover bone disease, osteoblast activity is increased, and the osteoid thickness is increased (Aa). The double labels are clear (Ab). In low-turnover bone disease, no osteoblasts or osteoclasts can be identified (Ba), and the double labels are blurred (Bb).

Table 2. Strengths and weaknesses of bone biopsy and different imaging modalities used in renal osteodystrophy.

	Strengths	Weaknesses
Bone biopsy	Gold standard Information about bone turnover, mineralization and volume (histomorphometry) Information about bone quality	Information about only one small spot of the skeleton Low reproducibility and high costs Procedural morbidity Is not available in every unit
DXA	Measurement of bone mineral density Estimation of fracture risk Low costs Low radiation	Information about only quantitative measurement of bone, No information about bone quality, such as bone turnover and bone architecture
TBS	Measurement of trabecular microarchitecture Estimation of fracture risk Low costs Low radiation	No information about dynamic parameters such as bone turnover and bone-formation rate
HR-pQCT	Good spatial resolution Differentiation between trabecular and cortical bone Volumetric BMD Low radiation	Costly Static measurement of bone
MRI	Measurement of microarchitecture of bone Measurement of cortical porosity Causes no radiation	Complicated scan protocols, largely replaced by HR-pQCT in research settings
^{18}F-NaF-PET	Noninvasive Measurement of bone turnover Gives a wider picture of the skeleton High reproducibility Fast	Costly Not available in every unit Causes radiation

The terms for different imaging modalities are explained in the text and in the Abbreviations section

2.4 Imaging techniques in renal osteodystrophy

Medical imaging has provided a significant contribution to clinical decision-making, and the development of bone imaging has contributed to the creation of several treatment algorithms (208). Although novel imaging techniques used in the evaluation of renal osteodystrophy are promising in terms of their ability to noninvasively quantify components of ROD, only a few imaging modalities can measure bone turnover. Of the imaging methods presented here, only dual-energy X-ray absorptiometry is used in clinical practice in Finland. Plain radiographical findings, e.g., in hands were previously used in diagnosing severe hyperparathyroid bone disease. This technique is currently

not routinely in clinical use and is not presented here. The other imaging techniques are for the time being used only in research settings.

2.4.1 Dual-energy X-ray absorptiometry

Dual-energy X-ray absorptiometry (DXA) is a valuable diagnostic tool for quantification of bone mineral density (BMD) and evaluation of fracture risk (209). The most common modality is axial measurement of the lumbar spine and the hip using a stationary scan table. DXA produces little radiation and obtains a rapidly acquired two-dimensional image with good resolution. The WHO international reference standard for osteoporosis is a T score of -2.5 or less at the femoral neck in the DXA. An important limitation of DXA is that surrounding calcifications may reduce the accuracy of two-dimensional BMD assessment. In the CKD population, BMD measured by DXA is a measurement of both trabecular and cortical bone. A low BMD may indicate any combination of osteopenia, osteoporosis or changes in bone due to renal osteodystrophy. Still, DXA is a valid tool also recommended by the KDIGO guidelines (169) to assess fracture risk and as a baseline measure before initiating treatment or for monitoring treatment response (209). BMD measured by DXA is predictive of fracture also in the CKD grades 3–5D population (210, 211). BMD does not provide information about bone turnover or the changes of microarchitecture in bone, and therefore, in clinical practice, additional information is needed before initiating treatment.

2.4.2 DXA-derived trabecular bone score

DXA-derived trabecular bone score (TBS) is a recently developed diagnostic tool for assessing the image texture obtained from standard DXA. TBS provides information about trabecular microarchitecture independent of BMD (212). TBS can be derived from available DXA images and requires no additional scanning. An advantage of TBS is that degenerative changes or overlapping vascular calcifications do not interfere with its measurement. Lower TBS at the lumbar spine is associated with higher risk of fragility fractures in patients with GFR less than 60ml/min independently of BMD or other risk factors (213). TBS scores are lower in hemodialysis patients than in controls without osteoporosis (214), and TBS correlates with T- and Z-scores measured by DXA at the lumbar spine and proximal femur in hemodialysis patients (215). Previous studies have demonstrated that TBS associates with trabecular microarchitecture and cortical width measured by bone histomorphometry and high-resolution peripheral computed tomography (216, 217). Still, in the diagnosis and management of osteoporosis in CKD grades 4–5D, further evaluation is needed before implementation of TBS into clinical practice is possible.

2.4.3 High-resolution peripheral computed tomography

High-resolution peripheral computed tomography (HR-pQCT) provides excellent spatial resolution and can differentiate between trabecular and cortical bone using a low radiation dose. HR-pQCT scans are usually performed on the distal tibia and radius. The distal tibia and radius consist mainly of cortical bone. Bone loss in CKD is partially due to cortical bone deterioration, and cortical bone loss can be more rapid than trabecular bone loss in CKD patients (218). HR-pQCT is associated with prevalent fractures in dialysis patients, and the association was stronger than between DXA and fractures (219). Parameters of distal radius HR-pQCT showed a negative correlation with bone-formation rate obtained by bone biopsy in one small study (178). Nevertheless, HR-pQCT is restricted to examination of the distal forearm and leg and requires expensive equipment. Therefore, HR-pQCT is used only in research settings.

2.4.4 Magnetic resonance imaging

Magnetic resonance imaging (MRI) was used in the past for imaging trabecular architecture but has largely been replaced by HR-pQCT due to complicated scan protocols that are not routinely available. MRI's main advantages are the direct acquisition of images and acquisition of functional information from bone, beyond the mineralized component (220). Advanced MRI techniques might provide useful additional information in the future about microarchitecture in bone, hopefully including the CKD population.

2.4.5 ^{18}F-sodium fluoride positron emission tomography

Positron emission tomography (PET) is an imaging method that enables measurement of molecular function in tissues and organs. PET utilizes the distribution of different positron-emitting tracers without interfering with normal body functions. Many different biological molecules can be labeled with short half-lived positron-emitting isotopes, and these labeled molecules can be measured and quantified by using PET scanners.

^{18}F-sodium fluoride positron emission tomography (^{18}F-NaF-PET) enables noninvasive quantitative studies of regional bone turnover (10, 221). ^{18}F-sodium fluoride (^{18}F-NaF) is a bone-seeking tracer, with a half-life of 110 minutes, that provides a unique way of assessing regional bone turnover (222). ^{18}F-fluoride has rapid and high affinity for bone and rapid plasma clearance, resulting in high tissue-to-background ratios and therefore high-quality images. ^{18}F-fluoride incorporates into bone at sites of high osteoblastic activity and newly mineralized bone (223). The highest uptake is seen in trabecular bone. The binding of ^{18}F-fluoride to plasma

protein is minimal, allowing imaging to be performed rather quickly after tracer administration (11). ^{18}F-Na^{-} is produced by 11-MeV proton irradiation of ^{18}O-water using a cyclotron.

There are two types of measurements that can be made with the tracer ^{18}F-NaF: *bone uptake* and *blood clearance to bone.* In order to measure blood clearance, dynamic PET scans are needed. Bone uptake can also be measured from static scans. It is important to understand the difference between these two measurements, because it can affect the interpretation of the results. In molecular imaging, uptake measurements are used most widely in oncology.

Standardized uptake values (SUVs) are common when expressing the PET tracer uptake in tumors (224). SUV is calculated by taking the activity concentration (kBq/ml) in the region of interest (ROI) and normalizing for injected activity and the subject's body weight. In oncology, where the tumors often are heterogeneous, the maximum SUV within the tumor is reported. In studies of metabolic bone disease, the uptake of tracer in bone is more uniform, and it is therefore preferable to express SUV by the mean value in bone, not the maximum. The limitation of measurements of bone uptake is that there is only a finite amount of tracer available to be shared between all competing tissues. Regional bone uptake measurements not only reflect the local demand for tracer at the measurement site but are influenced by competing demands from the other areas of the skeleton (225). In extensive metabolic disease of bone, this can cause flaws in the interpretation of the results.

Blood clearance to bone measurements differ from standardized bone uptake because blood clearance normalizes the rate of uptake of tracer into an organ by its concentration in arterial plasma. In PET studies, blood clearance is expressed as the clearance per mL of tissue (mL/min/mL). For example, in patients with extensive bone disease, such as Paget´s disease, or those being treated with potent anabolic agents such as teriparatide (226, 227), the arterial plasma concentration of tracer is reduced by the increased competition for tracer, and thus the local bone uptake is also reduced. Measurements of blood clearance are free of this limitation because the uptake is expressed relative to the de facto arterial concentration of tracer being delivered. Blood clearance may therefore be more reliable as an indicator of site-specific bone function than SUV (223). Plasma clearance should be used when measuring treatment response in osteoporosis and in cases where the bone disorder is systemic and affects the whole skeleton, as in renal osteodystrophy.

In quantitative ^{18}F-NaF-PET imaging, the Hawkins method was the first molecular imaging technique designed to measure plasma clearance (222). In this method, a 60-minute dynamic PET scan is performed. PET scanners have a limited field of view, approximately 15 centimeters, and therefore the dynamic scan is limited to this sized region of the skeleton—for example, the lumbar spine. When performing dynamic PET scans, a CT scan is also acquired for attenuation correction

of the PET images and for more precise definition of the ROIs. In the Hawkins method, a dynamic scan protocol consisting of twenty-four 5-second, four 30-second and fourteen 240-second time frames is performed, which give adequate time resolution to study the complete bone time activity curve (TAC). In order to calculate blood clearance of fluoride to bone, one must also measure the arterial input function (AIF). AIF can be measured by direct sampling using an arterial blood line (228), which is the most precise method. AIF can also be measured by using an image-derived input function from an ROI placed on the aorta (228) or by using a semi-population method using venous blood samples (229). The AIF and TACs for the various ROIs defined on the dynamic PET scans are combined in order to measure the blood clearance to bone in each ROI. The archived TACs and AIF can be analyzed using the Hawkins method to find the effective plasma flow (K_1) and plasma clearance to the bone K_i in each ROI. The Hawkins method is a compartmental model, where four constants are estimated: K_1 describes effective bone plasma flow to unbound bone, K_2 the reverse transport of tracer from the unbound pool back to plasma, K_3 describes the forwarded transport from unbound bone pool to bone mineral and K_4 the reverse flow; see Figure 6.

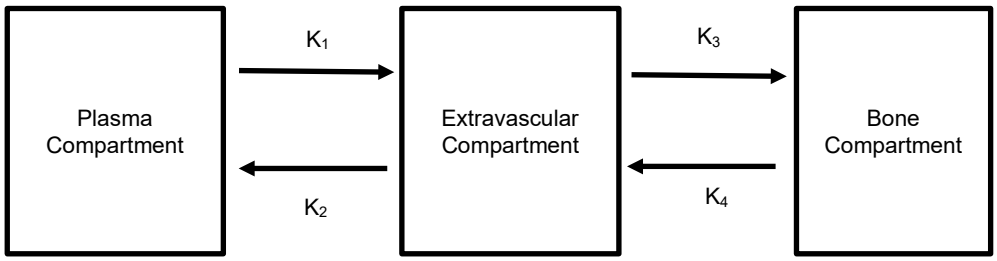

Figure 6.

K_i is calculated using the equation: $K_i = K_1 \times K_3/(K_2 - K_3)$ mL/min/mL (222). K_i stands for the plasma clearance of the tracer to bone. An alternative method to Hawkins is the Patlak analysis (230), which is a more easily performed alternative. The Patlak method still acquires a full dynamic PET scan to obtain a full input function from the time of tracer administration. The Patlak method assumes that K_4 (reverse flow) is small and enables the estimation of K_i (bone plasma clearance) from a straight-line graph.

^{18}F-NaF-PET has previously been used to investigate regional bone formation in patients with osteoporosis (12, 231). ^{18}F-NaF-PET has also shown potential to measure treatment effects of both anabolic and antiresorptive medications in osteoporosis patients with normal kidney function (12, 232). A few studies have evaluated the correlation between histomorphometric parameters from bone biopsy

and fluoride activity in the PET scan (233, 234). In a small study of patients on dialysis with renal osteodystrophy, there was a correlation between dynamic histomorphometric markers such as bone-formation rate and tracer activity in the PET scan (233).

In Table 3, strengths and weaknesses of bone biopsy and different imaging modalities are compared. In Figure 7, the progression of CKD-MBD, bone abnormalities that develop when CKD progresses and the imaging modalities that can be used in the evaluation of ROD are shown.

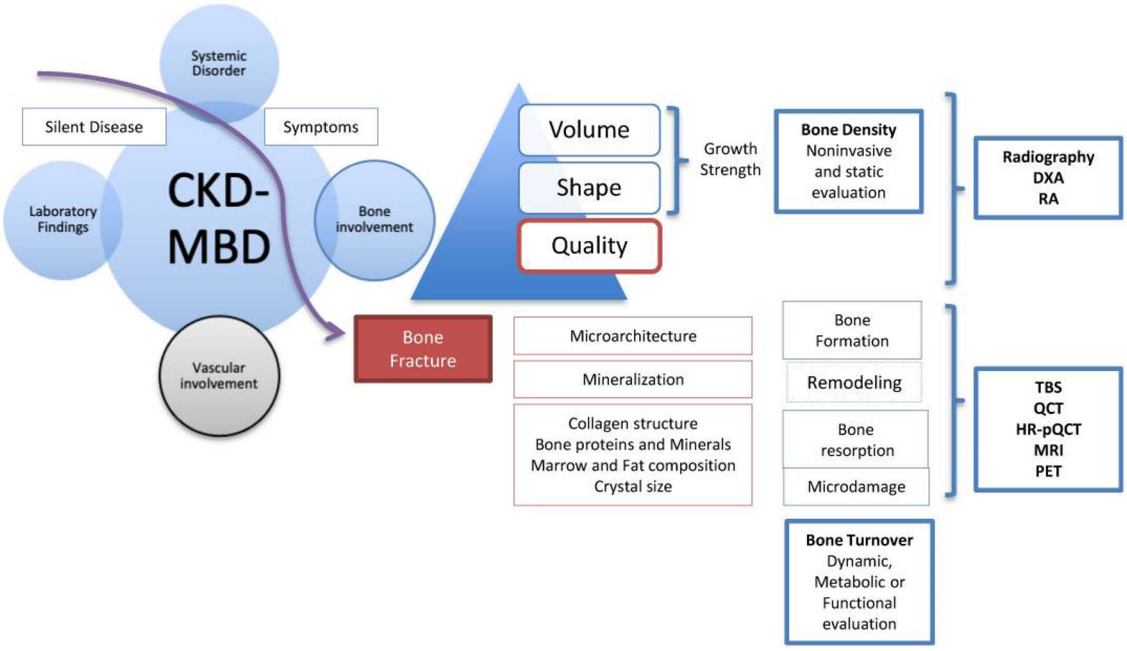

Figure 7. Progression of CKD-MBD from asymptomatic disease to bone fracture, bone parameters and associated imaging techniques. Figure reproduced from Diagnostics (Basel). 2021 Apr 26;11(5):772. Reproduced with permission.

As kidney disease progress, abnormalities in bone homeostasis develop, leading to changes in bone turnover, mineralization and volume, referred to as renal osteodystrophy. Bone density can be measured by DXA in order to estimate bone volume and strength. The microarchitecture of bone can be estimated using TBS or HR-pQCT. Bone turnover can be quantified using ^{18}F-NaF-PET imaging.

CKD-MBD – chronic kidney disease – mineral and bone disorder, DXA – dual-energy X-ray absorptiometry, RA – Radiographic absorptiometry, TBS- Trabecular bone score, QCT – Quantitative computerized tomography, HR-pQCT – High resolution-peripheral quantitative computerized tomography, MRI – Magnetic resonance imaging, PET – Positron emission tomography

2.5 Management of CKD-MBD

The management of patients with chronic kidney disease and disturbance in mineral homeostasis leading to impairment of bone remodeling and mineralization includes both risk assessment and medical treatment. Taking into consideration both the increased fracture risk in patients with chronic kidney disease and the high cardiovascular mortality and morbidity, it is important to assess risk factors in this patient group and optimize treatment. The treatment of osteoporosis and fracture is a complex entity, and in this review, the focus is set on the treatment of secondary hyperparathyroidism. However, there are several ongoing trials evaluating the effect of teriparatide in low-turnover bone disease and the effect of antiresorptive treatment in ESKD patients (clinicaltrials.gov NCT04522622 and NCT02792413). Treatment of secondary hyperparathyroidism is dependent on measurable surrogates of disordered mineral and bone disorder (235), such as calcium, phosphate, PTH and 25-hydroxyvitamin D. KDIGO guidelines recommend treatment decisions based on serial trends of these biomarkers (169), not a single measurement.

A major challenge in the treatment of patients with CKD-MBD is that the ability of the biomarkers in clinical use to estimate underlying bone disorder is limited, and bone biopsies are not easily available. Treatment decisions, especially the treatment of fractures or surgical interventions in CKD 4-5D patients, demand knowledge about the underlying bone disease, especially turnover. Diagnostic tools that could help in the evaluation of the subtypes of renal osteodystrophy would also be helpful in clinical practice.

2.5.1 Treatment of hyperphosphatemia and hypocalcemia

When it comes to the treatment of hyperphosphatemia in patients with CKD G3–5D, there is high-quality evidence that higher concentrations of phosphate are associated with mortality and cardiovascular outcomes (see Section 2.1.3.1) but no data demonstrating that lowering phosphate levels improves cardiovascular outcomes. This includes both treatment with phosphate-lowering agents and dietary restriction. KDIGO guidelines 2017 suggest that the prevention of hyperphosphatemia might be more important than treatment or normalization of phosphate levels, even though research supporting this assumption and the safety of such an approach is lacking. The recommendation is to focus on patients with persistent and progressive hyperphosphatemia aiming towards normal phosphate levels.

2.5.1.1 Dietary phosphate restrictions

Three major sources of phosphate can be recognized in the diet: 1) natural phosphate in unprocessed food (organic phosphate), 2) phosphates added to food during

processing (inorganic phosphate) and 3) phosphates in dietary supplements and medications. Organic phosphate is predominantly found in high-protein foods, such as meat and dairy products (235). Approximately 35–86% of phosphate is absorbed from these sources (236). From plant-derived food, < 50% is absorbed (237). The bioavailability of additives is thought to be nearly 100% (237). Dietary restriction of phosphate should not be obtained by reducing protein intake, as low protein intake worsens patient survival over time (238). Instead, education about the best food choices should be given, towards fresh and homemade foods rather than processed food, which contains excess additives.

2.5.1.2 Phosphate-lowering therapies

There are two types of phosphate binders: calcium-containing phosphate binders and calcium-free phosphate binders. Calcium-containing phosphate binders have raised concerns because there is evidence that the use of calcium-containing phosphate binders might increase calcification in CKD G3–G4 patients (239), and in addition, their effects on phosphate balance is weak (240). A meta-analysis of 140 trials evaluated the potential benefits and harms of different phosphate binders (241). No clinically important benefits of any phosphate binder on cardiovascular death, myocardial infarction, stroke, fracture or coronary calcification were found. In the dialysis population, sevelamer, a calcium-free phosphate binder, might lower all-cause mortality compared to calcium-based binders and causes less treatment-related hypercalcemia. The meta-analysis concluded that the effects of calcium-free phosphate binders on cardiovascular disease, vascular calcification and bone outcomes compared to placebo in CKD G2–G5 patients are uncertain.

Secondary hyperparathyroidism also raises phosphate levels by the impact of PTH releasing phosphate from bone (239), and thereby, treating high levels of PTH also will help the management of hyperphosphatemia (242).

2.5.1.3 Maintaining serum calcium

Epidemiological data linking higher calcium concentrations to increased mortality in the CKD population (243, 244) and novel studies linking higher concentrations of calcium to nonfatal cardiovascular events (245) have resulted in increased awareness of the calcium balance and the treatment of hypocalcemia in CKD-MBD. KDIGO guidelines 2017 (169) suggest an individual approach to the treatment of hypocalcemia, and mild hypocalcemia, especially if it is related to cinacalcet treatment in dialysis patients, does not need to be corrected. However, symptomatic or severe hypocalcemia should be corrected.

2.5.2 Treatment of abnormal PTH levels

KDIGO guidelines 2009 recommends a target range of PTH of 2–9 times the upper normal limit for the assay used for CKD stage 5D (1). However, in patients with CKD G3a to G5, the optimal level of PTH is not known. Elevated PTH levels might be an appropriate adaptive response to declining kidney function, and therefore, treatment should not be based on a single elevated PTH level in patients not yet on dialysis. However, when PTH is progressively rising or persistently above upper normal limits, modifiable factors such as hypocalcemia, hyperphosphatemia, phosphate intake and vitamin D deficiency should be addressed (169)

2.5.2.1 Calcitriol and vitamin D analogs

Calcitriol and other D vitamin analogs have been the primary treatment option for secondary hyperparathyroidism in CKD patients. These agents can successfully suppress PTH levels (246, 247), but again, trials that demonstrate improvement in patient-centered outcomes are lacking. Instead, several studies confirmed that calcitriol and D-vitamin analogs significantly increase the risk of hypercalcemia (248, 249). In CKD G3–G5 patients, KDIGO recommends not to use calcitriol or D-vitamin analogs routinely, but only in cases of severe and progressive secondary hyperparathyroidism (169). In CKD G5D patients, calcitriol and D-vitamin analogs are considered equal to cinacalcet medication. There are still no trials, which demonstrate clear benefits on patient-level outcomes with calcitriol or vitamin D analog treatment.

2.5.2.2 Calcimimetics

Cinacalcet increases the sensitivity of the calcium-sensing receptors in the parathyroid gland, thereby decreasing PTH synthesis and secretion (250). Cinacalcet effectively reduces PTH levels also in severe hyperparathyroidism (251) and simultaneous reductions in serum phosphate and calcium levels. Cinacalcet is a treatment option in patients on dialysis.

It is well established that cinacalcet treatment decreases PTH levels. However, the effects of cinacalcet treatment on cardiovascular morbidity and mortality and all-cause mortality are not that clear. Two randomized controlled trials, ADVANCE (252) and EVOLVE (253), were performed to investigate the impact of cinacalcet on hard clinical outcomes. In the ADVANCE study, which evaluated the effect of cinacalcet + low-dose vitamin D on vascular calcification, the primary outcome was negative, but in a post hoc analysis, calcification progression in the treatment group compared to high-dose vitamin D was slower. The primary outcome of the EVOLVE study, which evaluated whether treatment with cinacalcet in hemodialysis patients

reduces risk of mortality and cardiovascular events, was also negative. Subgroup analysis, however, showed a reduction in death and cardiovascular events in patients over the age of 65. Cinacalcet might also have a positive effect on fracture risk (254).

2.5.2.3 Parathyroidectomy

In patients with CKD stages 3–5D with severe hyperparathyroidism that is not responding to medical and pharmacological treatment, parathyroidectomy is recommended (169). Whether cinacalcet treatment or parathyroidectomy is preferable is not unambiguous (255, 256). A recent meta-analysis suggested a beneficial effect of parathyroidectomy on all-cause and cardiovascular mortality, but future trials are needed that compare outcomes between cinacalcet treatment and parathyroidectomy (257).

3 Aims

The aim of this study was to evaluate whether ^{18}F-sodium fluoride positron emission tomography can measure turnover in dialysis patients with renal osteodystrophy and to evaluate the relationship between bone turnover and vascular calcification. The following research questions were addressed in one or more studies, which are referred to by their Roman numerals:

1) To investigate whether fluoride activity measured by dynamic ^{18}F-NaF PET scan correlates with histomorphometric parameters obtained by bone biopsy (I)

2) To evaluate whether ^{18}F-NaF PET could work as a diagnostic tool in the evaluation of the subgroups of renal osteodystrophy in dialysis patients (I-II, IV)

3) To compare bone turnover–based classification of renal osteodystrophy with the unified classification system that includes parameters of turnover, volume and mineralization and to compare the two classifications to ^{18}F-NaF PET (II)

4) To evaluate the relationship between vascular calcification and bone qualities, such as bone mineral metabolism and bone density (III)

5) To evaluate the relationship between two different ways of measuring fluoride uptake in the ^{18}F-NaF PET scan, bone uptake and plasma clearance to bone (IV)

4 Materials and Methods

4.1 Study population

Thirty-two patients with end-stage renal disease were recruited from the Kidney Center in Turku. The patients received either hemodialysis or peritoneal dialysis. The inclusion criteria included dialysis vintage for at least three months and biochemical abnormalities indicating mineral and bone disorder. These abnormalities included long-term elevated PTH and hyperphosphatemia. The patients were excluded in cases of pregnancy, previous parathyroidectomy or bisphosphonate medication in the past six months. During the study period, ongoing medication for secondary hyperparathyroidism remained unchanged.

For validation of the PET scan, seven healthy subjects were also recruited. Assessment of routine laboratory tests to rule out underlying kidney or bone disease was done. The control group underwent a dynamic and static PET scan; no bone biopsy was performed (I,II). Features of the study group in studies I–IV are shown in Table 3.

Table 3. Features of the study group.

Study	N	Group	Bone biopsy	PET scan
I and II	26	Dialysis patients	26/26	26/26
	7	Healthy controls	0/7	7/7
III	32	Dialysis patients	28/32 in two patients only static measurements	31/32
IV	28	Dialysis patients	26/28	28/28

Table 4. Disease characteristics and medication of the whole study group.

No. of patients	**32**
Female sex (%)	13 (41)
Age, years (median, range)	66 (37–83)
History of diabetes (type I and II) (%)	12 (38)
History of cardiovascular disease (%)	19 (59)
History of myocardial infarction (%)	6 (19)
Dialysis vintage, months (median, IQR)	10 (6–30)
Dialysis modality (PD/HD) (%)	50/50
Cause of ESRD	
Diabetic nephropathy (%)	11 (34)
Hypertension/arteriosclerosis (%)	4 (13)
Polycystic kidney disease (%)	7 (22)
Glomerulonephritis (%)	6 (19)
Other/unknown (%)	4 (13)
Laboratory parameters	
fS-calcium-ion 1.16 mmol/l–1.30 mmol/l (mean, SD))	1.17 (0.08)
fP-phosphorus 0.71–1.23 mmol/l (median, IQR)	1.68 (0.48)
fP-iPTH 15–65 ng/l (median, IQR)	319 (188–508)
P- D-25 > 50 nmol/l (median, IQR)	70 (49–95)
S- D- 1.25 37–216 pmol/l (median, IQR)	31 (24–52)
P-tALP 35–105 U/l (median, IQR)	84 (57–128)
Medication	
Calcimimetic (%)	5 (16)
Alfacalcidol, Paricalcitol (%)	21 (66)
Calcium carbonate (%)	28 (88)
Cholecalciferol (%)	29 (91)
Sevelamer/lanthanum carbonate (%)	18 (56)
Corticosteroid (%)	2 (6)

Data are presented as mean (SD) for normal distribution variables or median (interquartile range) for non-normal distribution variables. Modified from Aaltonen et al 2020 (I)

4.2 Clinical study design

This study was a cross-sectional cohort. All the participants underwent a dynamic and static ^{18}F-NaF-PET scan. Before the dynamic scan, a CT scan for attenuation was obtained, and after that a CT scan of the heart for estimating calcification score of the coronary arteries. The injection of ^{18}F-NaF was given simultaneously with the initiation of the dynamic PET scan. A 60-minute dynamic PET scan was done, followed by a 10-minute static PET scan.

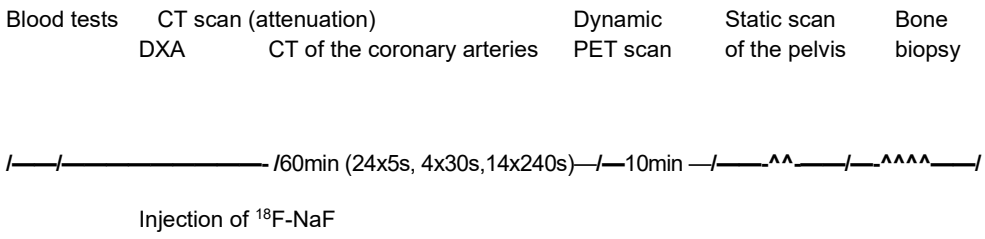

Figure 8. General study outline.

A bone biopsy was performed within 4–6 weeks after the PET scan. The bone biopsy was performed as a part of the study protocol. Dual-energy X-ray was done within one year of the PET scan (III). Aortic calcification score was collected from medical records and was used if the scan was done within two years of the PET scan (III).

4.3 Laboratory assessment

The laboratory tests and biochemical markers were obtained in the morning before dialysis sessions or on the morning of the bone biopsy. In all study participants, excluding the control group, serum ionized calcium, alkaline phosphatase, phosphate, 25-hydroxyvitamin D, 1.25-dihydroxyvitamin D, intact parathyroid hormone, albumin, acid-base balance, full blood count, and creatinine were performed. In addition, a coagulation status including full blood count, activated partial thromboplastin time (APTT) and the international normalized ratio (INR) was obtained prior to the bone biopsy. The laboratory tests were performed, and analysed by the laboratory of Turku University Hospital.

4.4 Bone biopsy and histomorphometry

A bone biopsy was obtained from the anterior iliac crest vertically under local anesthesia. The bone biopsies were performed in the outpatient clinic in Turku University Hospital. A SnareCoil Mermaid Medical RBN-86 8Gx15cm needle (Mermaid Medical Inc., USA) was used to obtain the bone biopsy. All the patients received oxycodone 10 milligram per os one hour before the procedure. Double labelling was achieved by tetracycline. Tetracycline 500 milligrams was administered three times a day for two days, followed by a ten-day drug-free interval, followed by a further two days of administration of tetracycline. The bone biopsy was performed 7–10 days after the second label.

The bone biopsies were fixed in 70% ethanol immediately after the procedure and transported to the Musculoskeletal Research Unit of Kuopio, where the histomorphometric analyses are done. The biopsies were first embedded in 70%

ethanol for at least 48h, then moved to stronger ethanol solutions before embedding in polymethyl methacrylate. The samples where then cut into 5-µm thick sections and stained with modified Masson-Goldner trichrome stain for static parameters. For the dynamic parameters, unstained sections were used. A semiautomatic image analyzer was used for analyzing all histomorphometric parameters (Bioquant Osteo II, Bioquant Image Analysis Corporation, Nashville, TN, USA).

Histomorphometric markers, both structural and remodeling parameters, were measured, including static and dynamic histomorphometric parameters. In cases of single tetracycline labels, the ASBMR Histomorphometry Nomenclature Committee recommendation for single labels was used (191), and a value for MAR of 0.3 µm/day was used when calculating BFR. All the bone biopsies were analysed by an independent histomorphometrist, who was blinded to the PET-results and to the clinical history and detail of the study.

Two ways of classifying the subgroups of renal osteodystrophy were used: bone turnover–based and TMV-based classification of ROD. In the bone turnover–based classification, Malluche's reference values of bone turnover was used (I). In the unified TMV–based classification system, the whole histopathological picture was evaluated, i.e., bone formation rate, activation frequency and mineralized surfaces as well as osteoclast and osteoblast activities, eroded surfaces, osteoid width and the existence of peritrabecular fibrosis (19). Analysis was done by an experienced histomorphometrist (H.Kröger) (I,II). In bone turnover –based classification of ROD, bone turnover was classified as normal when Ac.f was between 0.49 and 0.72/year and/or BFR/BS was 18.0–38.0 µm/year (21, 203, 204). In the unified TMV classification of ROD, the values for normal turnover were set based on the results of Recker et al. (200, 201). The range for normal turnover in men was Ac.f 0.12–0.6 and BFR/BS 3.6–18.8 µm/year; in postmenopausal women, Ac.f 0.11–0.49/year and BFR/BS 6–22 µm/year; and in premenopausal women, Ac.f 0.04–0.26/year and BFR/BS 3–13 µm/year.

4.5 ^{18}F-sodium fluoride positron emission tomography

The PET scans were performed in the Turku PET Centre using a Discovery VCT scanner (GE Healthcare). The production of ^{18}F-fluoride, [18F]F− was done by 11-MeV proton irradiation of ^{18}O-water using a cyclotron. The quality control tests of the tracer ^{18}F-NaF are conformed to the European Pharmacopeia.

The study subjects were positioned supine, so that the lumbar vertebra was in the field of view. The width of the dynamic scanner is 15 centimeters. A cannula was inserted in a peripheral vein for injection of the tracer. A 60-minute dynamic scan of the lumbar spine (L1–L4) was done, followed by a 10-minute static scan of the pelvis. An intravenous injection of 200 MBq ^{18}F-NaF was given simultaneously as

the dynamic PET scan was initiated. The dynamic PET scan consisted of twenty-four 5-second, four 30-second and fourteen 240-second time frames. In addition, low-dose CT scans were done for attenuation correction and image segmentation.

4.5.1 Region of interest

In order to generate bone-specific time-activity curves (TACs) (kilo becquerels per milliliter), we manually drew the region of interest (ROI) in the lumbar spine. Images from the attenuation CT were fused with the PET images for optimizing the correct anatomic location.

ROIs were defined by drawing an ROI within each vertebral body (L1–L4), avoiding the end-plates and disk space. In the static PET scan of the pelvis, we drew ROIs on the iliac crest on both the left and the right side, in the region from which the bone biopsy was later obtained. The mean values for the right and the left ROI where reported. The ROIs of the lumbar spine and the iliac crest are shown in Figure 9.

The picture frames and the activity of the injected tracer ^{18}F-NaF, were determined together with the physicist in charge of the VCT scanner to ensure that the reconstruction produced quantitative image voxel values in all time frames. Images were reconstructed by filtered back-projection resulting in 44 x 3.27 mm slices for each frame. CARIMAS, a medical image analysis software invented in

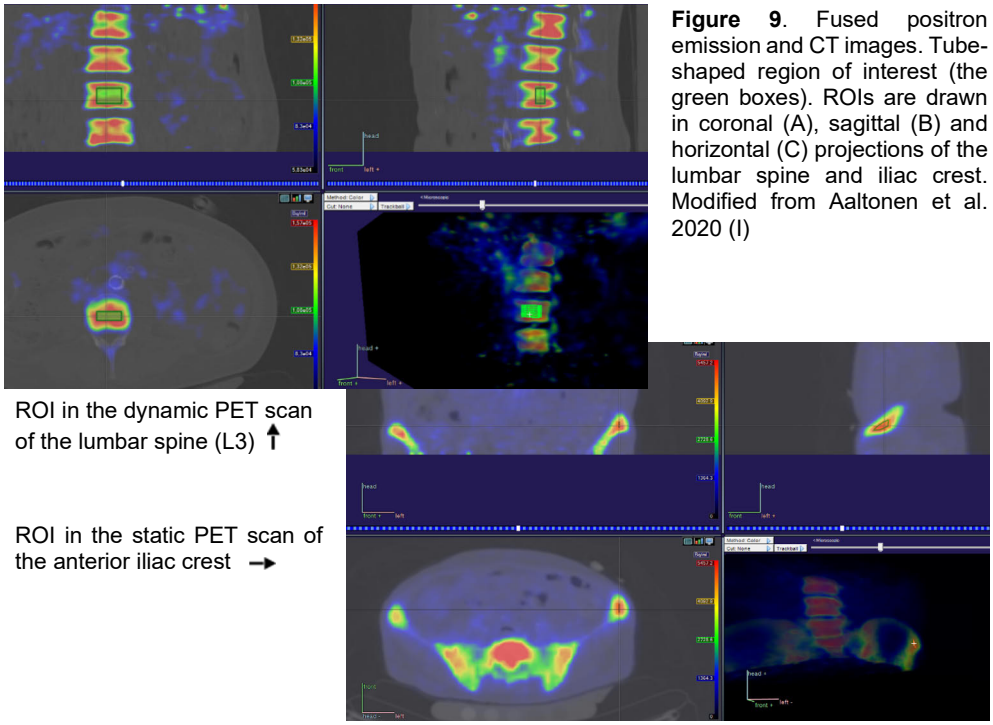

Figure 9. Fused positron emission and CT images. Tube-shaped region of interest (the green boxes). ROIs are drawn in coronal (A), sagittal (B) and horizontal (C) projections of the lumbar spine and iliac crest. Modified from Aaltonen et al. 2020 (I)

Turku PET Centre to facilitate the interpretation of experimental PET scans (downloadable at https://turkupetcentre.fi/carimas/carimasce/), was used for analyzing the images (Figure 9).

4.5.2 Arterial input function

It is necessary to measure the arterial input function in order to calculate plasma clearance of fluoride to bone. In this study we used blood clearance of fluoride to bone. [^{18}F]F$^-$ in plasma and blood cells is in balance, and results obtained using plasma and blood input correlate perfectly. We used an image-derived input function (AIF) by placing an ROI over the abdominal aorta (258). Extra caution was exercised when drawing the aorta ROI, because image-derived AIFs can present technical challenges.

4.5.3 Patlak graphical analysis

Patlak analysis was used to estimate the blood clearance off [^{18}F]F$^-$ to bone, that is, the net influx rate, K_i from the dynamic PET scans. Graphical analysis for a three-compartment model as described by Hawkins was used (222) to calculate the fluoride bone influx rate. In Patlak analysis (230), the fluoride to bone rate, K_i, is estimated based on the following equation:

$$\frac{C_t(t)}{C_b(t)} = K_i \left[\frac{\int_0^t C_b(t)dt}{C_b(t)} \right] + V$$

Tissue activity concentration is $C_t(t)$ at time t measured using the ROI approach. The blood concentration of the tracer is $C_b(t)$ and V is the effective distribution volume of the tracer; mL/mL. K_i (mL/min/mL) is the net uptake of fluoride to bone, assuming that fluoride is irreversibly bound to the bone. The Patlak method assumes that K_4 (reverse flow) is small and enables the estimation of K_i (bone plasma clearance) from a straight-line graph (Figure 10).

Figure 10. Patlak graphical analysis estimating K_i from a straight-line graph in a 60-minute dynamic PET scan. Modified from Aaltonen et al. (IV).

Fractional uptake rate (FUR), which is an approximation of Patlak K_i (259), was calculated for the static scan of the pelvis. FUR is calculated by dividing the bone activity concentration by area-under-curve of blood activity from ^{18}F-fluoride administration time to the time of static scan. Activity measurements were corrected for radioactive decay to the time of injection.

4.5.4 Standardized bone uptake values (IV)

Standardized uptake value (SUV) measurements provide a simple method of quantifying [^{18}F]F$^-$ uptake to bone. This method does not require dynamic scans or knowledge of the AIF (258). SUV was calculated using the mean activity concentration within the ROIs of L1–L4 in the lumbar spine. Bone uptake (SUV) of [^{18}F]NaF was estimated by the following formula:

$$SUV = \frac{C_t(t)}{ID/m}$$

$C_t(t)$ stands for the mean tracer activity within the ROI, *ID* is the injected dose and m is the body weight of the patient.

4.6 Arterial calcification (III)

4.6.1 Abdominal aortic calcification score

In order to estimate the abdominal aortic calcification (AAC) score, lateral lumbar radiography that included the abdominal aorta was performed using standard radiographic equipment. The scoring system described by Kauppila et al. (133) was used to calculate the AAC score. In this method, the posterior and anterior prospects of the abdominal aorta are divided into four segments; this division is bound by the first four lumbar vertebrae (L1–L4). A total of eight segments are evaluated, both the anterior and the posterior walls of the aorta. The calcification was graded 0, 1, 2 or 3, which means that the total score could range from 0–24 when the severity score for the anterior and posterior walls of the aorta were summed. All the radiographs were analysed by two independent researchers. The mean score was used in the analysis.

4.6.2 Coronary artery calcification score

Before initiation of the ^{18}F-NaF-PET scan a computed tomography (CT) of the heart was done on all the participants. CT scans were performed using a GE Discovery VCT 48 slices CT/PET device (GE healthcare). For calculation of the coronary artery

calcification (CAC) score, the method presented by Agatston et al. (260) was used. In this method, the calcification score for each coronary artery is calculated, and the score is expressed in Agatston units (AU). In the absence of CAC, Agatston score is 0 and in the presence of CAC Agatston score is 1 or greater. CAC grade is reported as 0, 1–100 (mild), 101–400 (moderate), or >400 (severe).

4.7 Dual-energy X-ray absorptiometry (III)

Dual-energy X-ray absorptiometry (DXA) is an X-ray based imaging method that is widely used in the diagnosis of osteoporosis (261). Bone mineral density (BMD) was measured from the proximal femur (femoral neck) and the lumbar spine (L1–L4). A DXA imaging device (Hologic QDR 4500C, Hologic Inc., USA) was used. We reported BMD as grams per centimeter. The results of individual patients were reported as T-scores.

4.8 Statistical analysis

SAS 9.4 for windows and JMP Pro 13 and 14 were used for statistical analysis for background variables. Characteristics of the study population were expressed as mean and standard deviation (SD) and/or median or range and interquartile range (IQR). Normality tests for fluoride activity in the ^{18}F-NaF PET scan and bone histomorphometric parameters were done both visually and together with the Shapiro-Wilk test. Nonparametric statistical testing was used if the parameters failed the normality test.

For estimating the correlation between histomorphometric parameters and fluoride activity, the Spearman rank correlation test was used (I). For estimating the difference between means in different groups, we used one-way analysis of variance (ANOVA) after logarithm transformation (I, II), and for pairwise comparison of different groups, we used Tukey's method (II). Fluoride activity in the PET scan and histomorphometric parameters were compared based on turnover using the Wilcoxon test (I, II, IV).

The receiver operating characteristics (ROC) curve for log-transformed data were assessed, and based on the ROC curve, we obtained the area under the curve (AUC) and calculated sensitivity, specificity, and positive and negative predictive values. AUC of 0.6–0.7 was considered poor, 0.7–0.8 fair, 0.8–0.9 good and 0.9–1 excellent (I, II). Kappa statistics were calculated to estimate the reliability of two different methods, ^{18}F-NaF PET and bone histomorphometry (II).

Association between aortic and coronary calcification score (AAC and CAC) and different bone qualities was studied with a linear model including relevant background variables in the model (gender, age, smoking, calcium carbonate

medication, dialysis vintage and diabetes). Assumptions for the model were checked using studentized residuals. Logarithmic transformation was used for some variables to fulfill the model assumptions. Pearson correlation coefficients were calculated between two continuous variables (III). A p value of 0.05 (two-tailed) or less was considered statistically significant.

4.9 Ethical considerations

This study was conducted in accordance with the Declaration of Helsinki as revised in 1964. The study was approved by the Ethics Committee of the Hospital District of South Western Finland. All subjects gave written informed consent. The study is registered in clinicaltrials.gov protocol registration and result system (NCT02967042).

5 Results

5.1 Correlation between ^{18}F-NaF-PET and bone histomorphometry (I)

In study I, 26 patients underwent a bone biopsy and an ^{18}F-NaF-PET scan. The average age was 68 and an equal number of females and males participated. Fifty percent were on hemodialysis, and 50% on peritoneal dialysis. Average dialysis vintage was 12 months. Based on bone histomorphometry, using Malluche´s reference values of normal bone turnover, 12% had high-turnover bone disease, 23% normal-turnover and 65% low-turnover bone disease. In the ^{18}F-NaF-PET scan, turnover was defined as high if fluoride activity was 0.055 mL/min/mL or higher and as low if fluoride activity was 0.040 mL/min/mL or lower. The cut-off values of fluoride activity in the PET scan were set according to the reference values of turnover based on the studies of Malluche. The flow diagram of patients is shown in Figure 11.

Fluoride activity in the ^{18}F-NaF-PET scan was measured in the lumbar spine and at the iliac crest. A mean value of the fluoride activity in L1–L4 was calculated, $K_{i\ mean}$, as was the mean value for the fluoride activity in the left and right anterior iliac crest, $FUR_{mean.}$ $K_{i\ mean}$ and FUR_{mean} were directly compared to both static and dynamic histomorphometric variables using the Spearman rank correlation test.

As dynamic variables, we used bone formation rate (BFR/BS), activation frequency (Ac.f), and mineralized surfaces (MS/BS) and mineralization lag time (Mlt). As static variables, we used osteoclast and osteoblast activities (Oc.S/BS and Ob.S/BS) and eroded surfaces (ES/BS). There was a statistically significant correlation between fluoride activity in the lumbar spine and anterior iliac crest and a majority of the static and dynamic variables measured (Table 5.) In Figure 12 are shown the correlations between $K_{i\ mean}$ and BFR and FUR_{mean} and Ac.f.

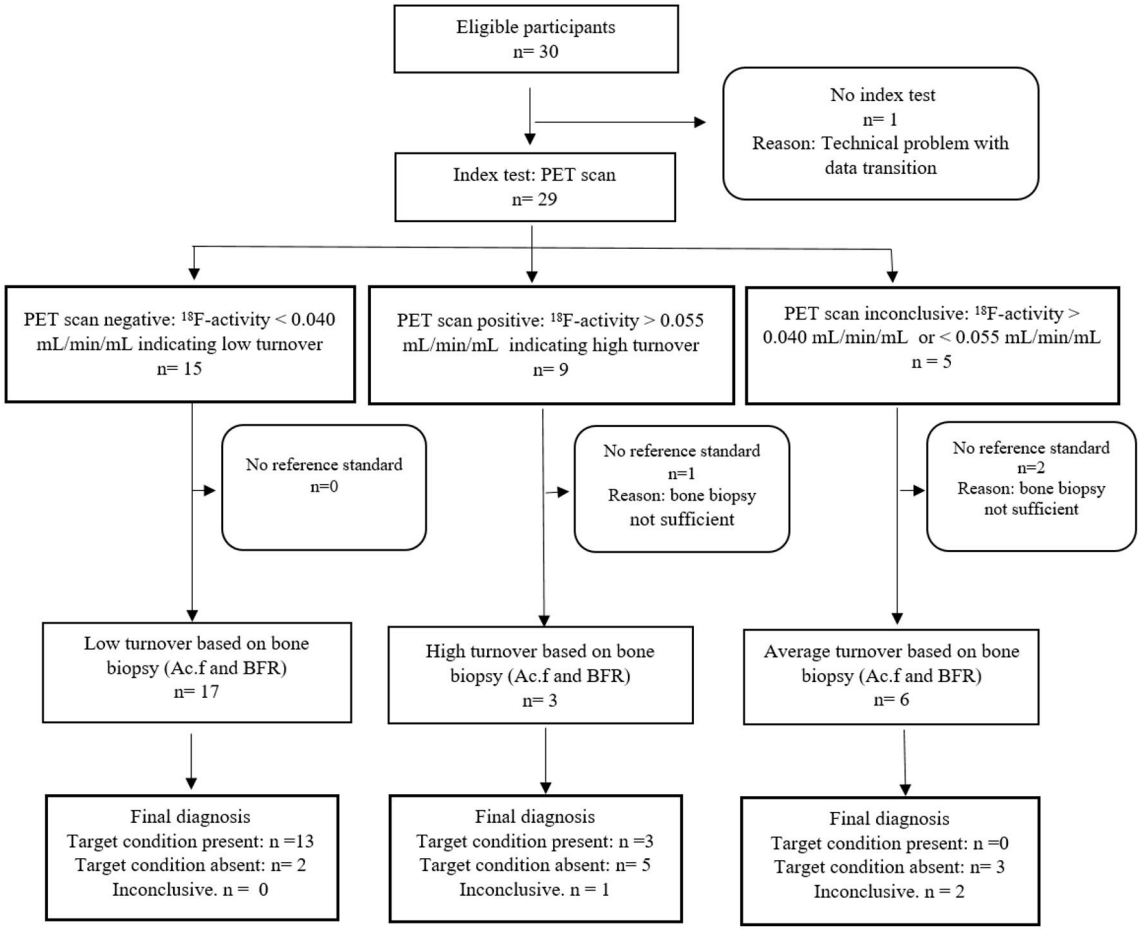

Figure 11. Flow chart of the patients. Modified from Aaltonen et al. 2020 (I).

Table 5. Correlation between histomorphometric markers and fluoride activity in the PET scan.

No. of patients = 26	$K_{i\ mean}$ (L1-L4)	FUR_{mean} (iliac crest)
Bone formation rate ($\mu m^3/\mu m^2$/1 day)	r_s= 0.63, p < 0.001	r_s = 0.66, p < 0.001
Erosion surface per bone surface (µm/day)	r_s = 0.57, p = 0.002	r_s = 0.60, p = 0.002
Osteoclast surface per bone surface (%)	r_s = 0.62, P < 0.001	r_s = 0.62, p < 0.001
Osteoblast surface per bone surface (%)	r_s = 0.49, p = 0.01	r_s = 0.58, p = 0.003
Mineralized surface per bone surface	r_s= 0.55, p = 0.003	r_s= 0.57, p = 0.003
Activation frequency (/year)	r_s = 0.60, p = 0.002	r_s = 0.65, p < 0.001
Osteoid thickness (Lm)	p = 0.10	r_s = 0.48, p = 0.01
Osteoid volume per bone volume (%)	p = 0.16	p = 0.10
Mineralization lag time (day)	p = 0.16	p = 0.25

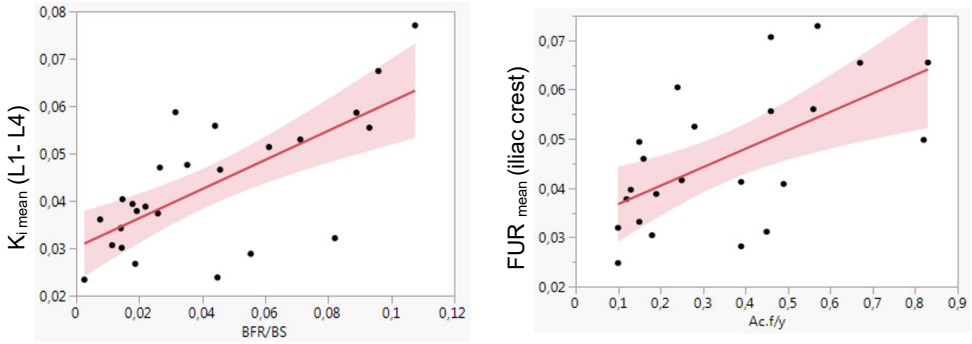

Figure 12. Correlation between fluoride activity in the PET scan and dynamic histomorphometric parameters. Modified from Aaltonen et al. 2020 (I).

In order to test ^{18}F-NaF-PET's diagnostic accuracy to discriminate low-turnover bone disease from non-low-turnover, we defined the ROC curve after equalizing the study group for parametric measurements using a natural logarithm. In ROC analysis for discriminating low turnover from non-low turnover in patients on dialysis, fluoride activity in the PET scan had an AUC of 0.82. The sensitivity was 76% and specificity 78%. In Figure 13 are shown images of the lumbar spine of patients with high-turnover bone disease, normal bone turnover and low-turnover bone disease.

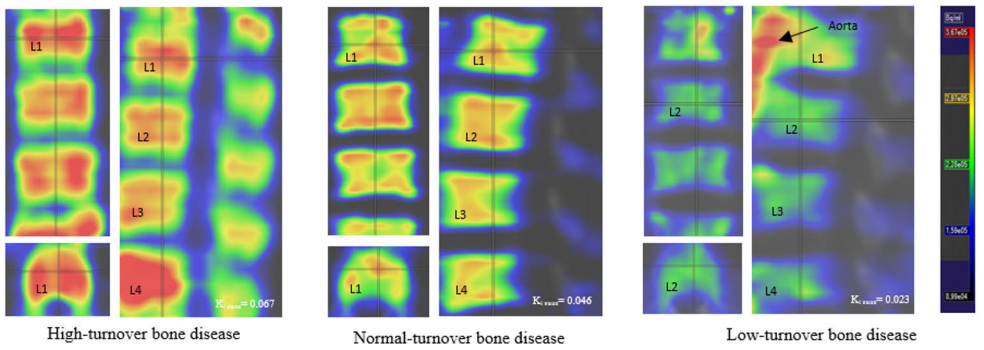

Figure 13. Images of patients with high, normal and low bone turnover using Carimas image analysis software. Modified from Aaltonen et al. 2020 (I).

5.2 Comparison between bone turnover–based and TMV-based classification of renal osteodystrophy (II)

The second publication focused on comparing ways of classifying renal osteodystrophy and how these classifications correlate with the fluoride activity in the PET scan. All the bone biopsies were re-evaluated. The study population was the same as in article I, except for one more included patient and one excluded by the histomorphometrist (the bone biopsy did not reach required standards). The classification of the subgroups of renal osteodystrophy was done based on Malluche's reference values, turnover-based classification of ROD, and the unified TMV–based classification, where the range of normal turnover was set based on the results of the group of Recker et al. In bone turnover–based classification of ROD, 61% had low-turnover bone disease and 12% had high-turnover bone disease. In unified TMV–based classification of ROD, 23% had low-turnover bone disease/adynamic bone disease and 42% had high-turnover/hyperparathyroid bone disease; see Figure 14.

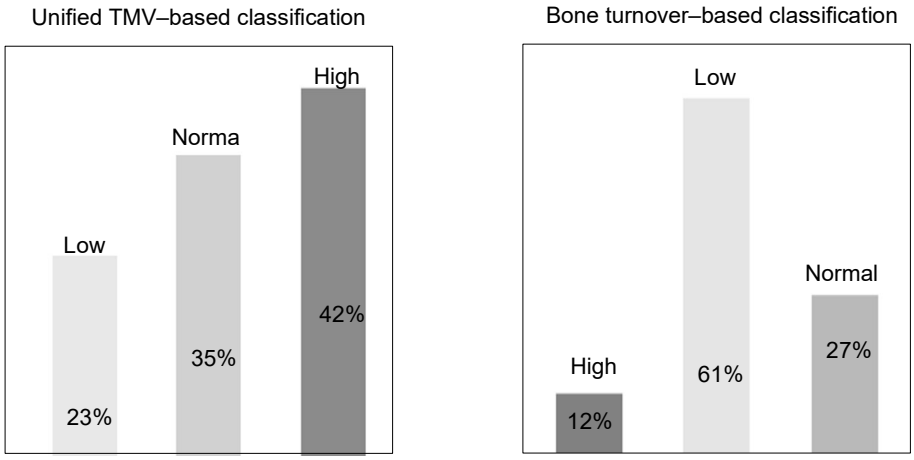

Figure 14. Distribution of high-, normal- and low-turnover bone disease in unified TMV–based classification of ROD and in bone turnover–based classification of ROD (II).

In Table 6 are shown histomorphometric parameters and fluoride activity in the PET scan in the lumbar spine and at the anterior iliac crest according to the classification of ROD in both groups. Even though the distribution of the subgroups of ROD differ in the two classification groups, the two classifications are statistically associated with each other. In cases of low bone turnover/adynamic bone disease, when unified TMV–based classification was used, all cases matched, but in cases of

hyperparathyroid bone disease, only three cases of 11 matched. Patients with normal bone turnover/normal bone or mild hyperparathyroid bone disease in the unified TMV–based classification were classified as low turnover when using Malluche's reference values, and patients with high turnover/hyperparathyroid bone disease were classified as normal bone turnover.

Table 6. Imaging and histomorphometric parameters in high-, normal- and low-turnover bone disease.

Unified TMV–based classification	High-turnover hyperparathyroid bone (n=11)	Normal-turnover Mild hyper-parathyroid bone/normal (n=9)	Low-turnover Adynamic bone disease (n=6)	p-value
BFR/BS ($\mu m^3/\mu m^2/y$)	26.0 (20.2–34.0)	9.7 (7.5–16.3)	5.2 (2.3–5.7)	< 0.001
Ac.f (1/year)	0.56 (0.46–0.67)	0.25 (0.16–0.39)	0.13 (0.11–0.17)	<0.001
Erosion surface / bone surface (µm/day)	3.8 (2.8–4.8)	1.9 (0.90–3.2)	1.5 (0.09–2.1)	0.01
Osteoclast surface / bone surface (%)	2.5 (1.4–3.5)	0.9 (0.23–1.31)	0.7 (0.001–1.9)	0.01
Osteoblast surface / bone surface (%)	4.9 (3.2–14.0)	2.9 2.0–4.0)	0.12 (0.001–0.3)	<0.001
Mineralized surface / bone surface	6.6 (5.1–9.5)	3.2 (2.6–6.9)	1.9 (1.4–2.7)	0.002
Osteoid thickness (Lm)	7.4 (6.6–10.0)	5.6 (4.5–6.7)	5.5 (4.9–6.7)	0.02
Osteoid volume / bone volume (%)	5.1 (3.4–6.1)	3.6 (2.1–4.6)	2.6 (2.2–5.2)	0.09
Mineralization lag time(day)	33.8 (25.5–35.9)	44.4 (30.3–79.6)	106.7 (99.6.0–174)	0.009
Mean K_i (L1–L4) mL/min/mL	0.056 (0.051–0.067)	0.039 (0.037–0.047)	0.032 (0.026–0.037)	0.003
Mean FUR (hip) mL/min/mL	0.060 (0.050–0.071)	0.041 (0.035–0.049)	0.032 (0.029–0.038)	0.002

Turnover-based classification	High-turnover (n=3)	Normal-turnover (n=7)	Low-turnover (n=16)	p-value
Bone formation rate ($\mu m^3/\mu m^2$/1 day)	35.0 (33.9–39.3)	24.8 (20.2–30.0)	7.5 (53–12.5)	< 0.001
Activation frequency (/year)	0.82 (0.67–0.83)	0.49 (0.46–0.57)	0.19 (0.15–0.31)	< 0.001
Erosion surface / bone surface (µm/day)	4.0 (2.4–6.9)	3.8 (2.8–4.8)	1.6 (0.7-2.9)	0.03
Osteoclast surface / bone surface (%)	3.5 (1.4–6.7)	2.5 (1.4–3.3)	0.8 (0.11–1.7)	0.02
Osteoblast surface / bone surface (%)	7.2 (3.2–16.9)	4.9 (3.2–14.0)	2.0 (0.2–4.6)	0.005
Mineralized surface / bone surface	9.5 (9.4–10.7)	6.5 (5.1–9.2)	2.9 (2.0–5.5)	0.002
Osteoid thickness (Lm)	8.7 (7.2–10.0)	7.4 (6.1–10.6)	5.7 (5.0–6.8)	0.02
Osteoid volume / bone volume (%)	6.8 (5.5–7.8)	3.5 (3.4–5.7)	3.0 (2.4–4.0)	0.02
Mineralization lag time(day)	31.4 (22.3–34.8)	33.8 (25.5–35.9)	57.6 (33.1–100.5)	0.05
Mean K_i (L1-L4) mL/min/mL	0.067 (0.055–0.077)	0.053 (0.032–0.059)	0.038 (0.031–0.045)	0.02
Mean FUR (hip) mL/min/mL	0.065 (0.050–0.066)	0.056 (0.041–0.073)	0.039 (0.032–0.046)	0.01

In unified TMV–based classification, the reference values for normal turnover (Recker et al., mean ± 1SD) in men was BFR/BS 3.6–18.8 um/y and Ac.f 0.12–0.6; in postmenopausal women BFR/BS 6–22 um/y and Ac.f 0.11–0.49 /y; and in premenopausal women BFR/BS 3–13um/y and Ac.f 0.04–0.26 /y. In turnover-based classification, Malluche's reference values for normal turnover were used: BFR/BS 18–38 um/y and Ac.f 0.49–0.74 /y. $K_{i\ mean}$ (L1–L4) reflects the fluoride activity in the lumbar spine and FUR_{mean} (hip) at the anterior iliac crest. $p < 0.05$ is statistically significant. Modified from Aaltonen et al. 2021 (II).

In Figure 15 is shown the mean fluoride activity in the lumbar spine $K_{i\ mean}$ (L1–L4) in the two classification groups: turnover-based and unified TMV–based classification. In addition, the mean fluoride activity of the control group is shown (Tukey's box-plot figure). The mean fluoride activity of the control group in the lumbar spine was 0.039 (0.038–0.044) mL/min/mL and at the anterior iliac crest (FUR_{mean}) 0.037 (0.032–0.044) mL/min/mL. In the unified TMV–based classification, the mean fluoride activity for normal turnover was 0.039 (0.037–0.047) in the lumbar spine ($K_{i\ mean}$) and 0.041 (0.035–0.049) at the anterior crest (FUR_{mean}). In turnover-based classification, fluoride activity in the lumbar region ($k_{i\ mean}$) for normal turnover was 0.053 (0.032–0.059) and at the anterior iliac crest 0.056 (0.041–0.073).

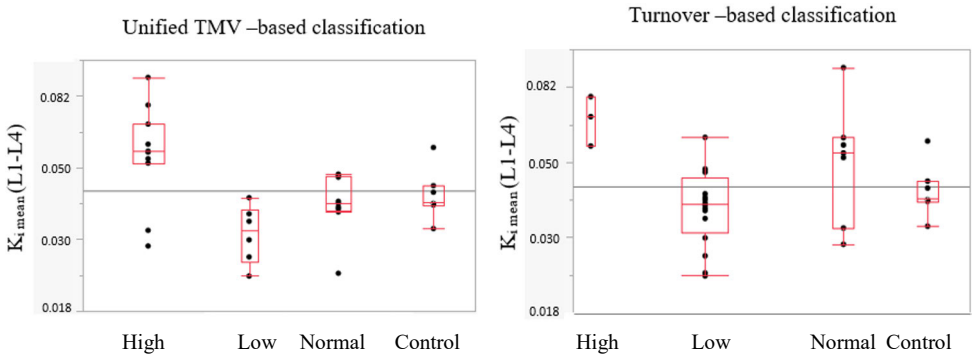

Figure 15. Fluoride activity in the lumbar spine according to unified TMV–based and turnover-based classification of ROD and in the control group. Modified from Aaltonen et al. 2021 (II).

In order to test ^{18}F-NaF-PET as a diagnostic tool in the evaluation of the subgroups of ROD, we defined the ROC curve. High turnover/hyperparathyroid bone disease was defined as fluoride activity higher than the cut-off value 0.055 mL/min/mL. Low turnover/adynamic bone disease was defined as fluoride activity below 0.038 mL/min/mL. We also assessed the ROC curve to test PTH's ability to discriminate between the subgroups of ROD. The cut-off value for PTH to discriminate between high turnover/hyperparathyroid bone disease and other types of ROD was set at 450 ng/ml. The cut-off value for PTH to discriminate between low turnover/adynamic bone disease from other types of ROD was set at 180 ng/ml.

In ROC analysis using unified TMV–based classification of ROD, ^{18}F-NaF-PET´s ability to discriminate between high turnover/hyperparathyroid bone disease and other types of ROD was good. The area under the curve (AUC) was 0.86, sensitivity 82% and specificity 100%. When assessing ROC analysis for ^{18}F-NaF-PET to discriminate between low turnover/adynamic bone disease and non-low-

turnover bone disease, AUC was 0.87, sensitivity 100% and specificity 70% (Table 7a).

In ROC analysis using bone turnover–based classification of ROD using Malluche´s reference values for turnover, the ROC curve could not be defined for patients with high turnover, because of the scarcity of patients. When assessing ROC analysis for ^{18}F-NaF-PET to discriminate between low turnover/adynamic bone disease and non-low-turnover bone disease, AUC was 0.83, sensitivity was 63% and specificity 80% (Table 7b).

In ROC analysis for PTH to discriminate high turnover/hyperparathyroid bone disease from other types of ROD, PTH had an AUC of 0.69, sensitivity was 55% and specificity 87%. When assessing ROC analysis for PTH to discriminate between low turnover/adynamic bone disease and non-low turnover using unified TMV-based classification, PTH had an AUC of 0.78, sensitivity was 67% and specificity 85% (Table 7a and 7b).

Table 7. **a** and **b** ^{18}F-NaF PET´s diagnostic accuracy in low- and high-turnover bone disease.

7a. ^{18}F-NaF PET strength to recognize low turnover	**AUC**	**Criterion**	**Sensitivity %**	**Specificity %**
^{18}F-fluoride activity in the PET scan unified TMV–based	0.87	Cut-off < 0.038 Ml/min/Ml	100%	70%
^{18}F-fluoride activity in the PET scan turnover-based	0.83	Cut-off < 0.038 Ml/min/Ml	63%	80%
PTH – unified TMV–based	0.78	< 185 ng/ml	67%	85%
PTH – turnover-based	0.68	< 185 ng/ml	31%	80%

7b. ^{18}F-NaF PET strength to recognize high turnover	**AUC**	**Criterion**	**Sensitivity %**	**Specificity %**
^{18}F-fluoride activity in the PET scan unified TMV–based	0.86	Cut-off > 0.055 Ml/min/Ml	82%	100%
PTH – unified TMV-based	0.69	> 450ng/ml	55%	87%

Modified from Aaltonen et al. 2021 (II)

5.3 Association between vascular calcification and bone histomorphometry (III)

The study group in the third publication comprised 32 end-stage renal disease patients, of whom 41% were female. 50% were on peritoneal dialysis and 50% in hemodialysis. The average age was 66 years. Thirty-eight percent had diabetes and

22% were smokers; 33% had osteoporotic values in the DXA scan (T-score -2.5 or less). According to histomorphometric parameters, 22% had low turnover/adynamic bone disease, 39% had high turnover/hyperparathyroid bone disease and 39% had normal turnover or mild hyperparathyroid bone disease.

The median AAC score was 8 (range 0–17) and the median CAC was 397 (range 0–1980). CAC score was calculated in all patients, and AAC score was estimated in 24/32 patients. Only 6.3% had CAC scores equal to 0, and as many as 50% had CAC scores higher than 400. Respectively, 12.5% had AAC scores equal to 0 and 62.5% had AAC scores higher than 8/24 (Figure 16). Fifty-nine percent of the study population had a history of cardiovascular disease. Both CAC and AAC were significantly higher in patients with verified cardiovascular disease. Overall, a substantial percent of the study population had severe and extensive atherosclerotic disease.

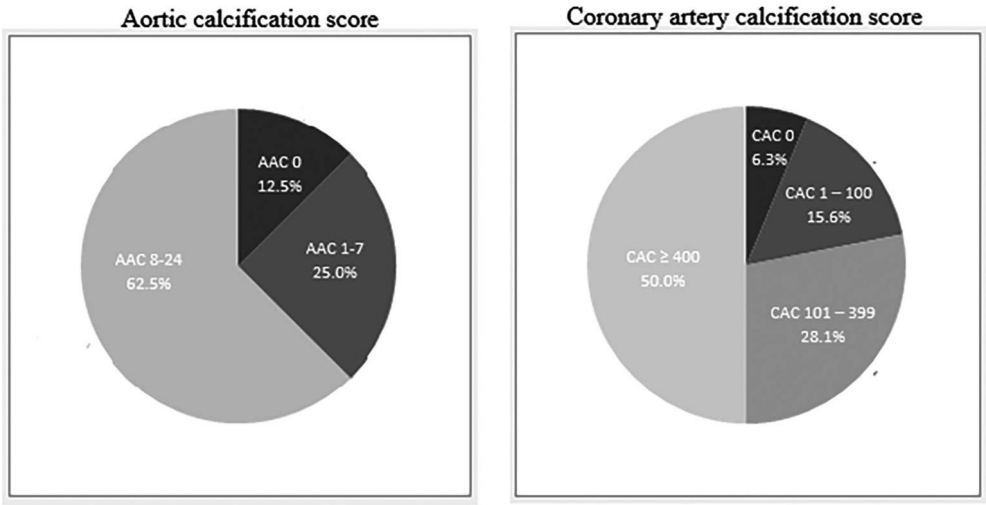

Figure 16. Distribution of aortic calcification and coronary artery scores in the study population. Modified from Aaltonen et al. (III).

There was no difference between fluoride activity measured by ^{18}F-NaF-PET, histomorphometric parameters or in bone density when comparing patients on hemodialysis and peritoneal dialysis, non-diabetic to diabetic patients, or patients with high and low calcification scores.

Association between vascular calcification (AAC and CAC) and bone metabolism measured by ^{18}F-NaF-PET, bone histomorphometry, laboratory parameters and bone density measured by DXA were tested using a model adjusted to age and sex. We tested both log-transformed calcification scores and calcification

scores. We found a positive association between CAC and Ki, adjusted for age and sex, p = 0.01. In addition, a positive association between CAC and PTH, p = 0.04 and between ES/BS and AAC, p = 0.04 was discovered, both adjusted for age and sex. We found no association between calcification scores and any other parameter measured.

5.4 Standardized bone uptake and blood clearance to bone in ^{18}F-NaF-PET scan (IV)

The study population in the fourth publication comprised 28 patients. Dynamic PET scan data were available for 31 patients, but in three patients, static calculations could not be done and they were excluded. As in the third study, 50% were on peritoneal dialysis treatment and 50% on hemodialysis. Median dialysis vintage was 10 months, range 3–94 months. The median coronary calcification score was 266, range 0–1979. Distribution of the subtypes of renal osteodystrophy was the same as in study II: 42% had high-turnover bone disease, 35% normal turnover and 23% low-turnover bone disease.

Pet studies

Blood clearance to bone, $K_{i\ mean}$, was measured in the lumbar spine, L1–L4, and fractional uptake rate, FUR_{mean}, at the anterior iliac crest. These measurements were obtained from the dynamic ^{18}F-NaF-PET scan. In addition, standardized uptake values (SUVs) were measured in both the lumbar spine and at the anterior iliac crest, $SUV_{mean.}$ These parameters were obtained from the static ^{18}F-NaF-PET scan 48–60 minutes from the initiating of the tracer. Both the dynamic and static measurements were compared to histomorphometric parameters using the Spearman rank correlation test. As shown in studies I and II, there was a clear correlation between fluoride activity in the dynamic ^{18}F-NaF-PET scan and histomorphometric parameters. When comparing histomorphometric parameters to SUVs, a weak correlation between SUV_{mean} (L1–L4) and erosion surface (p=0.02, r_s = 0.46) was shown, but no statistically significant correlation with any other parameter.

In order to test a simplified measurement of fluoride activity in the PET scan, we adjusted the fluoride activity measured in the lumbar spine, SUV_{mean} to the mean uptake of fluoride in blood 48–60 minutes from initiation of the dynamic PET scan, resulting in corrected SUV ($SUV_{corr).}$ This mean uptake of fluoride in blood was obtained from the image-derived arterial input function. SUV_{corr} of the lumbar spine correlated significantly with blood clearance to bone, K_i in the lumbar spine, r_s = 0.92 (Figure 17). SUV_{corr} also correlated significantly with histomorphometric parameters (Table 8).

Table 8. Correlation between standardized bone uptake values and histomorphometric parameters.

Histomorphometry	SUV_{mean} L1–L4	SUV_{mean} hip	SUV_{corr}
Bone formation rate	p = 0.23	0.21	r_s = 0.57, p = 0.003
Activation frequency	p = 0.29	0.13	r_s = 0.60, p = 0.002
Osteoclast activity	p = 0.59	0.11	r_s = 0.66, p = 0.008
Osteoblast activity	p = 0.11	0.57	r_s = 0.339, p = 0.05
Erosion surface per bone surface	r_s = 0.45, p = 0.02	r_s = 0.46, p = 0.02	r_s = 0.61, p = 0.001
Mineralized surface per bone surface	p = 0.32	0.23	r_s = 0.61, p = 0.005

Modified from Aaltonen et al. (IV)

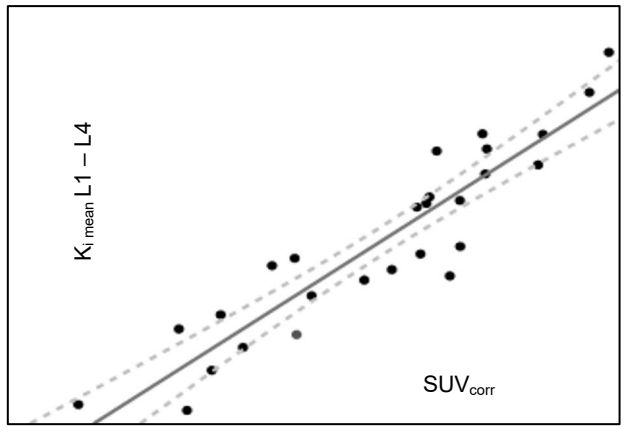

Figure 17. Correlation between corrected bone uptake values and blood clearance to bone. Modified from Aaltonen et al. (IV)

Elimination rate of fluoride and total blood clearance were calculated in all patients. There was no significant differences in either elimination rate or total blood clearance of fluoride when comparing patients with high-, normal- or low-turnover bone disease. There was not a statistically significant difference in SUV between different turnover groups, but SUV_{corr} was significantly higher in patients with high-turnover bone disease compared to patients with low-turnover bone disease.

6 Discussion

6.1 Correlation between ^{18}F-NaF-PET and histomorphometric parameters obtained by bone biopsy in patients on dialysis (I)

Study I showed a strong correlation between histomorphometric parameters obtained by bone biopsy and fluoride activity measured at the lumbar spine and at the anterior iliac crest in dynamic PET scans in patients on dialysis. A few studies have been published prior to this study (233, 262) showing a correlation between histomorphometric parameters in dialysis patients and dynamic PET scans using ^{18}F-fluoride as a tracer. Both studies were small. The study of Messa in 1993 included 11 patients on dialysis in which bone biopsies were obtained in eight patients. As histomorphometric markers, they used bone formation rate; reference values were not reported. In the study of Frost et al., seven patients on dialysis with suspected adynamic bone disease were included together with 12 osteoporotic women; as histomorphometric parameters for turnover, they used mineral apposition and bone formation rate.

In our study, fluoride activity in the dynamic PET scan correlated strongly with dynamic parameters such as bone formation rate and activation frequency, which represent turnover. Fluoride activity also correlated with several static histomorphometric parameters such as osteoclast and osteoblast activity and eroded surfaces. As reference values for normal bone turnover, we used the results of Malluche et al., being the most cited in this field of nephrological research (21, 203, 204). When using Malluche´s reference values for normal turnover, a majority of the patients presented with low-turnover bone disease (65%) and only three out of 26 patients had high-turnover bone disease. ^{18}F-NaF-PET had an AUC of 0.82 to identify patients with low turnover, when the cut-off level of tracer activity was set at < 0.04 mL/min/mL. PET imaging was superior to PTH to diagnose low-turnover bone disease. Because of too few patients, AUC for high turnover could not be performed.

Bone biopsy is the gold standard for diagnosing the subtypes of renal osteodystrophy. It is also the only available method to reliably measure treatment response. However, bone biopsy is not widely available, is not easily reproducible

and gives information of only one site of the skeleton. Bone biopsy is an invasive procedure. Both the procedure and the analysis require expertise that is not on hand in every center and not even in every country in Europe. In addition, the histomorphometric analyses are slow. A limitation of bone biopsies is that there are no universally accepted reference values for normal bone turnover.

Several noninvasive imaging methods have been evaluated in research settings in the CKD population, such as DXA and HR-pQCT. DXA is recommend to assess fracture risk also in the CKD population but is not able to identify the underlying bone disorder (169). HR-pQCT can detect microarchitectural changes in cortical and trabecular bone and can measure bone density (178). However, these imaging methods are static and are not able to measure bone turnover. ^{18}F-NaF-PET generates information of dynamic qualities of bone and quantifies bone turnover. This method gives a more extensive picture of the skeleton than bone biopsy and is noninvasive. ^{18}F-NaF-PET has been used successfully in studies evaluating osteoporosis medication (12, 232).

However, several disconcerting factors must be taken into account when interpreting the PET results. Previous studies indicate that patients with osteoporosis have lower tracer uptake in bone than patients with osteopenia or healthy controls (231). Also age can affect tracer uptake, even though more research is needed to estimate the significance of this finding (263). Dynamic PET scans are not feasible in clinical practice, and more simplified methods are needed.

The results of this study highlight that bone metabolism can be measured by ^{18}F-NaF-PET imaging also in patients on dialysis and that ^{18}F-NaF-PET appears to be a promising future diagnostic method in the evaluation of the subgroups of renal osteodystrophy.

6.2 Comparison between bone turnover–based and unified TMV–based classification of renal osteodystrophy (II)

In study II, a clear disproportion between bone turnover–based and unified TMV–based classification of renal osteodystrophy was discovered. This study is to our knowledge the first to compare different reference values of normal bone histomorphometry and to compare the results to ^{18}F-NaF-PET imaging, an objective measurement of bone metabolism. Reference values for normal histomorphometric parameters differ across studies. It is well established that many histomorphometric parameters show differences in men and women (200, 201, 206). There is variation according to age in several parameters, such as bone formation rate and osteoblast and osteoclast activities (205, 206). In addition, osteoclast activity increases and bone formation rate decreases in women after menopause (201).

In the majority of nephrological studies investigating bone biopsies, the reference values of Malluche et al. are used (21, 203, 204). The dynamic reference values of normal turnover from the studies of Malluche et al.—that is, bone formation rate and activation frequency—were obtained from 14 healthy males and 14 healthy females 20 – 83 years of age. In the studies of Recker et al., 96 healthy women and men underwent bone biopsies. The women underwent bone biopsies before and after menopause. In the studies of Recker et al. (200, 201), the normal range of dynamic histomorphometric parameters of bone turnover was substantially lower than in the studies of Malluche et al.

We used the reference values of Malluche et al. in the bone turnover classification of renal osteodystrophy. In unified TMV–based classification, we used the results of the studies of Recker et al., together with the overall histopathological picture, including osteoclast- and osteoblast activities, eroded surfaces, osteoid width and the existence of peritrabecular fibrosis. When using turnover-based classification of renal osteodystrophy, 61% of the patients had low-turnover bone disease and only 12% high-turnover bone disease. When using unified TMV–based classification of renal osteodystrophy, 42% has high-turnover bone disease and only 23% low-turnover bone disease. It seems that the reference values of Malluche overestimate low-turnover bone disease and underestimate high-turnover bone disease.

We tested the diagnostic accuracy of ^{18}F-NaF-PET in both classification groups. The cut-off value for fluoride activity in the PET scan was set at < 0.038 mL/min/mL for low turnover/adynamic bone, which agrees with the median fluoride activity of the control group. The cut-off value for high turnover was set at > 0.055 mL/min/mL. When using TMV-based classification of renal osteodystrophy, the diagnostic accuracy of ^{18}F-NaF-PET improves compared to turnover-based classification. The specificity of ^{18}F-NaF-PET to recognize high-turnover bone disease is 100% and sensitivity 82% with an AUC of 0.86. ^{18}F-NaF-PET's specificity to recognize low turnover is only 70%, but sensitivity is 100%, with an AUC of 0.87. In clinical practice, this suggests that ^{18}F-NaF-PET would confirm high-turnover bone disease with no false positive results, which is important before recommending parathyroidectomy or before initiating antiresorptive medication in cases of fractures in dialysis patients. In cases of low-turnover bone disease, ^{18}F-NaF-PET sensitivity is excellent with no false negative results, which is important when considering anabolic osteoporosis treatment. It is, however, good to acknowledge that ^{18}F-NaF-PET cannot, at least based on the knowledge we have at the moment, discriminate between patients with a mineralizing defect.

In the last decade, many studies have focused on finding a biomarker that can measure bone turnover in the CKD population. PTH is the main biomarker used for the evaluation of renal osteodystrophy in patients on dialysis (7, 197), even though

its diagnostic accuracy is limited. Biomarkers reflect the overall bone formation or bone resorption in the skeleton, and it is not unambiguous how well these parameters correlate with a bone biopsy from one small site of the skeleton. The assumption that bone metabolism differs in different sites of the skeleton is supported by PET studies confirming regional differences in bone metabolism (264). Also the lack of universal reference values of normal bone turnover challenge the reliability and comparability of different studies. PET imaging gives a wider picture of the skeleton. PET imaging could be an interesting research tool when investigating the usefulness of different biomarkers of bone turnover in the CKD population.

The results of this study challenge our conception of what reference values of normal bone turnover we should use in the CKD population. Should we consider age- and gender-adjusted reference values? More research and cooperation between units in different countries are needed to establish reference values for normal bone turnover in the CKD population. A European register, EUROD (https://www.eurod.net/welcome), was created in 2016, and one initiative is to update reference values for histomorphometric parameters in renal osteodystrophy. As in study I, ^{18}F-NaF-PET appears to be a promising new noninvasive diagnostic tool in patients with chronic kidney disease, even though further research is needed to establish the feasibility of the method in clinical practice.

6.3 Methodological aspects (I, II)

Bone biopsy is unquestionably the gold standard in evaluation of renal osteodystrophy in patients with CKD. There are, however, many challenging aspects when it comes to bone biopsies. Bone biopsies reflect only one small site of the skeleton. Even though bone biopsies are in clinical use and used also in clinical decision-making, no universal reference values for histomorphometric parameters are available. The histomorphometrist considers the overall histomorphometric picture when analyzing the bone biopsy, but in research settings, fixed reference values are needed. The techniques when obtaining bone biopsies also vary in different studies, and this also challenge the comparability of different studies.

Studies I and II aimed at evaluating ^{18}F-NaF-PET feasibility as a diagnostic tool in patients with renal osteodystrophy. Dynamic ^{18}F-NaF-PET scans have in previous studies proven to be precise in measuring bone turnover (11). As reference, we used histomorphometric parameters from the bone biopsy. The lack of reference values for histomorphometric parameters complicated the interpretation of the results. We used the historical reference values of Malluche (21, 203, 204) in study I. In study II we compared these reference values to unified TMV–based classification, where the results of the group of Recker (200, 201) were used when defining reference values for turnover. Studies I and II highlighted the need for universal histomorphometric

reference values in the CKD population. PET imaging gives a wider picture of the skeleton and could be a valuable tool also when searching for new clinical biomarkers to distinguish between the subgroups of renal osteodystrophy. The challenge when interpreting ^{18}F-NaF-PET scans is that dynamic scans are not feasible in clinical practice. PET scans also cause radiation, which must be taken into consideration.

6.4 Association between vascular calcification and bone mineral metabolism in end-stage renal disease (III)

Several studies have indicated a link between arterial calcification and bone turnover, and there is also evidence that improvement of bone turnover reduces progression of vascular calcification (8, 9, 26, 265). However, contradictory results have also been published (3, 266). In this study, there was a weak positive association between CAC and fluoride activity measured in the lumbar spine. However, there was no association between fluoride activity at the anterior iliac crest and CAC. Weak associations between CAC and PTH, and eroded surfaces and AAC, were also discovered. There were no associations between vascular calcifications and any other parameter measured.

This study cohort represents the typical dialysis population in Western countries. When comparing our cohort to the studies in which an association between arterial calcification and bone turnover was found, the patients in this study were older and the incidence of diabetes was greater. The median dialysis vintage was only 10 months, which could have had an impact on the results; the dialysis vintage range was, however, wide at 3–20 months. As many as 50% had manifested cardiovascular disease, and their CAC and AAC scores were on average higher. Fifty percent of the study population had CAC > 400, indicating extensive and severe atherosclerotic disease. In addition, the percentage of patients with low-turnover bone disease was much smaller than in the studies indicating a link between turnover and arterial calcifications, and this might have had an impact on the significance of the results. The results of this study strengthen the assumption of a link between vascular calcification and bone metabolism. However, one should keep in mind when interpreting the results that this was a cross-sectional, rather small study. PTH is a biomarker of turnover but has limited ability to diagnose the subgroups of renal osteodystrophy (7). The significance of the association between PTH and CAC remains unclear. Overall, some challenges when comparing different studies reporting associations between arterial calcifications and parameters of bone metabolism are the variability of study populations, the methods used to define bone turnover and calcification scores.

The strength of this study was that bone turnover was measured using both ^{18}F-NaF-PET imaging, which gives a more extensive picture of the skeleton, and histomorphometric parameters obtained by bone biopsy. Bone histomorphometry was analysed using the ASBMR Histomorphometry Nomenclature Committee recommendation for single labels (191), which is recommended by KDIGO. In addition, both coronary calcification score and aortic calcification score were measured. Both imaging methods are precise and validated to detect arterial calcifications.

A recent study showed an inverse association between trabecular bone score, including bone density, and vascular calcification (267). In our study, there was no association between arterial calcification and bone density and volume. Again, the small study population and the heterogeneity of the study population might diminish the association between arterial calcification and bone metabolism

In summary, one can state that indications of an association between arterial calcification and bone metabolism was also established in our study. However, our study also highlights the complexity when evaluating the link between arterial calcification and bone turnover in patients with extensive atherosclerotic disease and multiple comorbidities. In the presence of multiple factors contributing to the development of arterial calcifications, the impact of bone metabolism might be diminished. Future prospective studies are needed to establish the impact of improvement in bone turnover on vascular calcification,

6.5 Bone metabolic activity in dialysis patients using ^{18}F-NaF-PET—comparison between static and dynamic measurements (IV)

Dynamic ^{18}F-NaF-PET scans are precise and accurate in measuring bone metabolism but are not very practical in clinical practice. Standardized uptake values (SUVs) are widely used in the diagnostic field of oncology but are not validated for extensive metabolic bone diseases.

We have shown in study I and II that dynamic ^{18}F-NaF-PET can distinguish between high- and low-turnover bone disease. In this study, SUVs were measured from static scans in the lumbar spine and at the anterior iliac crest 48–60 minutes after tracer injection. SUVs did not correlate with histomorphometric parameters reflecting bone turnover and could not distinguish between high- and low-turnover bone disease. However, we detected that when correcting the SUVs with mean blood uptake of tracer 48–60 minutes from tracer injection, there was a strong correlation between SUV_{corr} and blood clearance to bone, $K_{i,}$ in the dynamic PET scan.

Radionuclide imaging using a dynamic ^{18}F-NaF-PET scan is a valuable tool when examining metabolic bone diseases. In dynamic PET scans, an arterial input function

is needed in order to measure blood clearance of fluoride to bone. In these scans, the rate of tracer uptake into an organ is normalized by the tracer concentration in blood. This method is very precise, because the tracer activity in the organ is proportional to the tracer activity in blood, and therefore kidney function or how extensive a metabolic bone disease is, does not affect the results.

One theory is that SUVs cannot be used in extensive metabolic bone disease. There is only a finite amount of tracer to be distributed into all competing bones, and therefore it is thought that regional bone uptake not only reflects the local demand for tracer but is also influenced by the competing areas of the skeleton (11). Similar challenges are likely to appear in the evaluation of renal osteodystrophy. In high-turnover bone disease, the metabolic activity in bones is high, and one would think the demand for tracer is high compared to low-turnover bone disease, where the metabolic activity of the bones is very low.

An unexpected result that has not been reported earlier was that there was no significant difference between the different turnover groups. We calculated fluoride elimination rate from blood and total blood clearance of fluoride in order to evaluate the impact of the distribution of fluoride to bone. There was no significant difference between the different turnover groups, which was unexpected. This indicates that other conditions overruled this possible effect and did not explain why SUVs measured from static scans did not work in this study population. All patients in this study were on dialysis, and their possible residual kidney function was not documented. One study using ^{18}F-FDG concluded that about 10 percent of the injected tracer dose was excreted in urine 70 minutes from the injection, but the excretion was highly variable (268). This could affect the SUV measurements. The patients in that study had normal kidney function. Studies of the impact of residual kidney function in the CKD population on standardized tracer uptake to bone have not been done.

Siddique et al. have proposed a simplified PET imaging method, where $^{18}F^-$ fluoride blood clearance to bone can be estimated from static scans (269). In that study, venous blood samples were obtained 30–60 minutes after a single tracer injection. These measurements correlated strongly with Patlak results. The conclusion was that $^{18}F^-$fluoride blood clearance to bone can be estimated from static scans and venous blood samples with a single injection of tracer.

This study suggests that blood clearance to bone can be estimated from static scans also when taking blood test 48–60 minutes from tracer injection. This method could also be useful in clinical practice before initiating osteoporosis medication in patients on dialysis or before considering parathyroidectomy. However, further research is needed to validate the method.

6.6 Limitation of the study

The limitation of the studies I–IV was the relatively small number of patients. The study population was heterogeneous, which could lead to challenges when interpreting the results. However, this study population was a valid example of the current dialysis population treated in clinical practice in Western countries. The histomorphometric parameters obtained by bone biopsy were not adjusted to age, and therefore we did not correct PET results for age either. Bone biopsies were obtained vertically, which could possibly have an impact on the interpretability and the comparability of studies in which bone biopsies were transiliac. One major limitation was that the control group was small and did not undergo a bone biopsy. It is not easy to get permission from an ethics committee to obtain bone biopsies from healthy controls. The fact that there are no universally accepted reference values for histomorphometric parameters, especially parameters measuring turnover, was a major challenge and could also be considered a limitation in testing a possible diagnostic imaging method. Also the fact that only PTH was measured as a biomarker for turnover is a limitation of this study.

Dynamic PET scans have successfully been used in a research setting in evaluation of regional bone metabolism. We used an image-derived input function, which is inferior to arterial blood sampling. One aim of this study was to evaluate whether ^{18}F-NaF-PET scan could work in clinical practice, and therefore an arterial bloodline was not an option. Image-derived input functions can present technical challenges, and therefore extra caution was exercised when drawing the region of interest on the aorta. The study population consisted of patients on dialysis. The residual function of the kidneys was not documented in this study population, which limited the possibilities of understanding the impact of kidney function on standardized uptake values.

6.7 Future implications

A majority of patients with end-stage kidney disease have abnormalities in mineral homeostasis impairing bone remodeling and mineralization, and the abnormalities are associated with increased morbidity and mortality in this patient group. The diagnostic accuracy of biomarkers in clinical use at this moment is not sufficient in advanced kidney disease. Bone biopsy is the gold standard, but it is not easily available. A diagnostic tool that could confirm or rule out high- or low-turnover bone disease before initiation of medical treatment or surgery would be highly welcomed in clinical practice.

^{18}F-NaF-PET has shown promising properties in the field of research when evaluating bone metabolism and treatment response of antiresorptive or anabolic osteoporosis medication. Based on the results of our study, ^{18}F-NaF-PET appears to

be an interesting diagnostic tool in clinical practice as well. ^{18}F-NaF-PET´s specificity to recognize high turnover is excellent and it could be used to confirm high-turnover bone disease, for example, before parathyroidectomy. An ongoing prospective trial (clinicaltrials.gov NCT04522622) investigates anabolic treatment in low-turnover disease using also ^{18}F-NaF-PET for measurement of bone turnover, giving us more information about both the imaging method and the effect of treatment. ^{18}F-NaF-PET sensitivity in low-turnover disease is very good. Further research is needed to validate a method that is feasible in clinical practice in the evaluation of CKD patients with renal osteodystrophy.

A randomized controlled trial assessing the changes in bone turnover after initiating cinacalcet medication in high-turnover bone disease with a follow-up of 18–24 months could be a future study design. ^{18}F-NaF-PET, bone biopsy, DXA and biomarkers of bone turnover would be obtained at baseline and after 18–24 months. Both dynamic and static measurements from the ^{18}F-NaF-PET scan would be measured and both imaging-derived AIF and venous blood tests for measuring AIF would be used. Research of new biomarkers of bone formation and bone resorption using ^{18}F-NaF-PET is also an interesting future field. ^{18}F-NaF-PET could also be a valuable research tool to assess the pathways and interactions between bone metabolism and the vasculature.

7 Conclusions

Fluoride activity measured by ^{18}F-NaF PET in patients on dialysis correlates with both static and dynamic histomorphometric parameters obtained by bone biopsy. The result of this study highlights that bone metabolism can also be measured by ^{18}F-NaF-PET imaging in patients on dialysis.

A clear disproportion between bone turnover–based and unified TMV–based classification of renal osteodystrophy was discovered. In nephrological research, bone turnover–based measurements using Malluche's reference values are most commonly used. A discussion is needed to assess what reference values of bone turnover should be used in the CKD population. ^{18}F-NaF PET seems a promising diagnostic tool to evaluate patients with renal osteodystrophy and to guide medication or surgical decisions. ^{18}F-PET diagnostic accuracy when using unified TMV–based classification of ROD was good, with both high specificity and sensitivity.

In this study population, there was a weak association between bone turnover measured by ^{18}F-NaF PET and coronary calcification. There was no association between histomorphometric parameters obtained from the bone biopsy. The association between bone turnover and arterial calcification is still controversial; both positive and negative studies have been published. This study population presented with extensive atherosclerosis, and the result of this study highlights the complexity of evaluating the link between vascular calcification and bone metabolism in patients with multiple comorbidities. In the presence of multiple factors contributing to the development of arterial calcification, the impact of bone metabolism might be diminished.

A simplified imaging method using ^{18}F-NaF PET, where static scans and venous blood samples are obtained 48–60 minutes after tracer injection, could provide an imaging method also feasible in clinical practice. More research and validation of the method are needed, however, before this method can be implicated in clinical practice.

Acknowledgements

This study was carried out at the Kidney Centre, Turku University Hospital and Turku PET Centre during the years 2016-2022. It was conducted within the Finnish Centre of Excellence in Cardiovascular and Metabolic Disease, supported by the Academy of Finland, the University of Turku, the Turku University Central Hospital, and the Åbo Akademi University.

I express my deepest gratitude to my supervisors Docent Kaj Metsärinne and Docent Niina Koivuviita for your guidance throughout this project. Without Your support and encourage, I would never have dared to start this project. I thank Kajus for always being supportive and positive. I admire your knowledge in this field, and your positive attitude toward research has been inspiring. I also thank you for making this research possible. I want to thank Niina for your guidance and help in practical issues, your energetic approach to almost everything and for introducing me to the world of research in Turku PET Centre. You have a magnificence ability to perceive entities, you have guided me in academic writing and your honest feedback challenging my thoughts, but at the same time believing in my own ideas have helped me a lot through the project.

I am grateful to Professor Markus Juonala for granting me permission to conduct this work at the Institute of Clinical Medicine, University of Turku. I warmly thank Professor Juhani Knuuti, director of Turku PET Centre, for providing facilities and an inspiring environment for research and I also thank the team in Kuopio Musculoskeletal Research Unit for your cooperation and expertise. I thank Docent Ilkka Kantola, the member of my supervisory committee, for his contribution to this thesis. I also gratefully thank Docent Satu Mäkelä for accepting the invitation to act as my opponent in the dissertation defense.

Professor Eero Honkanen and Docent Daniel Gordin are gratefully acknowledged for their review of this thesis and for their valuable comments and constructive criticism. I really enjoyed our conversations during the review process. I also thank Liz Prouty for revising the language in this thesis.

I sincerely want to thank all my co-authors for their contributions to the original publications. I especially thank Professor Heikki Kröger for your help and expertise in the field of bone histomorphometry. Our conversations and your support have

been of great value during this project. I also want to thank MSc Vesa Oikonen for helping me with PET analyses and methodology and Docent Marko Seppänen for your friendly support and expertise in the field of PET imaging. I warmly thank MSc Eliisa Löyttyniemi for your assistance in statistical analysis, you always seem to find the time to help. I also gratefully thank MD Xiaoyu Tong, MD Inari Burton and Dr Anna Kirjavainen for their contribution.

I am grateful to the staff of the Turku PET Centre: radiochemists, laboratory technicians, physicists, research nurses and other staff. You do an important work and it has been a privilege to work with you. I also want to thank Sauli Piirola and Chunley Han for your assistance in using Carimas and Marko Tättäläinen for always being patience and for helping with computer problems.

I thank MD Leena Martola for teaching me the bone biopsy procedure. I also thank the day care unit for the flexibility and positive attitude when introducing the bone biopsy procedure. Especially nurses Petra Virtanen and Hanna Piirainen are acknowledged.

I am grateful to all my colleagues in the Kidney Centre, Turku University Hospital for their support in my research work and for creating an enjoyable working atmosphere in the clinic. I especially thank Maija Heiro and Markus Hakamäki for your friendship and support during this process. I am grateful for the inspiring and supportive conversations with Tapio Hellman. I thank Johanna Päivärinta, Jonna Virtanen, Roosa Lankinen, Outi Leinonen and Risto Tertti for your support. I also warmly thank the whole staff of the Kidney Center.

Petra-Ann Salminen, my dearest friend, thank you for your support and friendship through all these years. Mats Boman, Jani Söderström, Suvi Vainiomäki, Liisa Viikari, Kata Noronen, Ilona Anttila, Pauliina Vaija, Satu Keronen, Kirsi Taimen, Antti Palomäki, Milja Söderström and all others. Thank you for all enjoyable moments, interesting conversations and support.

I am fortunate to have the family I do. My deepest gratitude to my mother, Mona, who has always encouraged and supported me throughout life and selflessly been there to help when needed. I am also grateful to my dear sister, Rie, for being there for me and for all the fun moments and adventures together.

Finally, I want to thank my husband Jarkko. You are my rock, I love you to the moon and back, thank you for all support, patience and unconditioned love. Ada and Filip, you are my stars and give meaning to my life.

This study was financially supported by grants from Finska Läkarsällskapet, the Perkle's Foundation, Munuaissäätiö, Turku University Medical Foundation, Turku University Foundation, The Finnish Cultural Foundation and Paulo Foundation.

Turku, January 2022
Louise Aaltonen

References

1. Kidney Disease: Improving Global Outcomes (KDIGO) CKD-MBD Work Group. KDIGO clinical practice guideline for the diagnosis, evaluation, prevention, and treatment of Chronic Kidney Disease-Mineral and Bone Disorder (CKD-MBD). Kidney Int Suppl. 2009 August 01;(113):S1-130. doi(113):1.
2. Guerin AP, London GM, Marchais SJ, Metivier F. Arterial stiffening and vascular calcifications in end-stage renal disease. Nephrol Dial Transplant. 2000 July 01;15(7):1014-21.
3. Barreto DV, Barreto FC, Carvalho AB, Cuppari L, Cendoroglo M, Draibe SA, et al. Coronary calcification in hemodialysis patients: the contribution of traditional and uremia-related risk factors. Kidney Int. 2005 April 01;67(4):1576-82.
4. Kendrick J, CheungAK, KaufmanJS, et al. FGF-23 associates with death, cardiovascular events, and initiation of chronic dialysis, JAmSocNephrol, 2011, vol. 22 (pg. 1913-1922)
5. Jadoul M, Albert JM, Akiba T, Akizawa T, Arab L, Bragg-Gresham JL, et al. Incidence and risk factors for hip or other bone fractures among hemodialysis patients in the Dialysis Outcomes and Practice Patterns Study. Kidney Int. 2006 October 01;70(7):1358-66.
6. Robertson L, Black C, Fluck N, Gordon S, Hollick R, Nguyen H, et al. Hip fracture incidence and mortality in chronic kidney disease: the GLOMMS-II record linkage cohort study. BMJ Open. 2018 April 12;8(4):e020312-020312.
7. Sprague SM, Bellorin-Font E, Jorgetti V, Carvalho AB, Malluche HH, Ferreira A, et al. Diagnostic Accuracy of Bone Turnover Markers and Bone Histology in Patients With CKD Treated by Dialysis. Am J Kidney Dis. 2016 April 01;67(4):559-66.
8. Asci G, Ok E, Savas R, Ozkahya M, Duman S, Toz H, et al. The link between bone and coronary calcifications in CKD-5 patients on haemodialysis. Nephrol Dial Transplant. 2011 March 01;26(3):1010-5.
9. Barreto DV, Barreto Fde C, Carvalho AB, Cuppari L, Draibe SA, Dalboni MA, et al. Association of changes in bone remodeling and coronary calcification in hemodialysis patients: a prospective study. Am J Kidney Dis. 2008 December 01;52(6):1139-50.
10. Even-Sapir E, Mishani E, Flusser G, Metser U. 18F-Fluoride positron emission tomography and positron emission tomography/computed tomography. Semin Nucl Med. 2007 November 01;37(6):462-9.
11. Blake GM, Park-Holohan SJ, Cook GJ, Fogelman I. Quantitative studies of bone with the use of 18F-fluoride and 99mTc-methylene diphosphonate. Semin Nucl Med. 2001 January 01;31(1):28-49.
12. Frost ML, Cook GJ, Blake GM, Marsden PK, Benatar NA, Fogelman I. A prospective study of risedronate on regional bone metabolism and blood flow at the lumbar spine measured by 18F-fluoride positron emission tomography. J Bone Miner Res. 2003 December 01;18(12):2215-22.
13. Chen J, Budoff MJ, Reilly MP, Yang W, Rosas SE, Rahman M, et al. Coronary Artery Calcification and Risk of Cardiovascular Disease and Death Among Patients With Chronic Kidney Disease. JAMA Cardiol. 2017 June 01;2(6):635-43.
14. Thompson GR, Forbat S, Underwood R. Electron-beam CT scanning for detection of coronary calcification and prediction of coronary heart disease. QJM. 1996 August 01;89(8):565-70.

15. Jha V, Garcia-Garcia G, Iseki K, Li Z, Naicker S, Plattner B, et al. Chronic kidney disease: global dimension and perspectives. Lancet. 2013 July 20;382(9888):260-72.
16. Chen TK, Knicely DH, Grams ME. Chronic Kidney Disease Diagnosis and Management: A Review. JAMA. 2019 October 01;322(13):1294-304.
17. Go, AS; Chertow, GM; Fan, D; McCullon, CE et al. Chronic kidney disease and the risks of death, cardiovascular events, and hospitalization. N.EnglJ.Med 2004 September 23;351(13):1296-305
18. Astor BC, Matsushita K, Gansevoort RT, van der Velde M, Woodward M, Levey AS, et al. Lower estimated glomerular filtration rate and higher albuminuria are associated with mortality and end-stage renal disease. A collaborative meta-analysis of kidney disease population cohorts. Kidney Int. 2011 June 01;79(12):1331-40.
19. Moe S, Drueke T, Cunningham J, Goodman W, Martin K, Olgaard K, et al. Definition, evaluation, and classification of renal osteodystrophy: a position statement from Kidney Disease: Improving Global Outcomes (KDIGO). Kidney Int. 2006 June 01;69(11):1945-53.
20. Malluche HH, Mawad H, Monier-Faugere MC. The importance of bone health in end-stage renal disease: out of the frying pan, into the fire? Nephrol Dial Transplant. 2004 March 01;19 Suppl 1:9.
21. Malluche HH, Monier-Faugere MC. Renal osteodystrophy: what's in a name? Presentation of a clinically useful new model to interpret bone histologic findings. Clin Nephrol. 2006 April 01;65(4):235-42.
22. Sprague SM. The role of the bone biopsy in the diagnosis of renal osteodystrophy. Semin Dial. 2000 June 01;13(3):152-5.
23. Nickolas TL, Cremers S, Zhang A, Thomas V, Stein E, Cohen A, et al. Discriminants of prevalent fractures in chronic kidney disease. J Am Soc Nephrol. 2011 August 01;22(8):1560-72.
24. Alem AM, Sherrard DJ, Gillen DL, Weiss NS, Beresford SA, Heckbert SR, et al. Increased risk of hip fracture among patients with end-stage renal disease. Kidney Int. 2000 July 01;58(1):396-9.
25. Tentori F, McCullough K, Kilpatrick RD, Bradbury BD, Robinson BM, Kerr PG, et al. High rates of death and hospitalization follow bone fracture among hemodialysis patients. Kidney Int. 2014 January 01;85(1):166-73.
26. London GM, Marchais SJ, Guerin AP, Boutouyrie P, Metivier F, de Vernejoul MC. Association of bone activity, calcium load, aortic stiffness, and calcifications in ESRD. J Am Soc Nephrol. 2008 September 01;19(9):1827-35.
27. Levey AS, Eckardt KU, Tsukamoto Y, Levin A, Coresh J, Rossert J, et al. Definition and classification of chronic kidney disease: a position statement from Kidney Disease: Improving Global Outcomes (KDIGO). Kidney Int. 2005 June 01;67(6):2089-100.
28. Eriksen EF, Axelrod DW, Melsen F. Bone Histomorphometry. New York,: Raven Press; 1994.
29. Clarke B. Normal bone anatomy and physiology. Clin J Am Soc Nephrol. 2008 November 01;3 Suppl 3:131.
30. Boyle WJ, Simonet WS, Lacey DL. Osteoclast differentiation and activation. Nature. 2003 May 15;423(6937):337-42.
31. Seeman E, Delmas PD. Bone quality--the material and structural basis of bone strength and fragility. N Engl J Med. 2006 May 25;354(21):2250-61.
32. Ubara Y, Fushimi T, Tagami T, Sawa N, Hoshino J, Yokota M, et al. Histomorphometric features of bone in patients with primary and secondary hypoparathyroidism. Kidney Int. 2003 May 01;63(5):1809-16.
33. Burr DB, Schaffler MB, Yang KH, Wu DD, Lukoschek M, Kandzari D, et al. The effects of altered strain environments on bone tissue kinetics. Bone. 1989;10(3):215-21.
34. Hadjidakis DJ, Androulakis II. Bone remodeling. Ann N Y Acad Sci. 2006 December 01;1092:385-96.

35. Frost HM. Skeletal structural adaptations to mechanical usage (SATMU): 2. Redefining Wolff's law: the remodeling problem. Anat Rec. 1990 April 01;226(4):414-22.
36. Agerbaek MO, Eriksen EF, Kragstrup J, Mosekilde L, Melsen F. A reconstruction of the remodelling cycle in normal human cortical iliac bone. Bone Miner. 1991 February 01;12(2):101-12.
37. Yasuda H, Shima N, Nakagawa N, Yamaguchi K, Kinosaki M, Mochizuki S, et al. Osteoclast differentiation factor is a ligand for osteoprotegerin/osteoclastogenesis-inhibitory factor and is identical to TRANCE/RANKL. Proc Natl Acad Sci U S A. 1998 March 31;95(7):3597-602.
38. Parfitt AM. Osteonal and hemi-osteonal remodeling: the spatial and temporal framework for signal traffic in adult human bone. J Cell Biochem. 1994 July 01;55(3):273-86.
39. Kenkre JS, Bassett J. The bone remodelling cycle. Ann Clin Biochem. 2018 May 01;55(3):308-27.
40. Gordin D., Soro-Paavonen A et al, FinnDiane Study Group. Osteoprotegerin is an independent predictor of vascular events in Finnish adults with type 1 diabetes. Diabetes Care, 2013 Jul;36(7):1827-33.
41. Silva BC, Bilezikian JP. Parathyroid hormone: anabolic and catabolic actions on the skeleton. Curr Opin Pharmacol. 2015 June 01;22:41-50.
42. Weinstein RS, Jilka RL, Parfitt AM, Manolagas SC. Inhibition of osteoblastogenesis and promotion of apoptosis of osteoblasts and osteocytes by glucocorticoids. Potential mechanisms of their deleterious effects on bone. J Clin Invest. 1998 July 15;102(2):274-82.
43. Quarles LD. Endocrine functions of bone in mineral metabolism regulation. J Clin Invest. 2008 December 01;118(12):3820-8.
44. Ben-Dov IZ, Galitzer H, Lavi-Moshayoff V, Goetz R, Kuro-o M, Mohammadi M, et al. The parathyroid is a target organ for FGF23 in rats. J Clin Invest. 2007 December 01;117(12):4003-8.
45. Krajisnik T, Bjorklund P, Marsell R, Ljunggren O, Akerstrom G, Jonsson KB, et al. Fibroblast growth factor-23 regulates parathyroid hormone and 1alpha-hydroxylase expression in cultured bovine parathyroid cells. J Endocrinol. 2007 October 01;195(1):125-31.
46. Galitzer H, Ben-Dov IZ, Silver J, Naveh-Many T. Parathyroid cell resistance to fibroblast growth factor 23 in secondary hyperparathyroidism of chronic kidney disease. Kidney Int. 2010 February 01;77(3):211-8.
47. Hu MC, Shi M, Zhang J, Quinones H, Kuro-o M, Moe OW. Klotho deficiency is an early biomarker of renal ischemia-reperfusion injury and its replacement is protective. Kidney Int. 2010 December 01;78(12):1240-51.
48. Komaba H, Goto S, Fujii H, Hamada Y, Kobayashi A, Shibuya K, et al. Depressed expression of Klotho and FGF receptor 1 in hyperplastic parathyroid glands from uremic patients. Kidney Int. 2010 February 01;77(3):232-8.
49. Prie D, Urena Torres P, Friedlander G. Latest findings in phosphate homeostasis. Kidney Int. 2009 May 01;75(9):882-9.
50. Shimada T, Hasegawa H, Yamazaki Y, Muto T, Hino R, Takeuchi Y, et al. FGF-23 is a potent regulator of vitamin D metabolism and phosphate homeostasis. J Bone Miner Res. 2004 March 01;19(3):429-35.
51. Felsenfeld AJ, Rodriguez M, Aguilera-Tejero E. Dynamics of parathyroid hormone secretion in health and secondary hyperparathyroidism. Clin J Am Soc Nephrol. 2007 November 01;2(6):1283-305.
52. Fukagawa M, Nakanishi S, Kazama JJ. Basic and clinical aspects of parathyroid hyperplasia in chronic kidney disease. Kidney Int Suppl. 2006 July 01;(102):S3-7. doi(102):3.
53. Gogusev J, Duchambon P, Hory B, Giovannini M, Goureau Y, Sarfati E, et al. Depressed expression of calcium receptor in parathyroid gland tissue of patients with hyperparathyroidism. Kidney Int. 1997 January 01;51(1):328-36.

54. Fukuda N, Tanaka H, Tominaga Y, Fukagawa M, Kurokawa K, Seino Y. Decreased 1,25-dihydroxyvitamin D3 receptor density is associated with a more severe form of parathyroid hyperplasia in chronic uremic patients. J Clin Invest. 1993 September 01;92(3):1436-43.
55. Kestenbaum B, Sampson JN, Rudser KD, Patterson DJ, Seliger SL, Young B, et al. Serum phosphate levels and mortality risk among people with chronic kidney disease. J Am Soc Nephrol. 2005 February 01;16(2):520-8.
56. Dhingra R, Sullivan LM, Fox CS, Wang TJ, D'Agostino RB S, Gaziano JM, et al. Relations of serum phosphorus and calcium levels to the incidence of cardiovascular disease in the community. Arch Intern Med. 2007 May 14;167(9):879-85.
57. Vart P, Nigatu YT, Jaglan A, van Zon SK, Shafique K. Joint Effect of Hypertension and Elevated Serum Phosphorus on the Risk of Mortality in National Health and Nutrition Examination Survey-III. J Am Heart Assoc. 2015 May 20;4(5):10.1161/JAHA.114.001706.
58. Sim JJ, Bhandari SK, Smith N, Chung J, Liu IL, Jacobsen SJ, et al. Phosphorus and risk of renal failure in subjects with normal renal function. Am J Med. 2013 April 01;126(4):311-8.
59. Voormolen N, Noordzij M, Grootendorst DC, Beetz I, Sijpkens YW, van Manen JG, et al. High plasma phosphate as a risk factor for decline in renal function and mortality in pre-dialysis patients. Nephrol Dial Transplant. 2007 October 01;22(10):2909-16.
60. Block GA, Hulbert-Shearon TE, Levin NW, Port FK. Association of serum phosphorus and calcium x phosphate product with mortality risk in chronic hemodialysis patients: a national study. Am J Kidney Dis. 1998 April 01;31(4):607-17.
61. Young EW, Albert JM, Satayathum S, Goodkin DA, Pisoni RL, Akiba T, et al. Predictors and consequences of altered mineral metabolism: the Dialysis Outcomes and Practice Patterns Study. Kidney Int. 2005 March 01;67(3):1179-87.
62. Pulskens WP, Verkaik M, Sheedfar F, van Loon EP, van de Sluis B, Vervloet MG, et al. Deregulated Renal Calcium and Phosphate Transport during Experimental Kidney Failure. PLoS One. 2015 November 13;10(11):e0142510.
63. Murer H, Hernando N, Forster I, Biber J. Regulation of Na/Pi transporter in the proximal tubule. Annu Rev Physiol. 2003;65:531-42.
64. Six I, Maizel J, Barreto FC, Rangrez AY, Dupont S, Slama M, et al. Effects of phosphate on vascular function under normal conditions and influence of the uraemic state. Cardiovasc Res. 2012 October 01;96(1):130-9.
65. Crouthamel MH, Lau WL, Leaf EM, Chavkin NW, Wallingford MC, Peterson DF, et al. Sodium-dependent phosphate cotransporters and phosphate-induced calcification of vascular smooth muscle cells: redundant roles for PiT-1 and PiT-2. Arterioscler Thromb Vasc Biol. 2013 November 01;33(11):2625-32.
66. Graciolli FG, Neves KR, dos Reis LM, Graciolli RG, Noronha IL, Moyses RM, et al. Phosphorus overload and PTH induce aortic expression of Runx2 in experimental uraemia. Nephrol Dial Transplant. 2009 May 01;24(5):1416-21.
67. Isakova T, Wahl P, Vargas GS, Gutierrez OM, Scialla J, Xie H, et al. Fibroblast growth factor 23 is elevated before parathyroid hormone and phosphate in chronic kidney disease. Kidney Int. 2011 June 01;79(12):1370-8.
68. Wolf M. Forging forward with 10 burning questions on FGF23 in kidney disease. J Am Soc Nephrol. 2010 September 01;21(9):1427-35.
69. Liu S, Zhou J, Tang W, Jiang X, Rowe DW, Quarles LD. Pathogenic role of Fgf23 in Hyp mice. Am J Physiol Endocrinol Metab. 2006 July 01;291(1):38.
70. Farrow EG, Davis SI, Summers LJ, White KE. Initial FGF23-mediated signaling occurs in the distal convoluted tubule. J Am Soc Nephrol. 2009 May 01;20(5):955-60.
71. Kuro-o M. Overview of the FGF23-Klotho axis. Pediatr Nephrol. 2010 April 01;25(4):583-90.
72. Faul C, Amaral AP, Oskouei B, Hu MC, Sloan A, Isakova T, et al. FGF23 induces left ventricular hypertrophy. J Clin Invest. 2011 November 01;121(11):4393-408.

73. Grabner A, Amaral AP, Schramm K, Singh S, Sloan A, Yanucil C, et al. Activation of Cardiac Fibroblast Growth Factor Receptor 4 Causes Left Ventricular Hypertrophy. Cell Metab. 2015 December 01;22(6):1020-32.
74. Gutierrez OM, Januzzi JL, Isakova T, Laliberte K, Smith K, Collerone G, et al. Fibroblast growth factor 23 and left ventricular hypertrophy in chronic kidney disease. Circulation. 2009 May 19;119(19):2545-52.
75. Scialla JJ, Wolf M. Roles of phosphate and fibroblast growth factor 23 in cardiovascular disease. Nat Rev Nephrol. 2014 May 01;10(5):268-78.
76. Scialla JJ, Astor BC, Isakova T, Xie H, Appel LJ, Wolf M. Mineral metabolites and CKD progression in African Americans. J Am Soc Nephrol. 2013 January 01;24(1):125-35.
77. Andrukhova O, Slavic S, Smorodchenko A, Zeitz U, Shalhoub V, Lanske B, et al. FGF23 regulates renal sodium handling and blood pressure. EMBO Mol Med. 2014 June 01;6(6):744-59.
78. Wolf MT, An SW, Nie M, Bal MS, Huang CL. Klotho up-regulates renal calcium channel transient receptor potential vanilloid 5 (TRPV5) by intra- and extracellular N-glycosylation-dependent mechanisms. J Biol Chem. 2014 December 26;289(52):35849-57.
79. Hu MC, Shi M, Zhang J, Addo T, Cho HJ, Barker SL, et al. Renal Production, Uptake, and Handling of Circulating alphaKlotho. J Am Soc Nephrol. 2016 January 01;27(1):79-90.
80. Sugiura H, Yoshida T, Shiohira S, Kohei J, Mitobe M, Kurosu H, et al. Reduced Klotho expression level in kidney aggravates renal interstitial fibrosis. Am J Physiol Renal Physiol. 2012 May 15;302(10):1252.
81. Bian A, Neyra JA, Zhan M, Hu MC. Klotho, stem cells, and aging. Clin Interv Aging. 2015 August 04;10:1233-43.
82. Hu MC, Shi M, Zhang J, Quinones H, Griffith C, Kuro-o M, et al. Klotho deficiency causes vascular calcification in chronic kidney disease. J Am Soc Nephrol. 2011 January 01;22(1):124-36.
83. Chang JR, Guo J, Wang Y, Hou YL, Lu WW, Zhang JS, et al. Intermedin1-53 attenuates vascular calcification in rats with chronic kidney disease by upregulation of alpha-Klotho. Kidney Int. 2016 March 01;89(3):586-600.
84. Hu MC, Shi M, Zhang J, Pastor J, Nakatani T, Lanske B, et al. Klotho: a novel phosphaturic substance acting as an autocrine enzyme in the renal proximal tubule. FASEB J. 2010 September 01;24(9):3438-50.
85. Vervloet MG, Massy ZA, Brandenburg VM, Mazzaferro S, Cozzolino M, Urena-Torres P, et al. Bone: a new endocrine organ at the heart of chronic kidney disease and mineral and bone disorders. Lancet Diabetes Endocrinol. 2014 May 01;2(5):427-36.
86. Monroe DG, McGee-Lawrence ME, Oursler MJ, Westendorf JJ. Update on Wnt signaling in bone cell biology and bone disease. Gene. 2012 January 15;492(1):1-18.
87. Ke HZ, Richards WG, Li X, Ominsky MS. Sclerostin and Dickkopf-1 as therapeutic targets in bone diseases. Endocr Rev. 2012 October 01;33(5):747-83.
88. Li X, Ominsky MS, Niu QT, Sun N, Daugherty B, D'Agostin D, et al. Targeted deletion of the sclerostin gene in mice results in increased bone formation and bone strength. J Bone Miner Res. 2008 June 01;23(6):860-9.
89. Yao GQ, Wu JJ, Troiano N, Insogna K. Targeted overexpression of Dkk1 in osteoblasts reduces bone mass but does not impair the anabolic response to intermittent PTH treatment in mice. J Bone Miner Metab. 2011 March 01;29(2):141-8.
90. Cejka D, Herberth J, Branscum AJ, Fardo DW, Monier-Faugere MC, Diarra D, et al. Sclerostin and Dickkopf-1 in renal osteodystrophy. Clin J Am Soc Nephrol. 2011 April 01;6(4):877-82.
91. Wilson PW, D'Agostino RB, Levy D, Belanger AM, Silbershatz H, Kannel WB. Prediction of coronary heart disease using risk factor categories. Circulation. 1998 May 12;97(18):1837-47.
92. Zimmermann J, Herrlinger S, Pruy A, Metzger T, Wanner C. Inflammation enhances cardiovascular risk and mortality in hemodialysis patients. Kidney Int. 1999 February 01;55(2):648-58.

93. Blacher J, Guerin AP, Pannier B, Marchais SJ, London GM. Arterial calcifications, arterial stiffness, and cardiovascular risk in end-stage renal disease. Hypertension. 2001 October 01;38(4):938-42.
94. London GM, Guerin AP, Marchais SJ, Metivier F, Pannier B, Adda H. Arterial media calcification in end-stage renal disease: impact on all-cause and cardiovascular mortality. Nephrol Dial Transplant. 2003 September 01;18(9):1731-40.
95. Okuno S, Ishimura E, Kitatani K, Fujino Y, Kohno K, Maeno Y, et al. Presence of abdominal aortic calcification is significantly associated with all-cause and cardiovascular mortality in maintenance hemodialysis patients. Am J Kidney Dis. 2007 March 01;49(3):417-25.
96. Stenvinkel P, Carrero JJ, Axelsson J, Lindholm B, Heimbürger O, Massy Z. Emerging biomarkers for evaluating cardiovascular risk in the chronic kidney disease patient: how do new pieces fit into the uremic puzzle? Clin J Am Soc Nephrol. 2008 Mar;3(2):505-21.
97. Wanner C, Krane V, März W, Olschewski M, Mann JF, Ruf G, et al. Atorvastatin in patients with type 2 diabetes mellitus undergoing hemodialysis. Diabetes and Dialysis Study Investigators. N Engl J Med. 2005 Jul 21; 353(3):238-48.
98. Zannad F, Kessler M, Lehert P, Grünfeld JP, Thuilliez C, et al. Prevention of cardiovascular events in end-stage renal disease: results of a randomized trial of fosinopril and implications for future studies. Kidney Int. 2006 Oct; 70(7):1318-24.
99. Eknoyan G, Beck GJ, Cheung AK, Daugirdas JT, Greene T, et al. Effect of dialysis dose and membrane flux in maintenance hemodialysis.Hemodialysis (HEMO) Study Group. N Engl J Med. 2002 Dec 19; 347(25):2010-9.
100. Fox CS, Larson MG, Vasan RS, Guo CY, Parise H, Levy D, et al. Cross-sectional association of kidney function with valvular and annular calcification: the Framingham heart study. J Am Soc Nephrol. 2006 February 01;17(2):521-7.
101. Ehara S, Kobayashi Y, Yoshiyama M, Shimada K, Shimada Y, Fukuda D, et al. Spotty calcification typifies the culprit plaque in patients with acute myocardial infarction: an intravascular ultrasound study. Circulation. 2004 November 30;110(22):3424-9.
102. Raggi P, Bellasi A, Ferramosca E, Islam T, Muntner P, Block GA. Association of pulse wave velocity with vascular and valvular calcification in hemodialysis patients. Kidney Int. 2007 April 01;71(8):802-7.
103. Amann K. Media calcification and intima calcification are distinct entities in chronic kidney disease. Clin J Am Soc Nephrol. 2008 November 01;3(6):1599-605.
104. Lindman BR, Bonow RO, Otto CM. Current management of calcific aortic stenosis. Circ Res. 2013 July 05;113(2):223-37.
105. Giachelli CM. The emerging role of phosphate in vascular calcification. Kidney Int. 2009 May 01;75(9):890-7.
106. Paloian NJ, Giachelli CM. A current understanding of vascular calcification in CKD. Am J Physiol Renal Physiol. 2014 October 15;307(8):891.
107. Cannata-Andia JB, Roman-Garcia P, Hruska K. The connections between vascular calcification and bone health. Nephrol Dial Transplant. 2011 November 01;26(11):3429-36.
108. Leskinen Y, Paana T, Saha H, Groundstroem K, Lehtimaki T, Kilpinen S, et al. Valvular calcification and its relationship to atherosclerosis in chronic kidney disease. J Heart Valve Dis. 2009 July 01;18(4):429-38.
109. Forster IC, Hernando N, Biber J, Murer H. Phosphate transporters of the SLC20 and SLC34 families. Mol Aspects Med. 2013 June 01;34(2-3):386-95.
110. Jono S, McKee MD, Murry CE, Shioi A, Nishizawa Y, Mori K, et al. Phosphate regulation of vascular smooth muscle cell calcification. Circ Res. 2000 September 29;87(7):10.
111. Chavkin NW, Chia JJ, Crouthamel MH, Giachelli CM. Phosphate uptake-independent signaling functions of the type III sodium-dependent phosphate transporter, PiT-1, in vascular smooth muscle cells. Exp Cell Res. 2015 April 10;333(1):39-48.

112. Shanahan CM, Crouthamel MH, Kapustin A, Giachelli CM. Arterial calcification in chronic kidney disease: key roles for calcium and phosphate. Circ Res. 2011 September 02;109(6):697-711.
113. Jimbo R, Shimosawa T. Cardiovascular Risk Factors and Chronic Kidney Disease-FGF23: A Key Molecule in the Cardiovascular Disease. Int J Hypertens. 2014;2014:381082.
114. Fyfe-Johnson AL, Alonso A, Selvin E, Bower JK, Pankow JS, Agarwal SK, et al. Serum fibroblast growth factor-23 and incident hypertension: the Atherosclerosis Risk in Communities (ARIC) Study. J Hypertens. 2016 July 01;34(7):1266-72.
115. Akhabue E, Montag S, Reis JP, Pool LR, Mehta R, Yancy CW, et al. FGF23 (Fibroblast Growth Factor-23) and Incident Hypertension in Young and Middle-Aged Adults: The CARDIA Study. Hypertension. 2018 July 01;72(1):70-6.
116. de Borst MH, Vervloet MG, ter Wee PM, Navis G. Cross talk between the renin-angiotensin-aldosterone system and vitamin D-FGF-23-klotho in chronic kidney disease. J Am Soc Nephrol. 2011 September 01;22(9):1603-9.
117. Dai B, David V, Martin A, Huang J, Li H, Jiao Y, et al. A comparative transcriptome analysis identifying FGF23 regulated genes in the kidney of a mouse CKD model. PLoS One. 2012;7(9):e44161.
118. Nasrallah MM, El-Shehaby AR, Salem MM, Osman NA, El Sheikh E, Sharaf El Din, U A. Fibroblast growth factor-23 (FGF-23) is independently correlated to aortic calcification in haemodialysis patients. Nephrol Dial Transplant. 2010 August 01;25(8):2679-85.
119. Scialla JJ, Lau WL, Reilly MP, Isakova T, Yang HY, Crouthamel MH, et al. Fibroblast growth factor 23 is not associated with and does not induce arterial calcification. Kidney Int. 2013 June 01;83(6):1159-68.
120. Leifheit-Nestler M, Grosse Siemer R, Flasbart K, Richter B, Kirchhoff F, Ziegler WH, et al. Induction of cardiac FGF23/FGFR4 expression is associated with left ventricular hypertrophy in patients with chronic kidney disease. Nephrol Dial Transplant. 2016 July 01;31(7):1088-99.
121. Hsu HJ, Wu MS. Fibroblast growth factor 23: a possible cause of left ventricular hypertrophy in hemodialysis patients. Am J Med Sci. 2009 February 01;337(2):116-22.
122. Vázquez-Sánchez S, Poveda J, Navarro-García JA, González-Lafuente L, et al. An Overview of FGF-23 as a Novel Candidate Biomarker of Cardiovascular Risk..Front Physiol. 2021 Mar 9;12:632260. doi: 10.3389/fphys.2021.632260.
123. Grabner A, Schramm K, Silswal N, Hendrix M, Yanucil C, et al. FGF23/FGFR4-mediated left ventricular hypertrophy is reversible. Sci Rep. 2017 May 16; 7(1):1993.
124. Bellasi A, Raggi P. Vascular calcification in chronic kidney disease: usefulness of a marker of vascular damage. J Nephrol. 2011 June 01;24 Suppl 18:11.
125. Bellasi A, Raggi P. Techniques and technologies to assess vascular calcification. Semin Dial. 2007 April 01;20(2):129-33.
126. Rumberger JA, Brundage BH, Rader DJ, Kondos G. Electron beam computed tomographic coronary calcium scanning: a review and guidelines for use in asymptomatic persons. Mayo Clin Proc. 1999 March 01;74(3):243-52.
127. Goodman WG, Goldin J, Kuizon BD, Yoon C, Gales B, Sider D, et al. Coronary-artery calcification in young adults with end-stage renal disease who are undergoing dialysis. N Engl J Med. 2000 May 18;342(20):1478-83.
128. Russo D, Corrao S, Battaglia Y, Andreucci M, Caiazza A, Carlomagno A, et al. Progression of coronary artery calcification and cardiac events in patients with chronic renal disease not receiving dialysis. Kidney Int. 2011 July 01;80(1):112-8.
129. Achenbach S, Raggi P. Imaging of coronary atherosclerosis by computed tomography. Eur Heart J. 2010 June 01;31(12):1442-8.
130. Shantouf RS, Budoff MJ, Ahmadi N, Ghaffari A, Flores F, Gopal A, et al. Total and individual coronary artery calcium scores as independent predictors of mortality in hemodialysis patients. Am J Nephrol. 2010;31(5):419-25.

131. Watanabe R, Lemos MM, Manfredi SR, Draibe SA, Canziani ME. Impact of cardiovascular calcification in nondialyzed patients after 24 months of follow-up. Clin J Am Soc Nephrol. 2010 February 01;5(2):189-94.
132. Honkanen E., Kauppila L., Wikstrom B. et al. Abdominal aortic calcification in dialysis patients: results of the CORD study. Nephrol Dial Transplant (2008) 23: 4009-4015
133. Kauppila LI, Polak JF, Cupples LA, Hannan MT, Kiel DP, Wilson PW. New indices to classify location, severity and progression of calcific lesions in the abdominal aorta: a 25-year follow-up study. Atherosclerosis. 1997 July 25;132(2):245-50.
134. Wilson PW, Kauppila LI, O'Donnell CJ, Kiel DP, Hannan M, Polak JM, et al. Abdominal aortic calcific deposits are an important predictor of vascular morbidity and mortality. Circulation. 2001 March 20;103(11):1529-34.
135. Cho A, Jung HY, Park HC, Oh J, Kim J, Lee YK. Relationship between abdominal aortic calcification on plain radiograph and coronary artery calcification detected by computed tomography in hemodialysis patients. Clin Nephrol. 2020 March 01;93(3):123-9.
136. Peeters MJ, van den Brand, J A, van Zuilen AD, Koster Y, Bots ML, Vervloet MG, et al. Abdominal aortic calcification in patients with CKD. J Nephrol. 2017 February 01;30(1):109-18.
137. Zweig BM, Sheth M, Simpson S, Al-Mallah MH. Association of abdominal aortic calcium with coronary artery calcium and obstructive coronary artery disease: a pilot study. Int J Cardiovasc Imaging. 2012 February 01;28(2):399-404.
138. Bellasi A, Ferramosca E, Muntner P, Ratti C, Wildman RP, Block GA, et al. Correlation of simple imaging tests and coronary artery calcium measured by computed tomography in hemodialysis patients. Kidney Int. 2006 November 01;70(9):1623-8.
139. Bellasi A, Ferramosca E, Ratti C, Block G, Raggi P. Cardiac valve calcification is a marker of vascular disease in prevalent hemodialysis patients. J Nephrol. 2012 April 01;25(2):211-8.
140. Raggi P, Bellasi A, Gamboa C, Ferramosca E, Ratti C, Block GA, et al. All-cause mortality in hemodialysis patients with heart valve calcification. Clin J Am Soc Nephrol. 2011 August 01;6(8):1990-5.
141. Brandenburg VM, Kramann R, Rothe H, Kaesler N, Korbiel J, Specht P, et al. Calcific uraemic arteriolopathy (calciphylaxis): data from a large nationwide registry. Nephrol Dial Transplant. 2017 January 01;32(1):126-32.
142. Honda Y, Endo Y AD partment of Dermatology, Kyoto University Graduate School of Medicine, Tanizaki H, Fujisawa A, Kitoh A, Miyachi Y, et al. Calciphylaxis associated with acute renal failure in multicentric Castleman's disease. Eur J Dermatol. 2015 October 01;25(5):497-9.
143. Kalajian AH, Malhotra PS, Callen JP, Parker LP. Calciphylaxis with normal renal and parathyroid function: not as rare as previously believed. Arch Dermatol. 2009 April 01;145(4):451-8.
144. Kramann R, Brandenburg VM, Schurgers LJ, Ketteler M, Westphal S, Leisten I, et al. Novel insights into osteogenesis and matrix remodelling associated with calcific uraemic arteriolopathy. Nephrol Dial Transplant. 2013 April 01;28(4):856-68.
145. Shroff R, Long DA, Shanahan C. Mechanistic insights into vascular calcification in CKD. J Am Soc Nephrol. 2013 February 01;24(2):179-89.
146. Chen TY, Lehman JS, Gibson LE, Lohse CM, El-Azhary RA. Histopathology of Calciphylaxis: Cohort Study With Clinical Correlations. Am J Dermatopathol. 2017 November 01;39(11):795-802.
147. Fine A, Zacharias J. Calciphylaxis is usually non-ulcerating: risk factors, outcome and therapy. Kidney Int. 2002 June 01;61(6):2210-7.
148. Nigwekar SU, Zhao S, Wenger J, Hymes JL, Maddux FW, Thadhani RI, et al. A Nationally Representative Study of Calcific Uremic Arteriolopathy Risk Factors. J Am Soc Nephrol. 2016 November 01;27(11):3421-9.
149. Hayashi M, Takamatsu I, Kanno Y, Yoshida T, Abe T, Sato Y, et al. A case-control study of calciphylaxis in Japanese end-stage renal disease patients. Nephrol Dial Transplant. 2012 April 01;27(4):1580-4.

150. Danziger J. Vitamin K-dependent proteins, warfarin, and vascular calcification. Clin J Am Soc Nephrol. 2008 September 01;3(5):1504-10.
151. Baldwin C, Farah M, Leung M, Taylor P, Werb R, Kiaii M, et al. Multi-intervention management of calciphylaxis: a report of 7 cases. Am J Kidney Dis. 2011 December 01;58(6):988-91.
152. Nigwekar SU, Brunelli SM, Meade D, Wang W, Hymes J, Lacson E. Sodium thiosulfate therapy for calcific uremic arteriolopathy. Clin J Am Soc Nephrol. 2013 July 01;8(7):1162-70.
153. Liu SH, Chu HI. Treatment of Renal Osteodystrophy with Dihydrotachysterol (A.T.10) and Iron. Science. 1942 April 10;95(2467):388-9.
154. Lacativa PG, Franco FM, Pimentel JR, Patricio Filho PJ, Goncalves MD, Farias ML. Prevalence of radiological findings among cases of severe secondary hyperparathyroidism. Sao Paulo Med J. 2009 May 01;127(2):71-7.
155. Appelman-Dijkstra NM, Navas Canete A, Soonawala D. The rugger-jersey spine. Kidney Int. 2016 August 01;90(2):454.
156. Urena P, Bernard-Poenaru O, Ostertag A, Baudoin C, Cohen-Solal M, Cantor T, et al. Bone mineral density, biochemical markers and skeletal fractures in haemodialysis patients. Nephrol Dial Transplant. 2003 November 01;18(11):2325-31.
157. Jadoul M, Albert JM, Akiba T, Akizawa T, Arab L, Bragg-Gresham JL, et al. Incidence and risk factors for hip or other bone fractures among hemodialysis patients in the Dialysis Outcomes and Practice Patterns Study. Kidney Int. 2006 October 01;70(7):1358-66.
158. Tentori F, McCullough K, Kilpatrick RD, Bradbury BD, Robinson BM, Kerr PG, et al. High rates of death and hospitalization follow bone fracture among hemodialysis patients. Kidney Int. 2014 January 01;85(1):166-73.
159. Jorgensen HS, David K, Salam S, Evenepoel P, European Renal Osteodystrophy (EUROD) workgroup, an initiative of the CKD-MBD working group of the ERA-EDTA. Traditional and Non-traditional Risk Factors for Osteoporosis in CKD. Calcif Tissue Int. 2021 April 01;108(4):496-511.
160. Mortensen SJ, Mohamadi A, Wright CL, Chan JJ, Weaver MJ, von Keudell A, et al. Medications as a Risk Factor for Fragility Hip Fractures: A Systematic Review and Meta-analysis. Calcif Tissue Int. 2020 July 01;107(1):1-9.
161. Schnitzler CM, Pettifor JM, Mesquita JM, Bird MD, Schnaid E, Smyth AE. Histomorphometry of iliac crest bone in 346 normal black and white South African adults. Bone Miner. 1990 September 01;10(3):183-99.
162. Monier-Faugere MC, Malluche HH. Trends in renal osteodystrophy: a survey from 1983 to 1995 in a total of 2248 patients. Nephrol Dial Transplant. 1996;11 Suppl 3:111-20.
163. Ng AH, Omelon S, Variola F, Allo B, Willett TL, Alman BA, et al. Adynamic Bone Decreases Bone Toughness During Aging by Affecting Mineral and Matrix. J Bone Miner Res. 2016 February 01;31(2):369-79.
164. Malluche HH, Porter DS, Monier-Faugere MC, Mawad H, Pienkowski D. Differences in bone quality in low- and high-turnover renal osteodystrophy. J Am Soc Nephrol. 2012 March 01;23(3):525-32.
165. Cannata Andia JB. Aluminium toxicity: its relationship with bone and iron metabolism. Nephrol Dial Transplant. 1996;11 Suppl 3:69-73.
166. Ambrus C, Almasi C, Berta K, Deak G, Marton A, Molnar MZ, et al. Vitamin D insufficiency and bone fractures in patients on maintenance hemodialysis. Int Urol Nephrol. 2011 June 01;43(2):475-82.
167. Piraino B, Chen T, Cooperstein L, Segre G, Puschett J. Fractures and vertebral bone mineral density in patients with renal osteodystrophy. Clin Nephrol. 1988 August 01;30(2):57-62.
168. Carbonara CEM, Reis LMD, Quadros, K R D S, Roza NAV, Sano R, Carvalho AB, et al. Renal osteodystrophy and clinical outcomes: data from the Brazilian Registry of Bone Biopsies - REBRABO. J Bras Nefrol. 2020 January 20;42(2):138-46.

169. Ketteler M, Block GA, Evenepoel P, Fukagawa M, Herzog CA, McCann L, et al. Executive summary of the 2017 KDIGO Chronic Kidney Disease-Mineral and Bone Disorder (CKD-MBD) Guideline Update: what's changed and why it matters. Kidney Int. 2017 July 01;92(1):26-36.
170. Evenepoel P, Cunningham J, Ferrari S, Haarhaus M, Javaid MK, Lafage-Proust MH, et al. European Consensus Statement on the diagnosis and management of osteoporosis in chronic kidney disease stages G4-G5D. Nephrol Dial Transplant. 2021 January 01;36(1):42-59.
171. Ott SM. Histomorphometric measurements of bone turnover, mineralization, and volume. Clin J Am Soc Nephrol. 2008 November 01;3 Suppl 3:151.
172. Christiansen P, Steiniche T, Vesterby A, Mosekilde L, Hessov I, Melsen F. Primary hyperparathyroidism: iliac crest trabecular bone volume, structure, remodeling, and balance evaluated by histomorphometric methods. Bone. 1992;13(1):41-9.
173. Kelly PJ, Pocock NA, Sambrook PN, Eisman JA. Age and menopause-related changes in indices of bone turnover. J Clin Endocrinol Metab. 1989 December 01;69(6):1160-5.
174. D'Haens G, Verstraete A, Cheyns K, Aerden I, Bouillon R, Rutgeerts P. Bone turnover during short-term therapy with methylprednisolone or budesonide in Crohn's disease. Aliment Pharmacol Ther. 1998 May 01;12(5):419-24.
175. Fernandez-Martin JL, Martinez-Camblor P, Dionisi MP, Floege J, Ketteler M, London G, et al. Improvement of mineral and bone metabolism markers is associated with better survival in haemodialysis patients: the COSMOS study. Nephrol Dial Transplant. 2015 September 01;30(9):1542-51.
176. Lehmann G, Stein G, Huller M, Schemer R, Ramakrishnan K, Goodman WG. Specific measurement of PTH (1-84) in various forms of renal osteodystrophy (ROD) as assessed by bone histomorphometry. Kidney Int. 2005 September 01;68(3):1206-14.
177. Torres A, Lorenzo V, Hernandez D, Rodriguez JC, Concepcion MT, Rodriguez AP, et al. Bone disease in predialysis, hemodialysis, and CAPD patients: evidence of a better bone response to PTH. Kidney Int. 1995 May 01;47(5):1434-42.
178. Salam S, Gallagher O, Gossiel F, Paggiosi M, Khwaja A, Eastell R. Diagnostic Accuracy of Biomarkers and Imaging for Bone Turnover in Renal Osteodystrophy. J Am Soc Nephrol. 2018 May 01;29(5):1557-65.
179. Magnusson P, Sharp CA, Magnusson M, Risteli J, Davie MW, Larsson L. Effect of chronic renal failure on bone turnover and bone alkaline phosphatase isoforms. Kidney Int. 2001 July 01;60(1):257-65.
180. Drechsler C, Verduijn M, Pilz S, Krediet RT, Dekker FW, Wanner C, et al. Bone alkaline phosphatase and mortality in dialysis patients. Clin J Am Soc Nephrol. 2011 July 01;6(7):1752-9.
181. Maruyama Y, Taniguchi M, Kazama JJ, Yokoyama K, Hosoya T, Yokoo T, et al. A higher serum alkaline phosphatase is associated with the incidence of hip fracture and mortality among patients receiving hemodialysis in Japan. Nephrol Dial Transplant. 2014 August 01;29(8):1532-8.
182. Seibel MJ. Biochemical markers of bone turnover: part I: biochemistry and variability. Clin Biochem Rev. 2005 November 01;26(4):97-122.
183. Shidara K, Inaba M, Okuno S, Yamada S, Kumeda Y, Imanishi Y, et al. Serum levels of TRAP5b, a new bone resorption marker unaffected by renal dysfunction, as a useful marker of cortical bone loss in hemodialysis patients. Calcif Tissue Int. 2008 April 01;82(4):278-87.
184. Yamada S, Tsuruya K, Yoshida H, Taniguchi M, Haruyama N, Tanaka S, et al. The clinical utility of serum tartrate-resistant acid phosphatase 5b in the assessment of bone resorption in patients on peritoneal dialysis. Clin Endocrinol (Oxf). 2013 June 01;78(6):844-51.
185. Wheater G, Elshahaly M, Tuck SP, Datta HK, van Laar JM. The clinical utility of bone marker measurements in osteoporosis. J Transl Med. 2013 August 29;11:201-.
186. Vasikaran SD, Chubb SP, Ebeling PR, Jenkins N, Jones GR, Kotowicz MA, et al. Harmonised Australian Reference Intervals for Serum PINP and CTX in Adults. Clin Biochem Rev. 2014 November 01;35(4):237-42.

187. Evenepoel P, D'Haese P, Bacchetta J, Cannata-Andia J, Ferreira A, Haarhaus M, et al. Bone biopsy practice patterns across Europe: the European renal osteodystrophy initiative-a position paper. Nephrol Dial Transplant. 2017 October 01;32(10):1608-13.
188. Torres PU, Bover J, Mazzaferro S, de Vernejoul MC, Cohen-Solal M. When, how, and why a bone biopsy should be performed in patients with chronic kidney disease. Semin Nephrol. 2014 November 01;34(6):612-25.
189. Trueba D, Sawaya BP, Mawad H, Malluche HH. Bone biopsy: indications, techniques, and complications. Semin Dial. 2003 August 01;16(4):341-5.
190. Hernandez JD, Wesseling K, Pereira R, Gales B, Harrison R, Salusky IB. Technical approach to iliac crest biopsy. Clin J Am Soc Nephrol. 2008 November 01;3 Suppl 3:164.
191. Dempster DW, Compston JE, Drezner MK, Glorieux FH, Kanis JA, Malluche H, et al. Standardized nomenclature, symbols, and units for bone histomorphometry: a 2012 update of the report of the ASBMR Histomorphometry Nomenclature Committee. J Bone Miner Res. 2013 January 01;28(1):2-17.
192. Parfitt AM, Drezner MK, Glorieux FH, s JA, Malluche H, Meunier PJ, et al. Bone histomorphometry: standardization of nomenclature, symbols, and units. Report of the ASBMR Histomorphometry Nomenclature Committee. J Bone Miner Res. 1987 December 01;2(6):595-610.
193. Dempster DW, Ferguson-Pell MW, Mellish RW, Cochran GV, Xie F, Fey C, et al. Relationships between bone structure in the iliac crest and bone structure and strength in the lumbar spine. Osteoporos Int. 1993 March 01;3(2):90-6.
194. Chavassieux PM, Arlot ME, Meunier PJ. Intersample variation in bone histomorphometry: comparison between parameter values measured on two contiguous transiliac bone biopsies. Calcif Tissue Int. 1985 July 01;37(4):345-50.
195. Schober HC, Han ZH, Foldes AJ, Shih MS, Rao DS, Balena R, et al. Mineralized bone loss at different sites in dialysis patients: implications for prevention. J Am Soc Nephrol. 1998 July 01;9(7):1225-33.
196. Eriksen EF, Mosekilde L, Melsen F. Trabecular bone remodeling and balance in primary hyperparathyroidism. Bone. 1986;7(3):213-21.
197. Malluche HH, Mawad HW, Monier-Faugere MC. Renal osteodystrophy in the first decade of the new millennium: analysis of 630 bone biopsies in black and white patients. J Bone Miner Res. 2011 June 01;26(6):1368-76.
198. Malluche HH, Porter DS, Monier-Faugere MC, Mawad H, Pienkowski D. Differences in bone quality in low- and high-turnover renal osteodystrophy. J Am Soc Nephrol. 2012 March 01;23(3):525-32.
199. Ott SM. Bone histomorphometry in renal osteodystrophy. Semin Nephrol. 2009 March 01;29(2):122-32.
200. Recker RR, Akhter MP, Lappe JM, Watson P. Bone histomorphometry in transiliac biopsies from 48 normal, healthy men. Bone. 2018 June 01;111:109-15.
201. Recker RR, Lappe JM, Davies M, Kimmel D. Perimenopausal bone histomorphometry before and after menopause. Bone. 2018 March 01;108:55-61.
202. Ott SM. Renal Osteodystrophy-Time for Common Nomenclature. Curr Osteoporos Rep. 2017 June 01;15(3):187-93.
203. Malluche HH, Meyer W, Sherman D, Massry SG. Quantitative bone histology in 84 normal American subjects. Micromorphometric analysis and evaluation of variance in iliac bone. Calcif Tissue Int. 1982 September 01;34(5):449-55.
204. Malluche HH FM. Atlas of mineralized bone histology. Karger, Basel; 1986.
205. Vedi S, Kaptoge S, Compston JE. Age-related changes in iliac crest cortical width and porosity: a histomorphometric study. J Anat. 2011 May 01;218(5):510-6.
206. Rehman MT, Hoyland JA, Denton J, Freemont AJ. Age related histomorphometric changes in bone in normal British men and women. J Clin Pathol. 1994 June 01;47(6):529-34.

207. Tong X, Burton IS, Jurvelin JS, Isaksson H, Kroger H. Iliac crest histomorphometry and skeletal heterogeneity in men. Bone Rep. 2016 November 28;6:9-16.
208. Prescott JW. Quantitative imaging biomarkers: the application of advanced image processing and analysis to clinical and preclinical decision making. J Digit Imaging. 2013 February 01;26(1):97-108.
209. Cummings SR, Bates D, Black DM. Clinical use of bone densitometry: scientific review. JAMA. 2002 October 16;288(15):1889-97.
210. West SL, Lok CE, Langsetmo L, Cheung AM, Szabo E, Pearce D, et al. Bone mineral density predicts fractures in chronic kidney disease. J Bone Miner Res. 2015 May 01;30(5):913-9.
211. Iimori S, Mori Y, Akita W, Kuyama T, Takada S, Asai T, et al. Diagnostic usefulness of bone mineral density and biochemical markers of bone turnover in predicting fracture in CKD stage 5D patients--a single-center cohort study. Nephrol Dial Transplant. 2012 January 01;27(1):345-51.
212. Martineau P, Leslie WD. Trabecular bone score (TBS): Method and applications. Bone. 2017 November 01;104:66-72.
213. Naylor KL, Prior J, Garg AX, Berger C, Langsetmo L, Adachi JD, et al. Trabecular Bone Score and Incident Fragility Fracture Risk in Adults with Reduced Kidney Function. Clin J Am Soc Nephrol. 2016 November 07;11(11):2032-40.
214. Yavropoulou MP, Vaios V, Pikilidou M, Chryssogonidis I, Sachinidou M, Tournis S, et al. Bone Quality Assessment as Measured by Trabecular Bone Score in Patients With End-Stage Renal Disease on Dialysis. J Clin Densitom. 2017 December 01;20(4):490-7.
215. Brunerova L, Ronova P, Veresova J, Beranova P, Potoekova J, Kasalicky P, et al. Osteoporosis and Impaired Trabecular Bone Score in Hemodialysis Patients. Kidney Blood Press Res. 2016;41(3):345-54.
216. Ramalho J, Marques IDB, Hans D, Dempster D, Zhou H, Patel P, et al. The trabecular bone score: Relationships with trabecular and cortical microarchitecture measured by HR-pQCT and histomorphometry in patients with chronic kidney disease. Bone. 2018 November 01;116:215-20.
217. Hans D, Barthe N, Boutroy S, Pothuaud L, Winzenrieth R, Krieg MA. Correlations between trabecular bone score, measured using anteroposterior dual-energy X-ray absorptiometry acquisition, and 3-dimensional parameters of bone microarchitecture: an experimental study on human cadaver vertebrae. J Clin Densitom. 2011 September 01;14(3):302-12.
218. Nickolas TL, Stein EM, Dworakowski E, Nishiyama KK, Komandah-Kosseh M, Zhang CA, et al. Rapid cortical bone loss in patients with chronic kidney disease. J Bone Miner Res. 2013 August 01;28(8):1811-20.
219. Cejka D, Patsch JM, Weber M, Diarra D, Riegersperger M, Kikic Z, et al. Bone microarchitecture in hemodialysis patients assessed by HR-pQCT. Clin J Am Soc Nephrol. 2011 September 01;6(9):2264-71.
220. Griffith JF, Yeung DK, Leung JC, Kwok TC, Leung PC. Prediction of bone loss in elderly female subjects by MR perfusion imaging and spectroscopy. Eur Radiol. 2011 June 01;21(6):1160-9.
221. Al-Beyatti Y, Siddique M, Frost ML, Fogelman I, Blake GM. Precision of (1)(8)F-fluoride PET skeletal kinetic studies in the assessment of bone metabolism. Osteoporos Int. 2012 October 01;23(10):2535-41.
222. Hawkins RA, Choi Y, Huang SC, Hoh CK, Dahlbom M, Schiepers C, et al. Evaluation of the skeletal kinetics of fluorine-18-fluoride ion with PET. J Nucl Med. 1992 May 01;33(5):633-42.
223. Ishiguro K, Nakagaki H, Tsuboi S, Narita N, Kato K, Li J, et al. Distribution of fluoride in cortical bone of human rib. Calcif Tissue Int. 1993 April 01;52(4):278-82.
224. John W. Keyes. SUV: Standard Uptake or Silly Useless Value? Journal of Nuclear Medicine. 1995 October , 36;10:1836-9.
225. Blake GM, Moore AE, Fogelman I. Quantitative studies of bone using (99m)Tc-methylene diphosphonate skeletal plasma clearance. Semin Nucl Med. 2009 November 01;39(6):369-79.

226. Gnanasegaran G, Moore AE, Blake GM, Vijayanathan S, Clarke SE, Fogelman I. Atypical Paget's disease with quantitative assessment of tracer kinetics. Clin Nucl Med. 2007 October 01;32(10):765-9.
227. Blake GM, Siddique M, Frost ML, Moore AE, Fogelman I. Radionuclide studies of bone metabolism: do bone uptake and bone plasma clearance provide equivalent measurements of bone turnover? Bone. 2011 September 01;49(3):537-42.
228. Cook GJ, Lodge MA, Marsden PK, Dynes A, Fogelman I. Non-invasive assessment of skeletal kinetics using fluorine-18 fluoride positron emission tomography: evaluation of image and population-derived arterial input functions. Eur J Nucl Med. 1999 November 01;26(11):1424-9.
229. Blake GM, Siddique M, Puri T, Frost ML, Moore AE, Cook GJ, et al. A semipopulation input function for quantifying static and dynamic 18F-fluoride PET scans. Nucl Med Commun. 2012 August 01;33(8):881-8.
230. Patlak CS, Blasberg RG, Fenstermacher JD. Graphical evaluation of blood-to-brain transfer constants from multiple-time uptake data. J Cereb Blood Flow Metab. 1983 March 01;3(1):1-7.
231. Frost ML, Fogelman I, Blake GM, Marsden PK, Cook G. Dissociation between global markers of bone formation and direct measurement of spinal bone formation in osteoporosis. J Bone Miner Res. 2004 November 01;19(11):1797-804.
232. Frost ML, Siddique M, Blake GM, Moore AE, Schleyer PJ, Dunn JT, et al. Differential effects of teriparatide on regional bone formation using (18)F-fluoride positron emission tomography. J Bone Miner Res. 2011 May 01;26(5):1002-11.
233. Messa C, Goodman WG, Hoh CK, Choi Y, Nissenson AR, Salusky IB, et al. Bone metabolic activity measured with positron emission tomography and [18F]fluoride ion in renal osteodystrophy: correlation with bone histomorphometry. J Clin Endocrinol Metab. 1993 October 01;77(4):949-55.
234. Piert M, Zittel TT, Becker GA, Jahn M, Stahlschmidt A, Maier G, et al. Assessment of porcine bone metabolism by dynamic. J Nucl Med. 2001 July 01;42(7):1091-100.
235. Kalantar-Zadeh K, Gutekunst L, Mehrotra R, Kovesdy CP, Bross R, Shinaberger CS, et al. Understanding sources of dietary phosphorus in the treatment of patients with chronic kidney disease. Clin J Am Soc Nephrol. 2010 March 01;5(3):519-30.
236. Ramirez JA, Emmett M, White MG, Fathi N, Santa Ana CA, Morawski SG, et al. The absorption of dietary phosphorus and calcium in hemodialysis patients. Kidney Int. 1986 November 01;30(5):753-9.
237. Uribarri J, Calvo MS. Hidden sources of phosphorus in the typical American diet: does it matter in nephrology? Semin Dial. 2003 June 01;16(3):186-8.
238. Shinaberger CS, Greenland S, Kopple JD, Van Wyck D, Mehrotra R, Kovesdy CP, et al. Is controlling phosphorus by decreasing dietary protein intake beneficial or harmful in persons with chronic kidney disease? Am J Clin Nutr. 2008 December 01;88(6):1511-8.
239. Block GA, Wheeler DC, Persky MS, Kestenbaum B, Ketteler M, Spiegel DM, et al. Effects of phosphate binders in moderate CKD. J Am Soc Nephrol. 2012 August 01;23(8):1407-15.
240. Hill KM, Martin BR, Wastney ME, McCabe GP, Moe SM, Weaver CM, et al. Oral calcium carbonate affects calcium but not phosphorus balance in stage 3-4 chronic kidney disease. Kidney Int. 2013 May 01;83(5):959-66.
241. Ruospo M, Palmer SC, Natale P, Craig JC, Vecchio M, Elder GJ, et al. Phosphate binders for preventing and treating chronic kidney disease-mineral and bone disorder (CKD-MBD). Cochrane Database Syst Rev. 2018 August 22;8:CD006023.
242. Zitt E, Fouque D, Jacobson SH, Malberti F, Ryba M, Urena P, et al. Serum phosphorus reduction in dialysis patients treated with cinacalcet for secondary hyperparathyroidism results mainly from parathyroid hormone reduction. Clin Kidney J. 2013 June 01;6(3):287-94.
243. Lacson E, Wang W, Hakim RM, Teng M, Lazarus JM. Associates of mortality and hospitalization in hemodialysis: potentially actionable laboratory variables and vascular access. Am J Kidney Dis. 2009 January 01;53(1):79-90.

244. Floege J, Kim J, Ireland E, Chazot C, Drueke T, de Francisco A, et al. Serum iPTH, calcium and phosphate, and the risk of mortality in a European haemodialysis population. Nephrol Dial Transplant. 2011 June 01;26(6):1948-55.
245. Gallieni M, Caputo F, Filippini A, Gabella P, Giannattasio M, Stingone A, et al. Prevalence and progression of cardiovascular calcifications in peritoneal dialysis patients: A prospective study. Bone. 2012 September 01;51(3):332-7.
246. Baker LR, Muir JW, Sharman VL, Abrams SM, Greenwood RN, Cattell WR, et al. Controlled trial of calcitriol in hemodialysis patients. Clin Nephrol. 1986 October 01;26(4):185-91.
247. Hayashi M, Tsuchiya Y, Itaya Y, Takenaka T, Kobayashi K, Yoshizawa M, et al. Comparison of the effects of calcitriol and maxacalcitol on secondary hyperparathyroidism in patients on chronic haemodialysis: a randomized prospective multicentre trial. Nephrol Dial Transplant. 2004 August 01;19(8):2067-73.
248. Thadhani R, Appelbaum E, Pritchett Y, Chang Y, Wenger J, Tamez H, et al. Vitamin D therapy and cardiac structure and function in patients with chronic kidney disease: the PRIMO randomized controlled trial. JAMA. 2012 February 15;307(7):674-84.
249. Wang AY, Fang F, Chan J, Wen YY, Qing S, Chan IH, et al. Effect of paricalcitol on left ventricular mass and function in CKD--the OPERA trial. J Am Soc Nephrol. 2014 January 01;25(1):175-86.
250. Fox J, Lowe SH, Conklin RL, Nemeth EF. The calcimimetic NPS R-568 decreases plasma PTH in rats with mild and severe renal or dietary secondary hyperparathyroidism. Endocrine. 1999 April 01;10(2):97-103.
251. Block GA, Martin KJ, de Francisco AL, Turner SA, Avram MM, Suranyi MG, et al. Cinacalcet for secondary hyperparathyroidism in patients receiving hemodialysis. N Engl J Med. 2004 April 08;350(15):1516-25.
252. Floege J, Raggi P, Block GA, Torres PU, Csiky B, Naso A, et al. Study design and subject baseline characteristics in the ADVANCE Study: effects of cinacalcet on vascular calcification in haemodialysis patients. Nephrol Dial Transplant. 2010 June 01;25(6):1916-23.
253. EVOLVE Trial Investigators, Chertow GM, Block GA, Correa-Rotter R, Drueke TB, Floege J, et al. Effect of cinacalcet on cardiovascular disease in patients undergoing dialysis. N Engl J Med. 2012 December 27;367(26):2482-94.
254. Moe SM, Abdalla S, Chertow GM, Parfrey PS, Block GA, Correa-Rotter R, et al. Effects of Cinacalcet on Fracture Events in Patients Receiving Hemodialysis: The EVOLVE Trial. J Am Soc Nephrol. 2015 June 01;26(6):1466-75.
255. Kim WW, Rhee Y, Kim BS, Kim K, Lee CR, Kang SW, et al. Clinical outcomes of parathyroidectomy versus cinacalcet in the clinical management of secondary hyperparathyroidism. Endocr J. 2019 October 28;66(10):881-9.
256. Narayan R, Perkins RM, Berbano EP, Yuan CM, Neff RT, Sawyers ES, et al. Parathyroidectomy versus cinacalcet hydrochloride-based medical therapy in the management of hyperparathyroidism in ESRD: a cost utility analysis. Am J Kidney Dis. 2007 June 01;49(6):801-13.
257. Wang G, Liu H, Wang C, Ji X, Gu W, Mu Y. Cinacalcet versus Placebo for secondary hyperparathyroidism in chronic kidney disease patients: a meta-analysis of randomized controlled trials and trial sequential analysis. Sci Rep. 2018 February 15;8(1):3111-8.
258. Puri T, Blake GM, Siddique M, Frost ML, Cook GJ, Marsden PK, et al. Validation of new image-derived arterial input functions at the aorta using 18F-fluoride positron emission tomography. Nucl Med Commun. 2011 June 01;32(6):486-95.
259. Thie JA. Clarification of a fractional uptake concept. J Nucl Med. 1995 April 01;36(4):711-2.
260. Agatston AS, Janowitz WR, Hildner FJ, Zusmer NR, Viamonte M, Detrano R. Quantification of coronary artery calcium using ultrafast computed tomography. J Am Coll Cardiol. 1990 March 15;15(4):827-32.

261. Kanis JA, Melton LJ, Christiansen C, Johnston CC, Khaltaev N. The diagnosis of osteoporosis. J Bone Miner Res. 1994 August 01;9(8):1137-41.
262. Frost ML, Compston JE, Goldsmith D, Moore AE, Blake GM, Siddique M, et al. (18)F-fluoride positron emission tomography measurements of regional bone formation in hemodialysis patients with suspected adynamic bone disease. Calcif Tissue Int. 2013 November 01;93(5):436-47.
263. Derlin T, Janssen T, Salamon J, Veldhoen S, Busch JD, Schon G, et al. Age-related differences in the activity of arterial mineral deposition and regional bone metabolism: a 18F-sodium fluoride positron emission tomography study. Osteoporos Int. 2015 January 01;26(1):199-207.
264. Cook GJ, Lodge MA, Blake GM, Marsden PK, Fogelman I. Differences in skeletal kinetics between vertebral and humeral bone measured by 18F-fluoride positron emission tomography in postmenopausal women. J Bone Miner Res. 2000 April 01;15(4):763-9.
265. Mace ML, Gravesen E, Nordholm A, Egstrand S, Morevati M, Nielsen C, et al. Chronic Kidney Disease-Induced Vascular Calcification Impairs Bone Metabolism. J Bone Miner Res. 2021 March 01;36(3):510-22.
266. Salam S, Gallagher O, Gossiel F, Paggiosi M, Eastell R, Khwaja A. Vascular calcification relationship to vascular biomarkers and bone metabolism in advanced chronic kidney disease. Bone. 2021 February 01;143:115699.
267. Aleksova J, Kurniawan S, Vucak-Dzumhur M, Kerr P, Ebeling PR, Milat F, et al. Aortic vascular calcification is inversely associated with the trabecular bone score in patients receiving dialysis. Bone. 2018 August 01;113:118-23.
268. Bach-Gansmo T, Dybvik J, Adamsen T, Naum A. Variation in urinary excretion of FDG, yet another uncertainty in quantitative PET. Acta Radiol Short Rep. 2012 September 23;1(8):10.1258/arsr.2012.120038. eCollection 2012.
269. Siddique M, Blake GM, Frost ML, Moore AE, Puri T, Marsden PK, et al. Estimation of regional bone metabolism from whole-body 18F-fluoride PET static images. Eur J Nucl Med Mol Imaging. 2012 February 01;39(2):337-43.

TURUN
YLIOPISTO
UNIVERSITY
OF TURKU

Painosalama, Turku, Finland 2022

ISBN 978-951-29-8820-4 (PRINT)
ISBN 978-951-29-8821-1 (PDF)
ISSN 0355-9483 (Print)
ISSN 2343-3213 (Online)